NAA-SR-1582

REACTORS-RESEARCH AND TESTING

SODIUM GRAPHITE REACTOR QUARTERLY PROGRESS REPORT OCTOBER — DECEMBER, 1955

SECTION A EDITOR
A. B. MARTIN

SECTION B EDITOR
J. C. COCHRAN

ATOMICS INTERNATIONAL

A DIVISION OF NORTH AMERICAN AVIATION, INC.
P. O. BOX 309 CANOGA PARK, CALIFORNIA

ISSUE DATE

APRIL 15, 1956

CONTRACT AT(04-3)-49

DISTRIBUTION

Category: REACTORS-RESEARCH AND TESTING
(M-3679, 17th Ed.)

	Copy No.
AF Plant Representative, Baltimore	1
AF Plant Representative, Burbank	2
AF Plant Representative, Marietta	3
AF Plant Representative, Santa Monica	4
AF Plant Representative, Seattle	5-7
AF Plant Representative, Wood-Ridge	8
Aircraft Laboratory Design Branch	9
ANP Project Office, Fort Worth	10
Alco Products, Inc.	11
Argonne National Laboratory	12-23
Armed Forces Special Weapons Project, [illegible]a	24
Armed Forces Special Weapons Project [illegible]hington	25
Army Chemical Center	26
Atomic Energy Commission, Washin[illegible]	27-30
Battelle Memorial Institute	31
Bettis Plant	32-37
Brookhaven National Laboratory	38-40
Bureau of Ships	41
Chicago Operations Office	42
Chicago Patent Group	43
Chief of Naval Research	44
Combustion Engineering, [illegible] (CERD)	45
duPont Company, Aiken	46-49
duPont Company, Wilm[illegible]on	50
Engineer Research a[illegible]velopment Laboratories	51
Foster Wheeler Cor[illegible]tion	52
General Electric C[illegible]any (ANPD)	53-56
General Electric [illegible]pany, Richland	57-64
Hanford Operati[illegible]Office	65
Hartford Area [illegible]e	66
Iowa State Co[illegible]	67
Knolls Atom[illegible]ower Laboratory	68-71
Los Alamo[illegible]entific Laboratory	72-75
Massachu[illegible] Institute of Technology (Benedict)	76
Materia[illegible]boratory (WADC)	77
Materi[illegible]aboratory Plant Office (WADC)	78
Moun[illegible]oratory	79
Nati[illegible] Advisory Committee for Aeronautics, Cleveland	80
Na[illegible]l Advisory Committee for Aeronautics, Washington	81
N[illegible]al Lead Company of Ohio	82
Na[illegible]l Research Laboratory	83-84
New York Operations Office	85-86
North American Aviation, Inc. (Aerophysics Division)	87
Nuclear Development Corporation of America	88
Nuclear Metals, Inc.	89
Office of the Quartermaster General	90
Patent Branch, Washington	91
Phillips Petroleum Company (NRTS)	92-98
Powerplant Laboratory (WADC)	99
Pratt and Whitney Aircraft Division (Fox Project)	100
San Francisco Operations Office	101
Sylvania Electric Products, Inc.	102
Union Carbide Nuclear Company (ORNL)	103-106
USAF Project RAND	107
U.S. Naval Postgraduate School	108
U.S. Naval Radiological Defense Laboratory	109
UCLA Medical Research Laboratory	110
University of California Radiation Laboratory, Berkeley	111
University of California Radiation Laboratory, Livermore	112
Vitro Engineering Division	113
Vitro Laboratories	114
Technical Information Service, Oak Ridge	115-429
File	430-505

TABLE OF CONTENTS

		Page No.
I.	Full Scale SGR	9
II.	Nuclear Parameters of Sodium Graphite Lattices	10
	A. Introduction	10
	B. Thermal Utilization	10
	C. Average Macroscopic Cross Sections	11
	D. Thermal Diffusion Length	12
	E. Neutron Age, Fast Effect, Neutrons Produced Per Absorption in Fuel and Resonance Escape Probability	14
III.	Development of Hot Cell Facilities and Handling Techniques	17
IV.	Metallurgy of SGR Fuels	18
	A. Macrostructure of Main SRE Fuel	18
	B. Gamma Graphing of Main SRE Fuel	19
	C. MTR Irradiation of SRE Fuel Materials	19
	D. Evaluation of Experimental Cast Uranium Alloy Fuel Slugs	20
V.	Metallurgy of Breeder Fuels	21
VI.	Engineering Evaluation of Graphite	24
VII.	Zirconium Behavior in Liquid Sodium	27
VIII.	Nuclear Engineering and Physics	33
IX.	Land, Utilities, and Buildings	39
X.	Fuel Elements	39
	A. Fuel Elements	39
	B. Fuel Rod Model	43
	C. Fuel Rod Development	43
	D. Fuel Rod Testing	46
XI.	Moderator Can Fabrication and Testing	50
	A. Moderator Can Testing Program	50
	B. Moderator Can Head Flexure Tests	53
XII.	Heat Transfer	54
	A. Six Inch Wedgeplug Valve Tests	54
	B. Liquid Sodium Level Gage Program	58
	C. Tubular Heater Experiment	58
	D. Plugging Indicator Test Loop	60

TABLE OF CONTENTS (Continued)

		Page No.
	E. Sodium Detection	62
	F. Cold Trap Operational Tests	62
	G. Six Inch Sodium Pump Loop	62
	H. Fuel Element Deflection Study	64
	I. SRE Fuel Element Orifice Calibration	65
	J. SRE Evaporative Coolers	68
	K. SRE Main Air Blast Heat Exchanger	68
XIII.	Instrumentation and Control	68
	A. Instrumentation	68
	B. Control Rod Systems	69
	C. Safety Rod Systems	71
	D. Core Tank Galling Tests	73
	E. MoS_2 Irradiation Experiment	82
XIV.	Shielding	84
	A. Top Shield	84
	B. Fuel Handling Coffin	84
	C. Gallery Shielding	89
	D. Hot Cell Waste Disposal	89
	E. Fuel Cleaning Cell	90
	F. Sodium Pumps	90
	G. Sodium Service System	91
	H. Inert Gas System	92
	I. Viewing Device	92
XV.	Reactor Services	93
	A. Sodium Service Systems	93
	B. Toluene System	94
	C. Vent System	94
	D. Piping	94
	E. Vapor Trap Experiment	94
	F. Freeze Trap Experiment	95
	G. Tetralin Evaporative Cooler Tests	96
	H. Hydrogen in Helium	97
	I. Fuel Handling	98

TABLE OF CONTENTS (Continued)

		Page No.
XVI.	Reactor Operations	99
	A. SRE Operations Manual	99
	B. Reactor Personnel Training	99
	C. Preoperational Testing.	99
	References	100

LIST OF TABLES

I.	Parameters of Thermal Cycled One Inch Test Slugs.	18
II.	Measurement of Wear of Graphite Rearing Pieces	26
III.	Hot-Poisoned and Wet Critical Valuation of 1.5 Per Cent Boron-Nickel Rods.	35
IV.	Sodium Leak Rates.	57
V.	Time to Raise Average Pipe Temperature From Ambient to 350° F	61
VI.	Temperature Schedule of Cycled Prototype Control Rods with 316 SS Screw.	70
VII.	Dose Buildup Factor (B_r)-Point Isotropic Source.	85
VIII.	Constant for the Quadratic Representation of the Dose Buildup Factor	86
IX.	Capture Gamma Rays From Heavy Concrete	87
X.	Effect of NaK Temperature on Hydrogen Content of Helium	97
XI.	Reduction of Water Content of Tank Helium	98

LIST OF FIGURES

		Page No.
1.	Thermal Utilization in SGX Lattices	11
2.	Thermal Flux Weighted Average Absorption Cross Section of SGX Lattices	12
3.	Thermal Flux Weighted Average Transport Cross Section of SGX Lattices	13
4.	Relative Temperature of Thermal Neutrons in SGX (Calculated)	14
5.	Square of Diffusion Length in SGX Lattices	15
6.	Neutron Age in SGX Lattices (Calculated).	16
7.	Resonance Escape Probability in SGX Lattices	17
8.	Microstructures of Th-5.4% U Extruded Rod	22
9.	Sodium Expansion of Graphite	25
10.	Weight Gain in NaZr I	28
11.	Weight Gain in NaZr III.	29
12.	Section of Welded Zr-Zr Interface	31
13.	Effect of Thermocouple Response Time	34
14.	Effect of Rod Motion.	36
15.	Effect of Pump Boost Rate.	37
16.	Effect of Scram Delay Times.	38
17.	Reactor Building Showing Structural Progress	40
18.	Black Soot-Like Deposit Around Welds and Chill Blocks.	42
19.	"As Received" and Electropolished Slugs.	44
20.	Cutaway Rod for Fuel Rod Model	45
21.	Cyclograph Traces	47
22.	Cyclograph Traces	48
23.	Cyclograph Traces	49
24.	Slugs Showing Regions Bonded with Sodium	51
25.	Slugs Showing Voids Coinciding with Many External Burned Regions	52
26.	Thermocouple Locations for the Preliminary Test of Freeze Seal Number 2.	55

LIST OF FIGURES (Continued)

Page No.

27. Six Inch Valve Concurrent Flow Tests Showing the Temperature Gradients Across the Number 2 Freeze Seal . . 56
28. Level Probe and Indicator 59
29. Tubular Heater Test Setup Minus Kaylo Insulation 60
30. SRE Fuel Element Model 63
31. Upper Plenum Showing Fuel Channels 63
32. Orifice Plate Showing Pressure Taps 66
33. Orifice Plate Disassembled 66
34. Orifice Plate Assembly Mounted Co-Axially in Pipe 67
35. Section of the Keyway Showing Galling 72
36. Key Showing Groove Cut Through Thimble 72
37. ASTM-A301 and 304 CRES Specimens Before Testing. . . . 74
38. 304 CRES vs ASTM-A301 After Test Run with No Lubrication . 75
39. 304 CRES vs ASTM-A301 After 600 Cycles at 500° F in Argon, 200 psi Loading Pressure 77
40. SAE 4130, 304 CRES, and Haynes 25 Specimens Before Test . 78
41. SAE 4130, 304 CRES, and Haynes 25 Specimens After Tests with MoS_2 Lubrication 79
42. 304 CRES vs ASTM-A301 After Tests with MoS_2 Lubrication. 80
43. 304 CRES vs ASTM-A301 Lubricated with MoS_2 with Sodium Added 81
44. 304 CRES vs ASTM-A301 Lubricated with Sodium 83
45. Capture Gamma Ray Spectrum for Heavy Concrete 88

SECTION A
TECHNOLOGY OF THE SODIUM GRAPHITE REACTOR

I. FULL SCALE SGR

(E. F. Weisner and R. J. Gimera)

The study relating to the inherent safety features of the Sodium Graphite Reactor concept was continued with an investigation of the mechanical behavior of the fuel element itself during a power excursion. A nuclear incident caused by an uncontrolled power increase may be terminated without action on the part of operating personnel by one of the following methods, depending on the magnitude of the incident (that is, on the rate of power increase): (1) the negative temperature coefficient of reactivity may stop the excursion before serious damage results, (2) the power may continue to increase until the fuel element jacket fails, allowing the fuel to drop to the bottom of the core tank, or (3) the power may continue to increase until the fuel elements are shattered by the vaporization of a portion of the fuel. Vaporization of a portion of the fuel could result in either ejection of the fuel element from the reactor top shield or in buckling of the fuel element hanger rod.

Earlier studies have shown that a general pressure increase in the reactor core, due to vaporization of either sodium or fuel, will be vented to the heat exchanger vaults via the pipe line diaphragms at about 4 atmospheres absolute pressure and that this may occur as a result of a nuclear incident caused by a 2 per cent step increase in reactivity. The present study has investigated the possibility of ejection of a fuel element from the core or the buckling of a fuel element hanger rod as a result of local pressure increases; that is, sudden release of fuel vapor pressure upon rupture of a fuel jacket after a power surge. The results indicate that fuel vaporization cannot result in lifting of the fuel element from its seat in the top shield, but may result in buckling of the fuel hanger rod, jamming the fuel element in the upper sodium pool.

II. NUCLEAR PARAMETERS OF SODIUM GRAPHITE LATTICES

(W. W. Brown, W. J. Houghton, and R. A. Laubenstein)

A. INTRODUCTION

Analysis of the measured neutron distributions in exponential assemblies similar in structure to the cores of proposed sodium-graphite power reactors is continuing. The lattices consist of fuel elements inserted vertically into a stack of graphite 60 inches high. Elements can be spaced at 7, 9.5, and 12 inches in assemblies that are 42, 47.5 and 48 inches square respectively. A 57 inch square assembly for the 9.5 inch spacing was also used. Measurements were made in lattices loaded with elements consisting of 2.9 inch dia aluminum castings containing the following types of fuel: four 1 inch rods of 0.90 weight per cent enriched uranium, and seven 0.75 inch rods of either natural or 2.78 per cent enrichment. Six rod elements were made from the seven rod clusters by replacing the central fuel rod with either graphite or aluminum. The various lattices studied, their buckling values, the average relative thermal neutron fluxes in the aluminum, graphite, and uranium in a cell, and some typical thermal flux distributions in a cell have been given in previous reports.[1,2,3,4] The present report deals with the calculations from these data of thermal utilization, resonance escape probability, and other associated lattice parameters.

B. THERMAL UTILIZATION

The thermal utilization, defined as the fraction of the thermal neutrons in a cell that are absorbed in uranium, is given by

$$F = \frac{\Sigma_U V_U \bar{\phi}_U}{\Sigma_U V_U \bar{\phi}_U + \Sigma_{Al} V_{Al} \bar{\phi}_{Al} + \Sigma_C V_C \bar{\phi}_C}$$

where Σ, V and $\bar{\phi}$ are macroscopic absorption cross section, volume, and average thermal neutron flux and the subscripts U, Al, and C refer to uranium, aluminum and carbon respectively. The measured average fluxes for each lattice are given in Table I of reference 3 for the 4-rod and natural 7-rod loadings, and in reference 4 for the 2.78 per cent enriched fuel elements of 6 and 7 rods. The thermal utilizations calculated for each type of loading are given in Fig. 1 as a function of

lattice spacing. Values for the 6 rod lattices are very little below those for the corresponding 7 rod lattices.

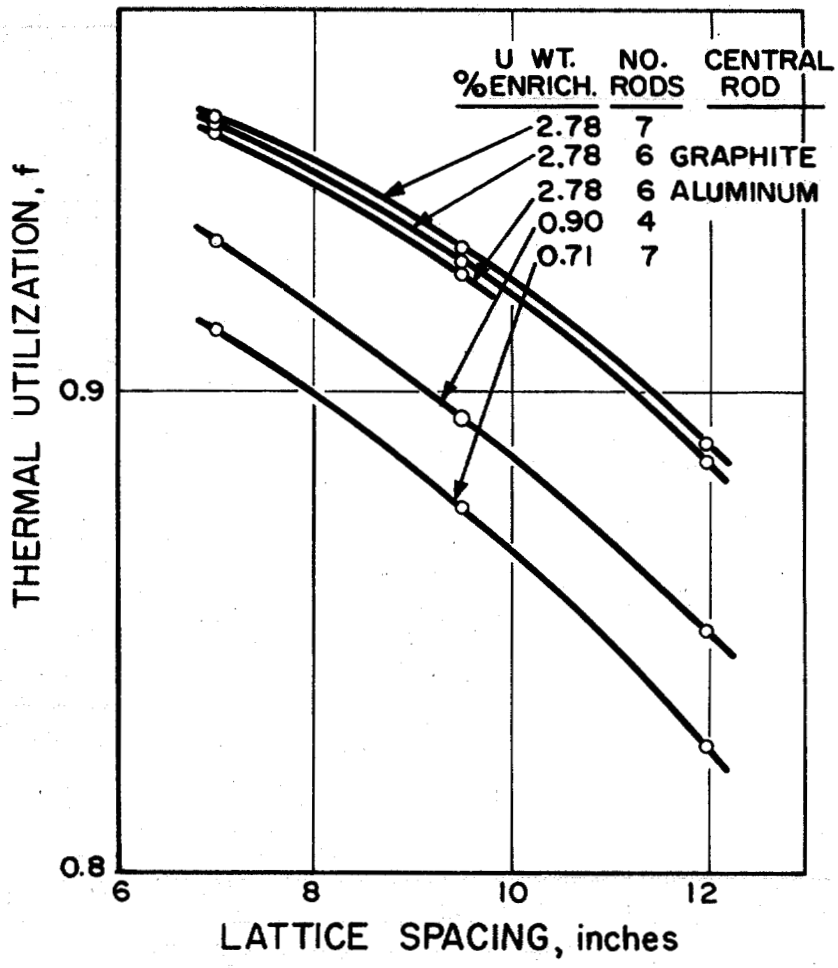

Fig. 1. Thermal Utilization in SGX Lattices

C. AVERAGE MACROSCOPIC CROSS SECTIONS

In a lattice the thermal neutron flux weighted average macroscopic absorption cross section is

$$\bar{\Sigma}_a = \frac{\Sigma_U \, V_U \, \bar{\phi}_U + \Sigma_{Al} \, V_{Al} + \bar{\phi}_{Al} + \Sigma_C \, V_C \, \bar{\phi}_C}{V_U \, \bar{\phi}_U + V_{Al} \, \bar{\phi}_{Al} + V_C \, \bar{\phi}_C}$$

where the Σ's are the Maxwell distribution average absorption cross sections of the materials indicated by the subscripts. The average transport cross section,

$\bar{\Sigma}_{tr}$, is given by a similar expression in which the Σ's are the transport cross sections of the materials. The values of these cross sections for each type of fuel loading is given as a function of lattice spacing in Fig. 2 and 3.

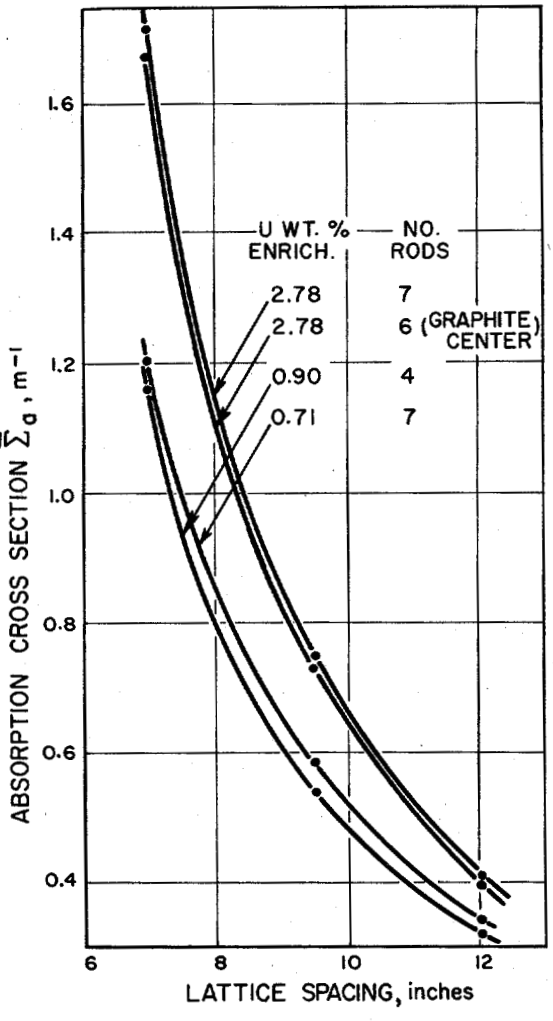

Fig. 2. Thermal Flux Weighted Average Absorption Cross Section of SGX Lattices

D. THERMAL DIFFUSION LENGTH

The thermal diffusion length, L, for a lattice can be obtained from the approximate expression[5]

$$L^2 = \frac{\sqrt{T}}{3\bar{\Sigma}_a \bar{\Sigma}_{tr} \sqrt{T_o}}$$

where T is the absolute temperature of the thermal neutrons in the lattice and T_o the temperature at which the cross sections have been evaluated, 293° K.

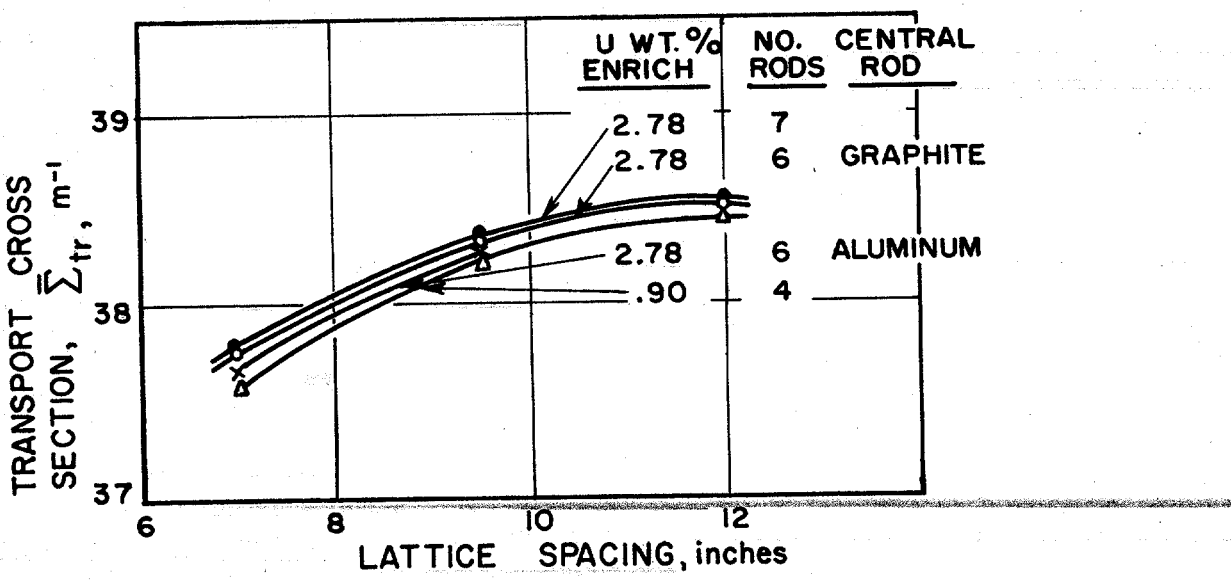

Fig. 3. Thermal Flux Weighted Average Transport Cross Section of SGX Lattices

The temperature has not been measured for these lattices but may be calculated from the expression[6]

$$T = T_o \left(1 + 1.20 \frac{\bar{\Sigma}_a}{0.8862\ \xi\ \Sigma_s}\right)$$

The factor 0.8862 is to convert the Maxwell averaged cross section Σ_a to the monokinetic value at 293° K. Σ_s and ξ are the macroscopic scattering cross section and average logarithmic energy decrement per collision respectively for the moderator. For graphite the values are 0.411 cm^{-1} and 0.158. The calculated relative temperatures $\frac{T}{T_o}$ are given in Fig. 4 and the values of L^2 obtained by using these temperatures in Fig. 5.

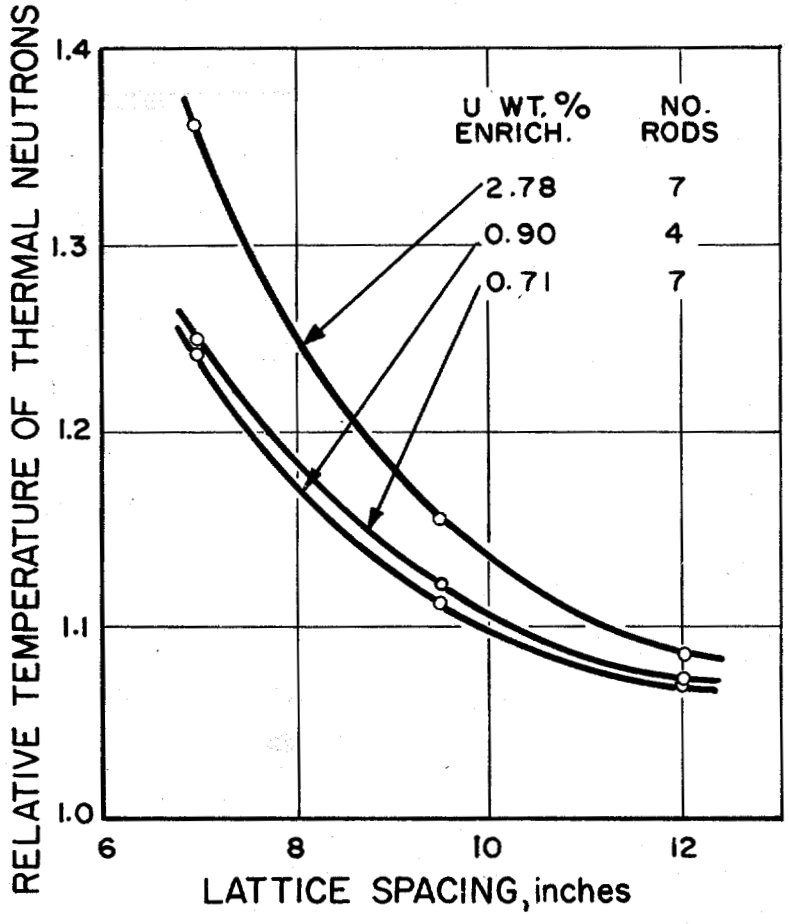

Fig. 4. Relative Temperature of Thermal Neutrons in SGX (Calculated)

E. NEUTRON AGE, FAST EFFECT, NEUTRONS PRODUCED PER ABSORPTION IN FUEL AND RESONANCE ESCAPE PROBABILITY

An approximate formula for the neutron age from fission to thermal energy in a lattice is given by[7]

$$\tau = 311 \left(1-0.289 \frac{\sigma_{in}}{\sigma_t} P + 0.048 \ln \frac{1043}{T}\right) \left(\frac{\rho}{\rho}\right)^2 \cdot \frac{V_{cell}}{V_{cell} - V_{Al}} \cdot \frac{V_{cell}}{V_C}$$

where σ_{in} and σ_t are the inelastic and total fast cross sections of uranium (1.85 and 7.10 barns respectively), and ρ and ρ_o are the measured and standard densities of AGOT graphite (ρ_o = 1.60 g cm^{-3}). P is the first collision probability in

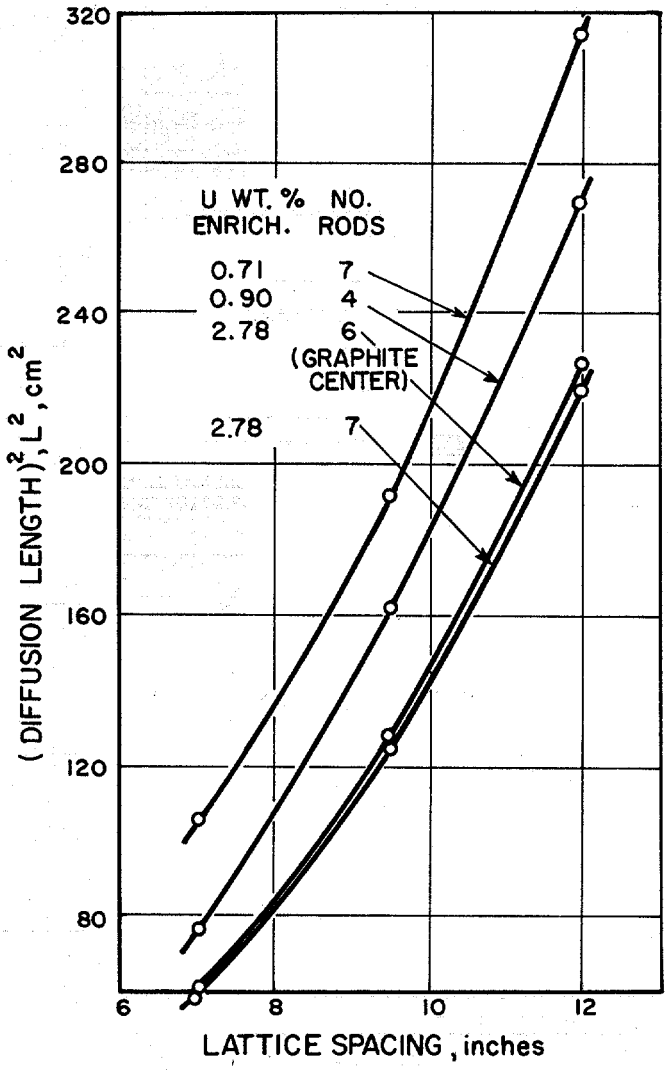

Fig. 5. Square of Diffusion Length in SGX Lattices

the fuel and has been calculated by J. E. Garvey[8] for solid and hollow cylinders. For the present calculation the 4, 6, and 7 rod elements have been approximated by hollow cylinders, following the model used by F. L. Fillmore.[9] The calculated ages are presented graphically in Fig. 6.

In terms of the first collision probability, P, the fast fission factor, ϵ, is given by[10]

$$\epsilon = 1 + \frac{0.04645P}{1 - 0.7861P}$$

Values of η, the number of neutrons per absorption in fuel were taken to be those calculated by E. R. Cohen[7] as a function of neutron temperature and fuel enrichment

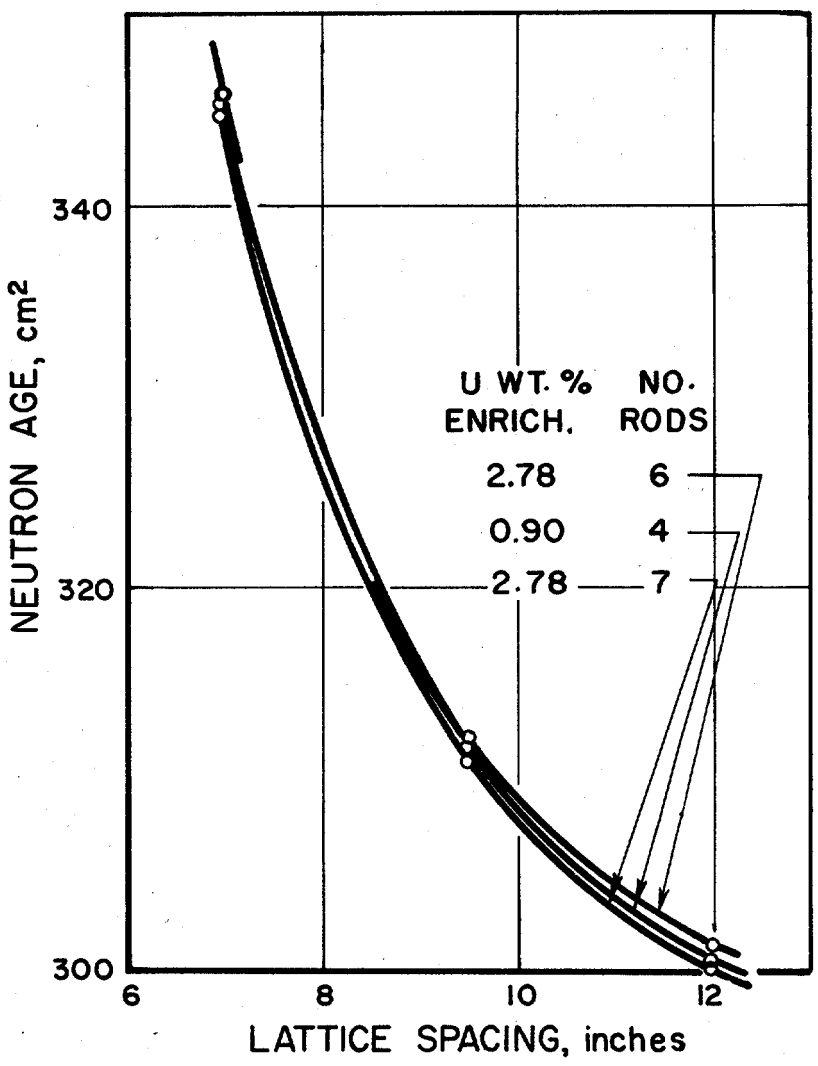

Fig. 6. Neutron Age in SGX Lattices (Calculated)

The measured bucklings, B^2, have been given in previous reports.[2, 3, 4] From the values of f, L, τ, ϵ, η, and B^2 for the lattices, the resonance escape probability p can be calculated from

$$p = \frac{(1 - B^2L^2)\ e^{B^2\tau}}{\eta\ \epsilon\ f}$$

Figure 7 shows the values of p that have been obtained for the lattices studies.

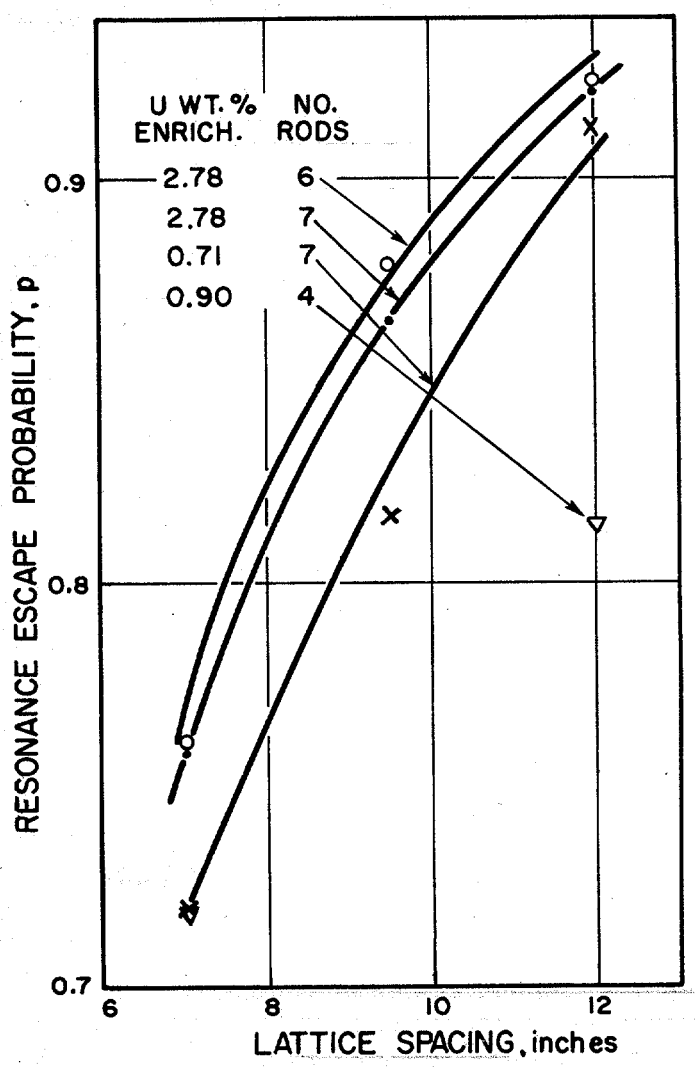

Fig. 7. Resonance Escape Probability in SGX Lattices

III. DEVELOPMENT OF HOT CELL FACILITIES AND HANDLING TECHNIQUES

(J. M. Davis)

During the period the SRE hot cell mockup and equipment development facilities have been set up and operated. The installation includes wooden cell mockup, overhead crane for the main cell, a small array of machine and hand tools, a mobile floor crane for manipulator handling and general utility, and the Master-Slave manipulators.

Several problems are currently being developed:

a. Equipment setup for opening and examining NAA 15A which will be irradiated at MTR (25 per cent complete)
b. Equipment for disassembling SRE fuel clusters (10 per cent complete)
c. Equipment for sectioning fuel slugs for specimen mounting (75 per cent complete)
d. Equipment for mounting and polishing metallurgical specimens (10 per cent complete).

IV. METALLURGY OF SGR FUELS

(B. R. Hayward, L. E. Wilkinson, G. G. Bentle and J. Walter)

A. MACROSTRUCTURE OF MAIN SRE FUEL

The alpha rolled beta treated 0.750 in. dia main fuel slugs for the SRE have a radial columnar structure as a result of a Hanford type heat treatment. The effect of this structure on reactor performance is not known. A few six inch long slugs were cut into one inch lengths for thermal cycling tests. The test specimens were cycled up to 500 times between 100° and 500° C at the rate of two cycles per hour. Results are shown in Table I.

TABLE I

PARAMETERS OF THERMAL CYCLED ONE INCH TEST SLUGS

Sample #	No. Cycles	Max. $\Delta\ell$ in	Max. $\Delta\ell$ %	Max. Δd in	Max. Δd%	Surface Condition
7222-2C	272	+.011	+1.2	-0.001	-0.13	wrinkled
9421-22E	272	+.013	+1.4	-0.003	-0.4	wrinkled
7222-2A	500	+.019	+1.9	-0.001	-0.13	wrinkled
7222-2F	500	+.021	+2.2	-0.000	--	wrinkled

The wrinkled condition of both the lateral and end surfaces exaggerate to a large extent the magnitude of the dimensional changes. Previously cycled specimens of alpha rolled unheat treated uranium indicated a length increase of 15-20 per cent as compared to the above specimens.

Attempts to simulate this columnar structure by heat treatment of other alpha rolled uranium have been unsuccessful. Samples of the columnar structure material were also annealed at 625° C for thirty minutes and sixty minutes, respectively. The amount of columnar area was somewhat reduced by this treatment but the effect was still strong.

X-ray patterns using the back reflection technique were taken at various radial areas within representative columnar structured slugs. Preliminary results indicate some preferred orientation in all areas of the slug. The outer radial areas indicated a higher degree of preferred orientation than the central area. This is probably indicative of the columnar structure.

B. GAMMA GRAPHING OF MAIN SRE FUEL

Continued evaluation for pre-irradiation data on the main SRE fuel slugs has included the non-destructive internal examination of 48 slugs. Some slugs contained known surface and end defects in the form of light and heavy seams and end cracks. A gamma graphing technique was used. The apparatus included a one curie radium source with X-ray film (Kodak Blue Brand) at a four foot exposure length using a mercury mask. Each slug was exposed for two 16 hour periods of 90° rotation. This technique does not indicate any internal flaws less than approximately 0.020 in. dia. The slugs without surface defects and with light seams showed no indication of internal flaws. Some of the heavy seams were indicated. All of the end cracks were clearly observed.

These same slugs will be carefully examined after reactor use and the effects of these known defects will be determined. The results of this overall data will enable more realistic specifications to be written for uranium slugs operating at high temperatures.

C. MTR IRRADIATION OF SRE FUEL MATERIALS

The initial capsule test in this program was discharged after only one MTR cycle. The failure to reach temperature has been resolved to be a result of both

a low neutron flux and errors in calculation. A redesigned capsule, using a multiple layer wall to reduce the thermal stress, has been evaluated and assembly will start after the approval of the MTR Safeguard Committee.

An additional part of this includes a simple flux monitoring device. This apparatus is designed to simulate neutron absorption properties of the main assembly containing the enriched fuel samples. By insertion just prior to the use of the fuel assembly, the flux monitor will indicate the flux level in that area. Potentially the problem of uncertain flux areas will be reduced. The measurements will also verify the calculations. Actually the flux will vary within a given area as a result of the surrounding experiments. It is thus important to study the MTR experiment schedule to obtain a reasonably consistent flux.

The flux monitoring capsule consists of a single nickel tube containing an inner liner of aluminum. Within the aluminum liner are six lead-boron compacts which simulate the actual fuel samples. Cobalt-aluminum monitoring wires will be placed on the outside nickel tube and at the surface and center of each of the lead-boron compacts.

D. EVALUATION OF EXPERIMENTAL CAST URANIUM ALLOY FUEL SLUGS

One of the primary purposes of ths sodium graphite experiment is to develop inexpensive fuel elements for long life at high temperatures. A promising technique is centrifugal casting. The alloys of interest include U-Zr (2 w/o Zr), U-Mo (1.2 w/o Mo), and U-Si (0.5 w/o Si). Fernald has developed a casting machine for production of test quantities of these alloy slugs (0.750 in. by 6 in.) for the SRE experimental fuel program. To date, development batches of alloys have been made and examined. The main variables studied include pouring temperature and mold speed. Twenty slugs of each alloy were studied at high and low pour temperatures and high and low mold rpm. Each slug was checked for dimensions. All slugs were gamma graphed for internal flaws. Representative slugs were also sectioned and examined both chemically and metallographically. Other slugs were machined to size and thermal cycled for dimensional stability. There were relatively small variations in the general quality of all of the alloy slugs. The following general characteristics were observed (1) Low mold speed and high pouring temperature give the best surface. (2) High mold speed and low pouring temperature give the highest density. (3) All slugs were slightly warped. (4) There is less internal porosity at low pouring temperature and high mold speed.

(5) The U-Si alloys had more surface defects than the other alloys. (6) All alloys showed good homogeneity of alloy content and metallurgical structure. (7) Representative slugs of all of the alloys were thermal cycled between 100° and 500° C. All slugs showed dimensional changes of less than 0.2 per cent in length with no observed change in the surface appearance.

This particular series of slugs were cast 0.030 in. oversize (0.780 in.). Several slugs of each alloy were machined to the SRE slug size tolerances. Refinements in the fabricating procedures are currently in progress to cast the slugs to the stated tolerances. With satisfactory performance of these designs the feasibility work on this program will be completed.

V. METALLURGY OF BREEDER FUELS

(B. R. Hayward and G. G. Bentle)

Larger diameter thorium feed material for the induction melting of thorium-uranium alloys was furnished to a supplier by National Lead Company. Improved melting procedures have been used in which the BeO melting crucible is replaced by $MgZrO_2$ coated graphite crucible. A bottom pour stopper rod technique also provides better melt control than the previous self pouring method. The coated graphite melting crucible causes an increase in the carbon content from the range of 100-150 ppm in the original thorium to 500-600 ppm. Since carbon is a high temperature strengthening element in thorium this may improve the high temperature strength of the alloy. Samples produced to date do not indicate that the increased carbon makes the extrusion and swaging operations more difficult.

In Fig. 8 is shown the results of microscopic examination of the extruded Th-U (5.4% U) alloy. The samples were mechanically polished and cathodically etched. This method of sample preparation does not indicate grain structure or delineate the phases which are present. The samples were taken from the front, middle, and back section of the extruded rod. Chemical analyses on these samples for uranium content indicate some small amount of segregation. However, there are discrepancies in analytical results between the laboratories at Nuclear Metals and Atomics International. The front of the extruded rod represents the bottom of the cast ingot. The photomicrographs illustrate the large quantity of inclusions present which tend to form in stringers and create some voids. The material

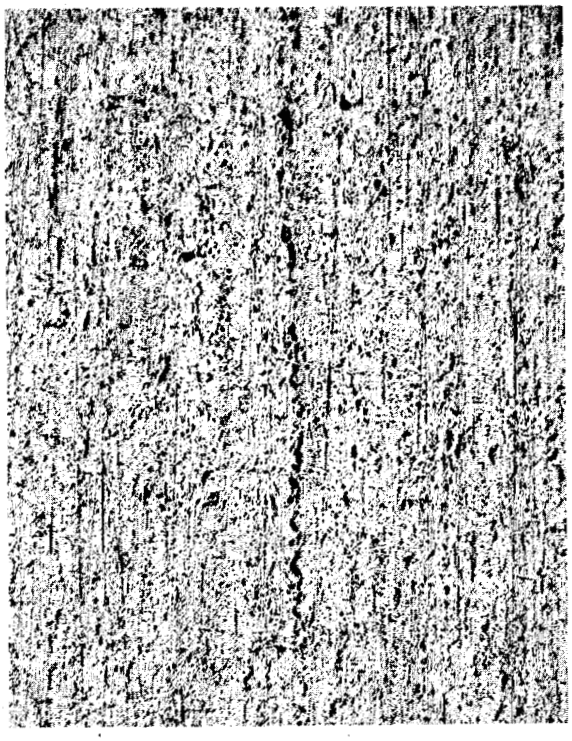

78-1A Longitudinal section-center First section from first slug, fewest oxides, most dark precipitate 50X

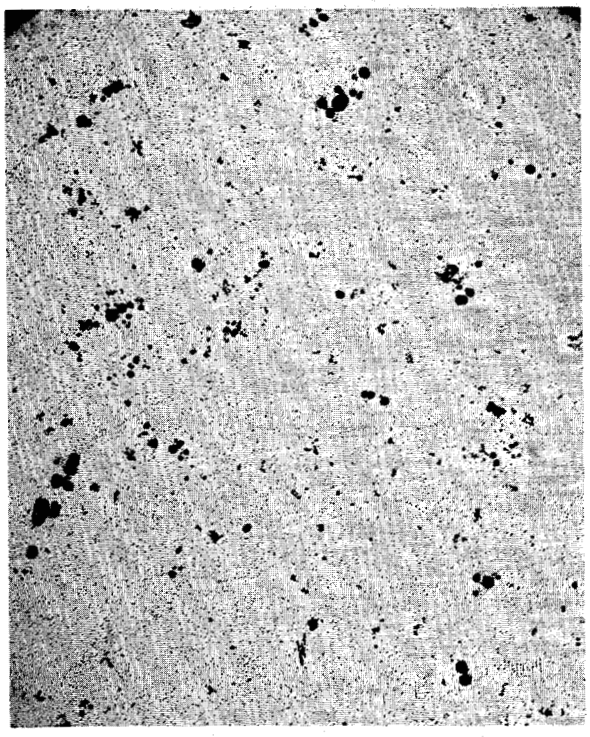

78-1C Cross section-center Middle section from first slug 100X

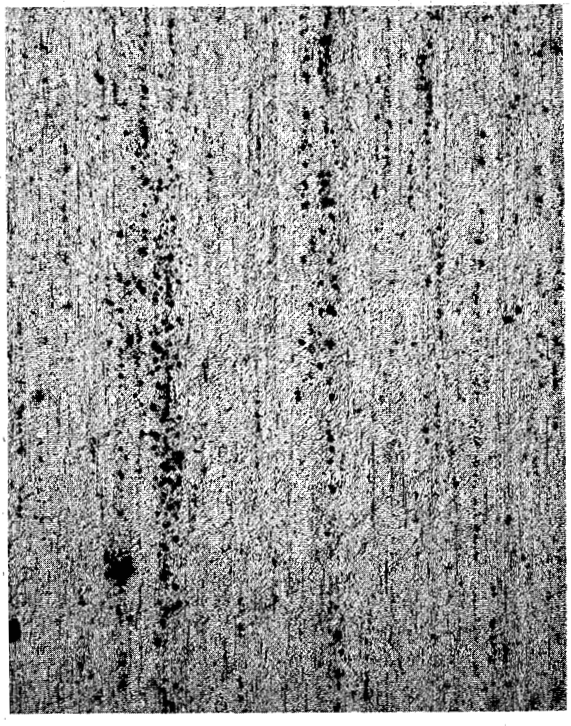

78-3A Longitudinal section. First section of third slug. Spherical oxides strung out in direction of extrusion 50X

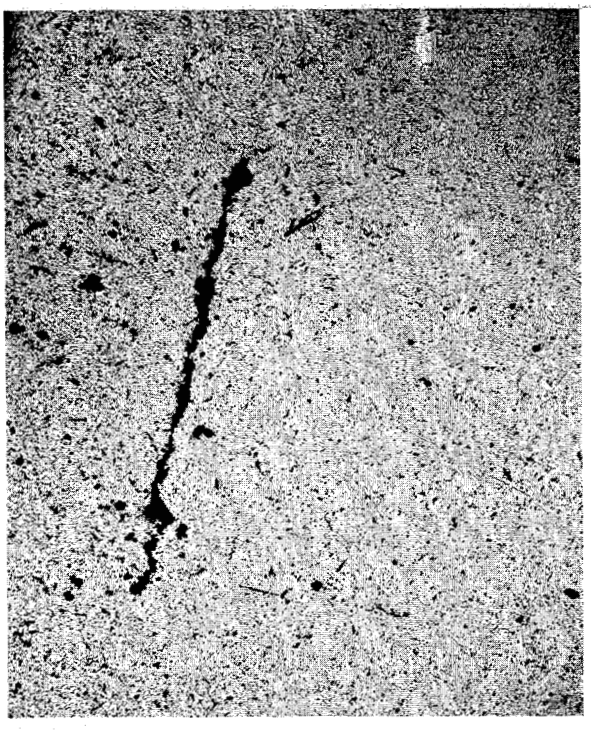

78-3C Cross section-edge. Middle section of third slug showing void area near surface 100X

Fig. 8. Microstructures of Th-5.4% U Extruded Rod

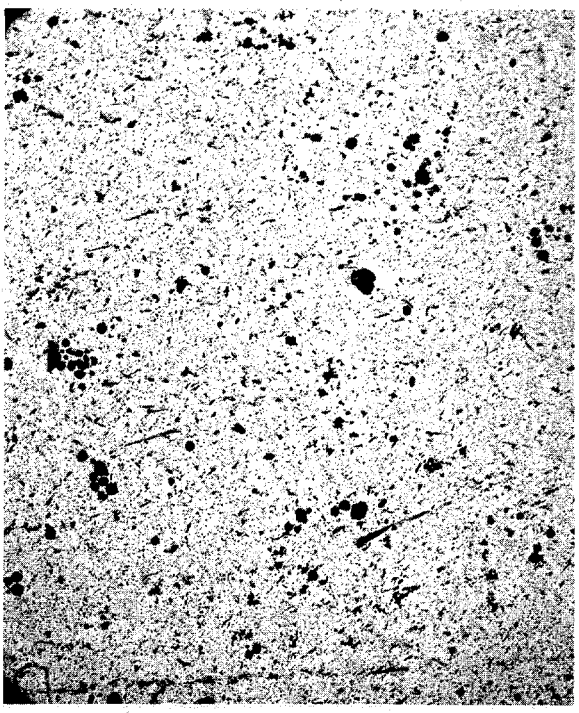

78-10C Cross section-center
Middle section of slug from center of rod, spherical oxides concentrated in center of slug 100X

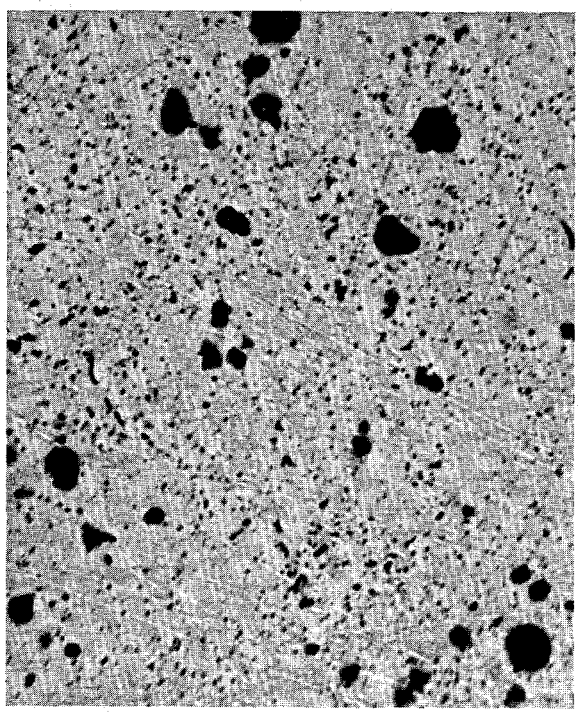

78-20C Cross section-center
Middle section of the end slug in the rod. - Fine black precipitate and large spherical oxides, 500X

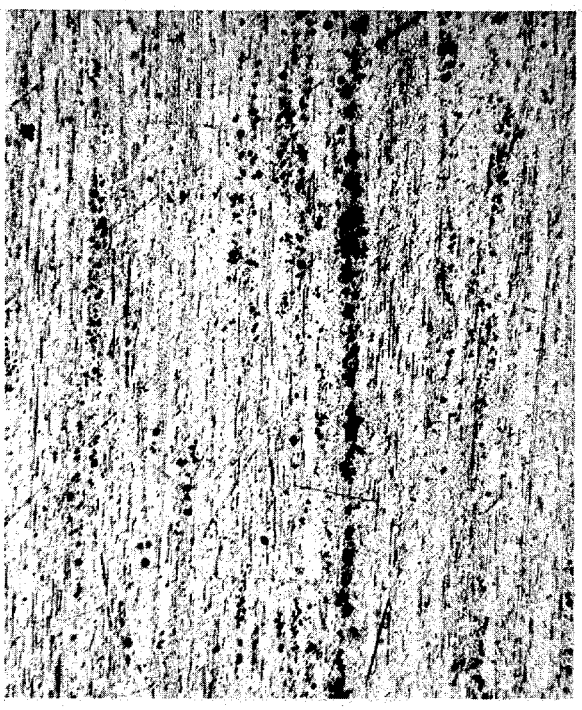

28-20F Transverse section
End section of last slug in rod
Many strung out oxides and void areas strung out with the oxides 50X

Average Hardness
KHN = 167
No constant variation between center and edge

Rockwell A = 39→40

UNCLASSIFIED

near the front of the extruded rod shows fewer inclusions and a larger quantity of an unknown dark precipitate type material than the middle or back sections. The form in which the uranium is present is not known.

VI. ENGINEERING EVALUATION OF GRAPHITE

(R. L. Carter, W. J. Greening, W. K. McCarty, and H. Taketani)

The improved equipment for thermal outgassing measurements on graphite test samples has been fabricated and is being assembled. This apparatus is equipped with a sample holder permitting quick change of test specimens, and with wide-range pressure gauges permitting accurate measurement of integrated volume of gas evolved from samples. Utilities for the apparatus are being installed and Quality Control personnel are being instructed in the principles of its operation. Initially the apparatus will be used to provide a survey of gas content of graphite being used in the SRE.

Specific problems to be encountered in the maintenance of proper pressure within SRE special moderator elements and special corner channel dummies have been considered in detail. It is not feasible to provide external ballast volumes to prevent large pressure excursions within the special moderator elements during core temperature changes. A more attractive alternative is to permit their unattended operation by means of a return duct through the top shield to the gas volume above the sodium plenum.

Length changes in standardized samples of TSP graphite have been measured during heating under sodium containing small quantities of potassium. It was established that addition of one per cent potassium to commercial sodium results in an alloy which attacks graphite, and causes it to spall and crack severely. On the other hand, heating under sodium purged of potassium by prior digestion with graphite led to approximately the same degree of attack (1.0 + 0.1 per cent in linear dilation) as that experienced under untreated commercial sodium. Figure 9 shows the relative linear expansion measured by means of a nickel dilatometer. Potassium content of the commercial sodium ~~used~~ was 1200 ppm while the purified sodium was found ~~by analysis~~ to contain around 480 ppm potassium. ~~It is noted that~~ this degree of purification is substantially below the 30 ppm potassium content reported achievable by this purification process in the literature. Nevertheless,

→ How else? By guess-work?

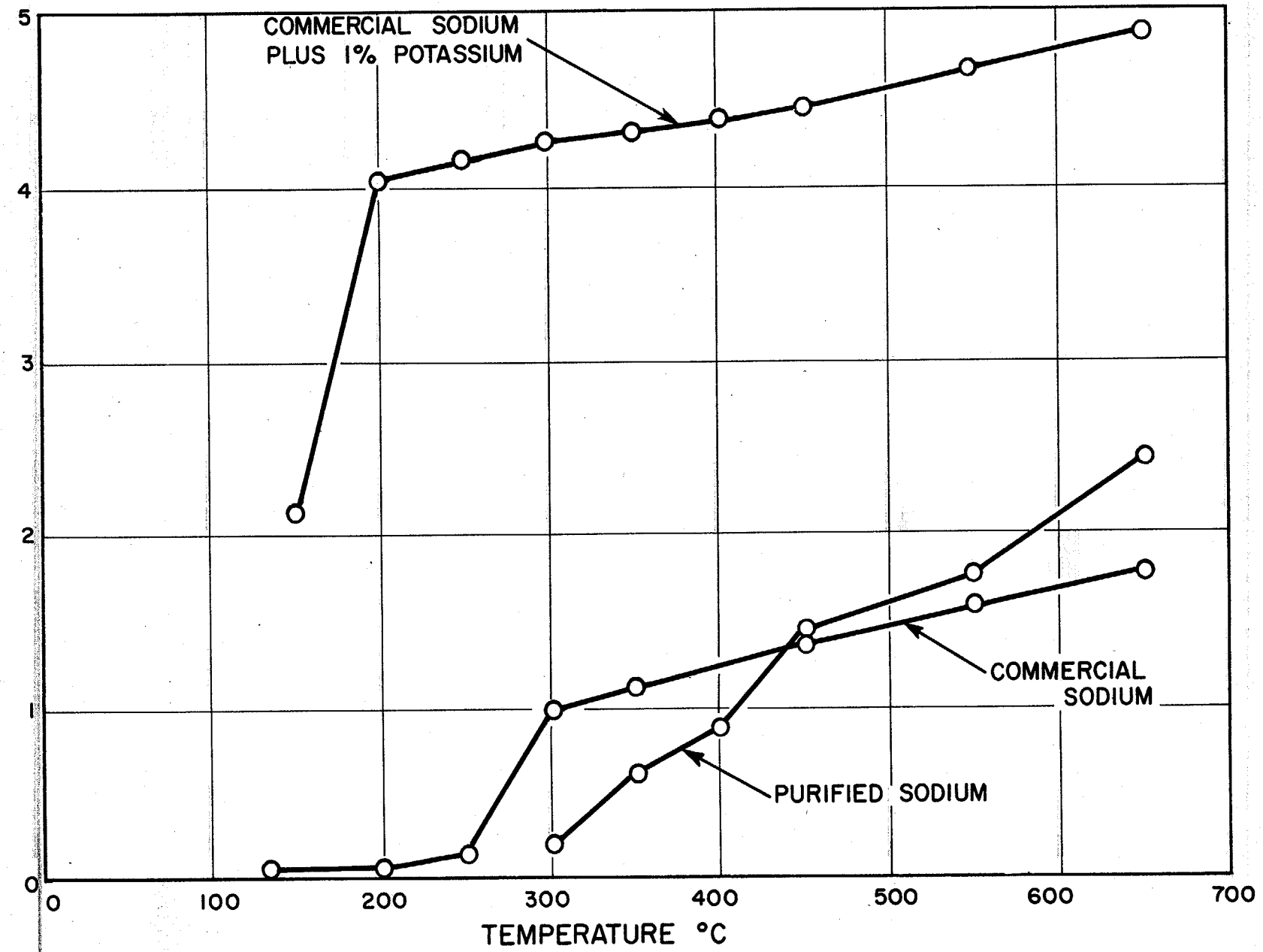

Fig. 9. Sodium Expansion of Graphite

from the lack of functional dependence between potassium concentration and degree of expansion of low concentrations, it can be concluded that a mechanism exists leading to a saturating reaction between pure sodium and TSP graphite at temperatures of 500° F and above. This results in physical expansion, but not disintegration of artificial graphite.

Samples of high density graphite obtained from National Carbon Company and from Great Lakes Carbon Company, with accurately determined physical dimensions, have been subjected to MTR irradiation of approximately 5×10^{19} nvt at temperatures above 300° C. The possible applicability of dense graphite in nuclear reactors at elevated temperatures depends upon verification of a stability equivalent to that found for standard grades now in use. The samples being tested have cooled radioactively and an apparatus has been built to collect gases evolved during irradiation and trapped in the stainless steel containers surrounding the samples. The first 5 samples have been opened, the quantity of gas evolved measured, and gas samples obtained for chemical analysis. Determination of length changes will be made after decanning is complete.

Tests which were initiated to determine the magnitude of abrasion characteristics of graphite in a dry atmosphere continue to show instead its excellent lubricative properties at high temperatures. Dew point of the desiccated helium atmosphere over the graphite-steel test bearing was determined to be -125° F. In all cases the bearings were observed to wear in, with a 50 per cent drop in torque after about a thousand cycles. Measurements of the wear of the graphite bearing pieces after conclusion of 1100° F wear tests are given in Table II.

TABLE II

MEASUREMENTS OF WEAR OF GRAPHITE REARING PIECES

Type Graphite	Preferred Orientation Crystalline C-Axis relative to contact plane	Bearing Load PSI	Cycles 180°/cy	Wear Rate In./cy x 10^{-8}
TSP	1	40	650,000	0.26
TSP	11	40	420,000	0.40
AUF	1	40	578,000	0.57
MYIA	unknown	59	122,000	1.2

It is seen that the lowest wear rate is experienced by the fine-grained highly purified TSP and, as would be expected, is lower for an orientation in which the crystals already tend to present favorable faces toward the wear plane. The similarly grained but unpurified AUF shows slightly greater wear, while the copper-aluminum impregnated MYIA is markedly inferior under these conditions.

VII. ZIRCONIUM BEHAVIOR IN LIQUID SODIUM

(G. G. Bentle, R. L. Carter, R. L. McKissen,
R. L. Eichelberger and R. B. Hinze)

In order to establish the dependence of oxygen transfer rate upon temperature of the sodium-zirconium interface, the NaZr I loop was operated at various different nominal temperatures. The cold trap maintained at all times at a temperature of 290 ± 10° F, insured that plugging indicators remained below this point. The corresponding oxygen solubility of 10 ppm was assumed to be the oxygen content of the sodium in the entire loop. Weighed zirconium samples were exposed for 200 hours or longer at temperatures of 1000° F, 925° F and 850° F. A summary of results is shown in Fig. 10. It is seen that essentially the same initial weight gain rates are experienced at 925° F as at 1000° F, but that a higher steady rate of oxidation is reached by the samples exposed at 1000° F. Presumably this effect is attributable to the higher rate of oxygen diffusion through the oxide layer into the parent metal at the higher temperature.

These data remain in radical disagreement with data obtained at KAPL showing weight gains under supposedly similar circumstances an order of magnitude lower. Continued investigations directed toward understanding of this discrepancy are discussed later.

It was determined that negligible weight gain was experienced during loop exposure at a zirconium-sodium interface temperature of 850° F. The points plotted in Fig. 10 actually show a slight measured loss in weight, believed attributable to mechanical removal of small quantities of oxide from the metal surface. These data indicate that oxidation of zirconium in cold-trapped liquid sodium can be kept to reasonable levels by limiting the sodium temperature to 850° F or below.

A static pot designed to reproduce more nearly KAPL experiments showing low contamination rates has been completed. In this device, subsequently referred

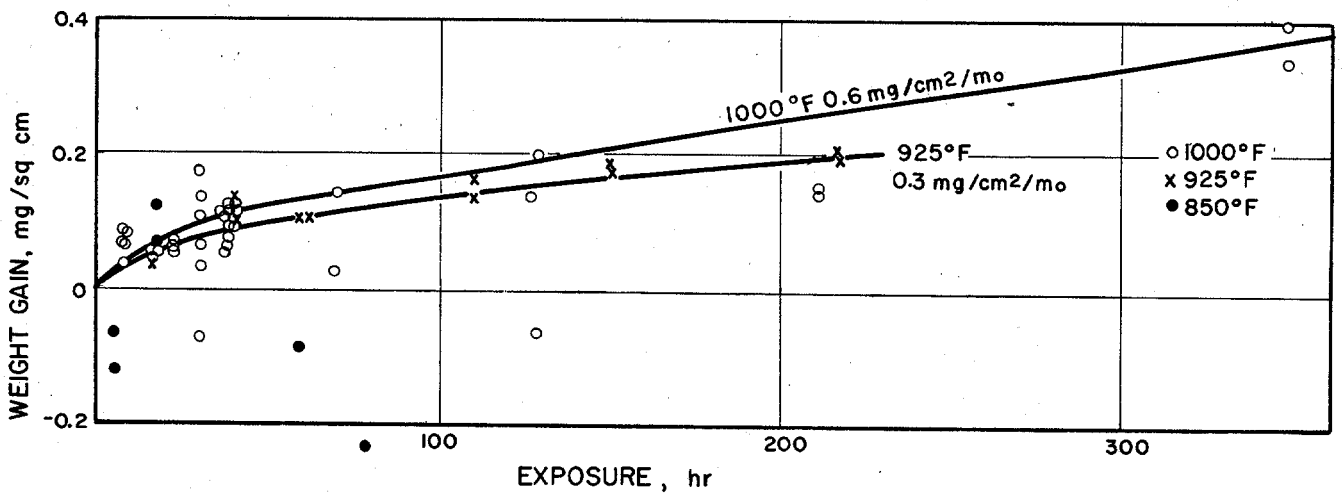

Fig. 10. Weight Gain in NaZr I

to as NaZr III, the oxygen content is supposedly maintained at the desired level by a cold trap which is connected to the bottom center of the pot. Thermal convection provides the only means of circulating the sodium by the cold trap connection at the bottom, by the heated outer circumference of the pot, and through the turret which carries the zirconium samples. As in the NaZr I loop, samples are changed by cooling the sodium to ~ 350° F, and reaching into the pot with a suitable grappling tool through a 2-in. valve. Diffusion of atmospheric gases into the pot is retarded by the rapid flow of inert gas (argon) used to cover the sodium out of a 6-in. length of 2-in. diameter pipe attached to the valve.

Zirconium samples exposed in the static pot show a higher weight gain than those exposed under similar conditions of temperature and sodium oxygen content in the NaZr loop.* It is observed from Fig. 11 that data obtained are extremely erratic, and it is difficult to obtain from them a reliable estimate as to the rate of weight gain after the oxide layer if formed.

*Subsequent to the period covered by this report, it was discovered that the controller used in this experiment was reading about 65° F low, and hence the curves plotted in Fig. 11 correspond to temperatures 65° F higher than stated. These reduce the magnitude of the discrepancy from results obtained in the NaZr I loop.

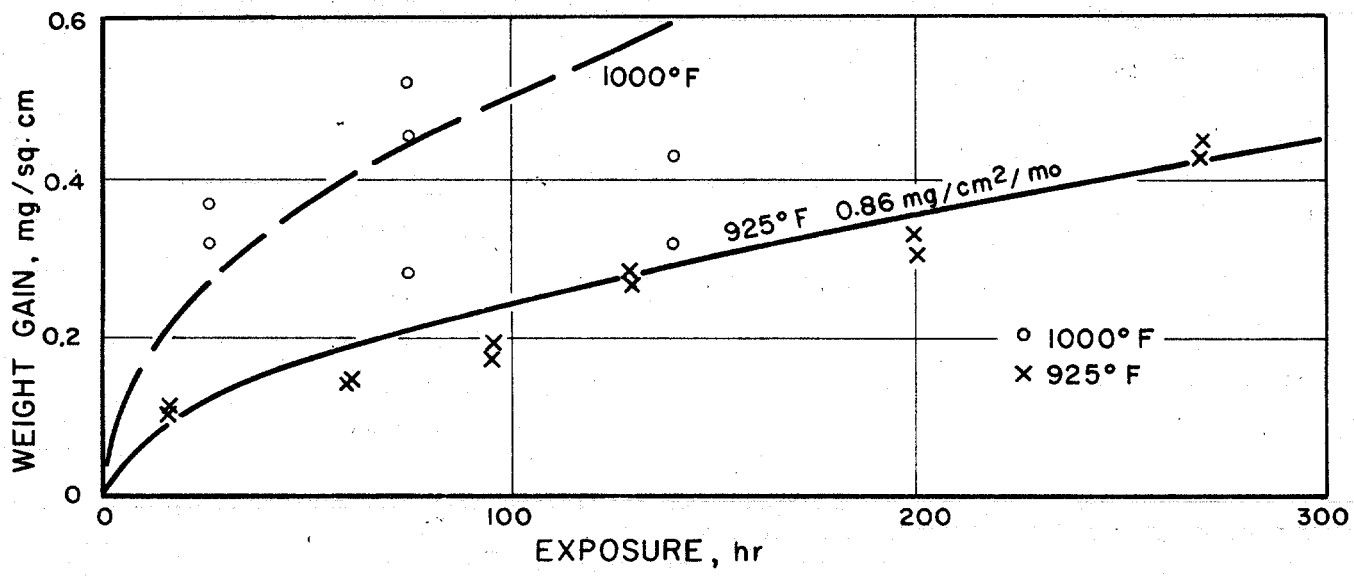

Fig. 11. Weight Gain in NaZr II

Several explanations for the elevated and erratic zirconium contamination rates have been advanced and are being investigated. The effect of introduction of a purging device to reduce the level of possible inert gas contamination will establish the contribution from this source. The possibility of contamination by atmospheric gases introduced during sample changing was eliminated through short term experiments both in NaZr I and NaZr III. These showed negligible short term pick-up by the zirconium during such an operation, and negligible change in plugging indicator reading immediately following it. Possible weight pick-up during the sample cleaning procedure was likewise eliminated as insignificant. Remaining to be evaluated as possible contributors to the erratic character of results are the temperature and convection inhomogeneities within the sample pot, and mechanical scaling of samples by the flowing sodium or by subsequent handling.

The second dynamic sodium loop, designated as NaZr II, has been completed. Sodium in this loop will be continuously purged of contaminants by flow through a

"hot trap" filled with turnings of Zr-Ti alloy. The loop was filled with sodium for a shake-down run, during which leaks were repaired and proper distribution of heaters was effected. This loop is scheduled for initiation of runs to determine the feasibility of the use of a hot trap to prevent contamination of zirconium in the immediate future.

Clean zirconium was found to self-weld under sodium at 1200° F. Two Zr bolts, one containing a sandwich of Zr and type 304 stainless steel washers which had bright surfaces and one containing a similar sandwich with unpolished surfaces were placed in a stainless steel capsule. Filtered sodium was added and the capsule sealed. After soaking for 30 days at 1200° F the samples were removed, cleaned and examined. The clean zirconium had self-welded, as seen in Fig. 12. The unpolished zirconium did not self-weld. Neither the polished nor the unpolished zirconium welded to the stainless steel. The washers were initially drawn into snug contact by a nut upon each bolt. Since the thermal expansion of stainless steel exceeds that of zirconium, the pressure applied between washers may be as high as the yield strength of zirconium at temperature, reduced by the ratio of appropriate cross sectional areas (approximately 1/3). Further experiments to fix more definitely the onset values of pressure and temperature leading to this effect are being undertaken.

M 559 Zr WASHERS POST Na

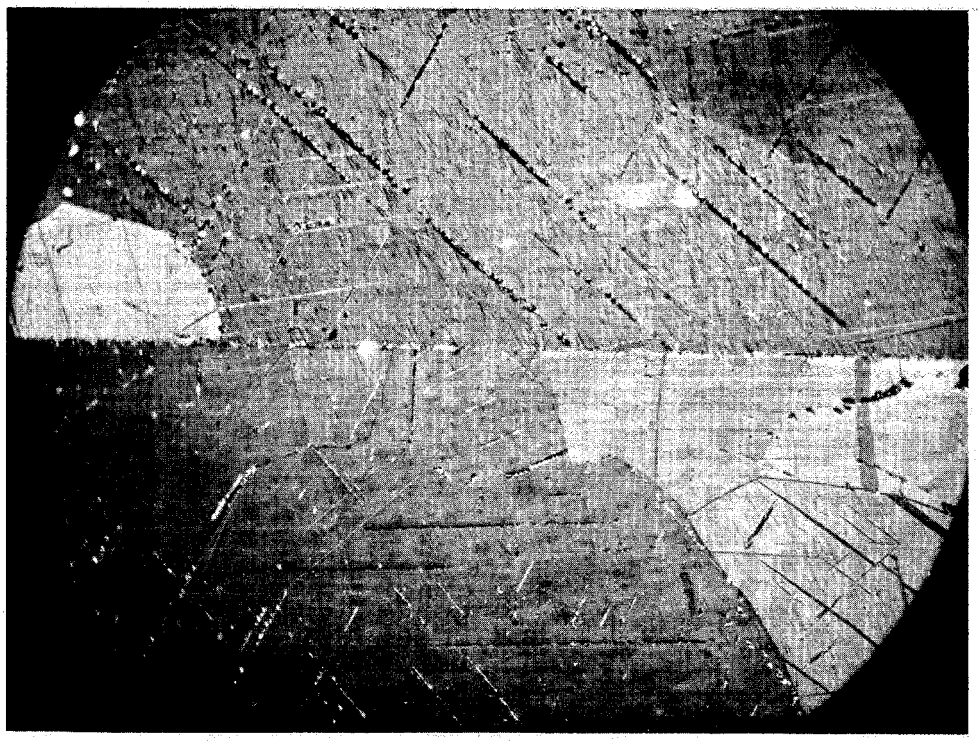

100 X PL

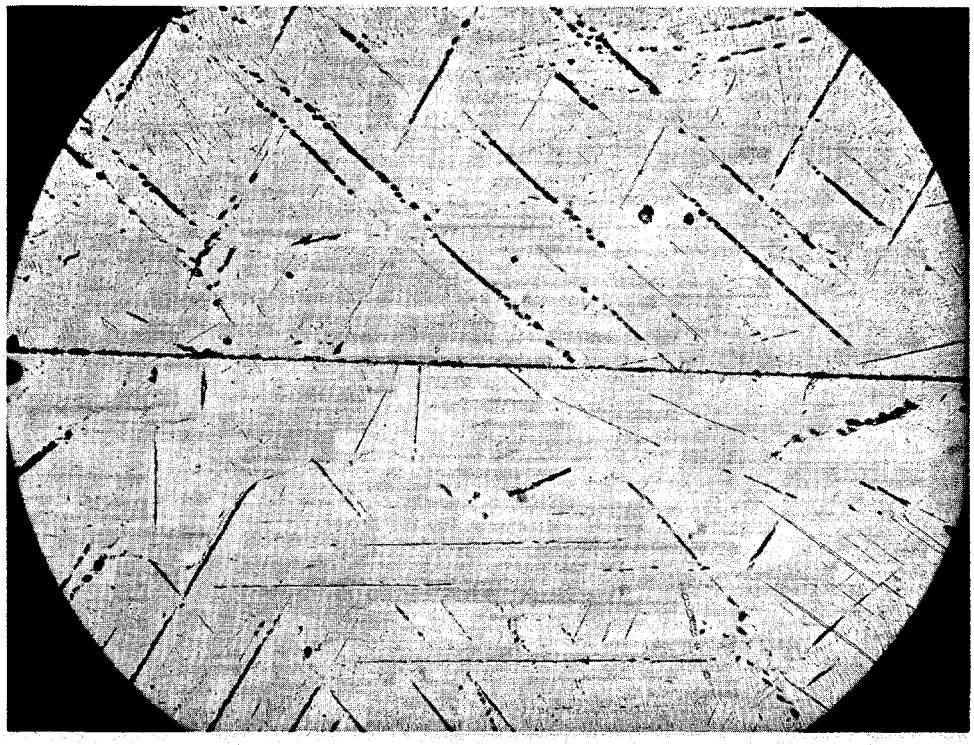

100 X BF

Fig. 12. Section of Welded Zr-Zr Interface

SECTION B
SODIUM REACTOR EXPERIMENT

VIII. NUCLEAR ENGINEERING AND PHYSICS

A. SYSTEMS ANALYSIS (H. Dieckamp, D. J. Cockeram and L. Blue

Analog computer studies of the SRE are being continued. Heat transfer in the core has been studied extensively with provisions for simulating the neutron kinetics and the negative temperature coefficient. Scram studies have been undertaken to determine the relative importance of subsequent measures in minimizing transients. These data are being evaluated in order to determine the need for special instrumentation and automatic action and the permissible time delays. Considerable work has been done to determine the relative control rod travel rates and rates of change of sodium flow required to give safe and convenient operation. Consideration is being given to incorporating the following features into the control system.

1. Coolant channel sodium outlet temperature thermocouples should have a minimum response time. This temperature will be a control indication of primary importance. The effect of thermocouple response time is shown for a representative transient in Fig. 13. T_c out is the actual coolant channel sodium outlet temperature. T'_c out is the above temperature as indicated by a thermocouple having a 5 sec response time. For comparison, T_p out, the outlet sodium temperature from the upper plenum, is shown.
2. The coolant channel sodium outlet temperature recorder should have an expanded scale.
3. Sodium pump boost rates should be decreased to the order of 10%/min. Because of the temperature coefficient of reactivity, sodium flow rate has a strong effect on reactivity. It seems undesirable for the control ability of sodium flow to overlap the control rates of the control rods. Sodium flow should be used to control temperatures and rods should be used to control power as a result of the response times associated

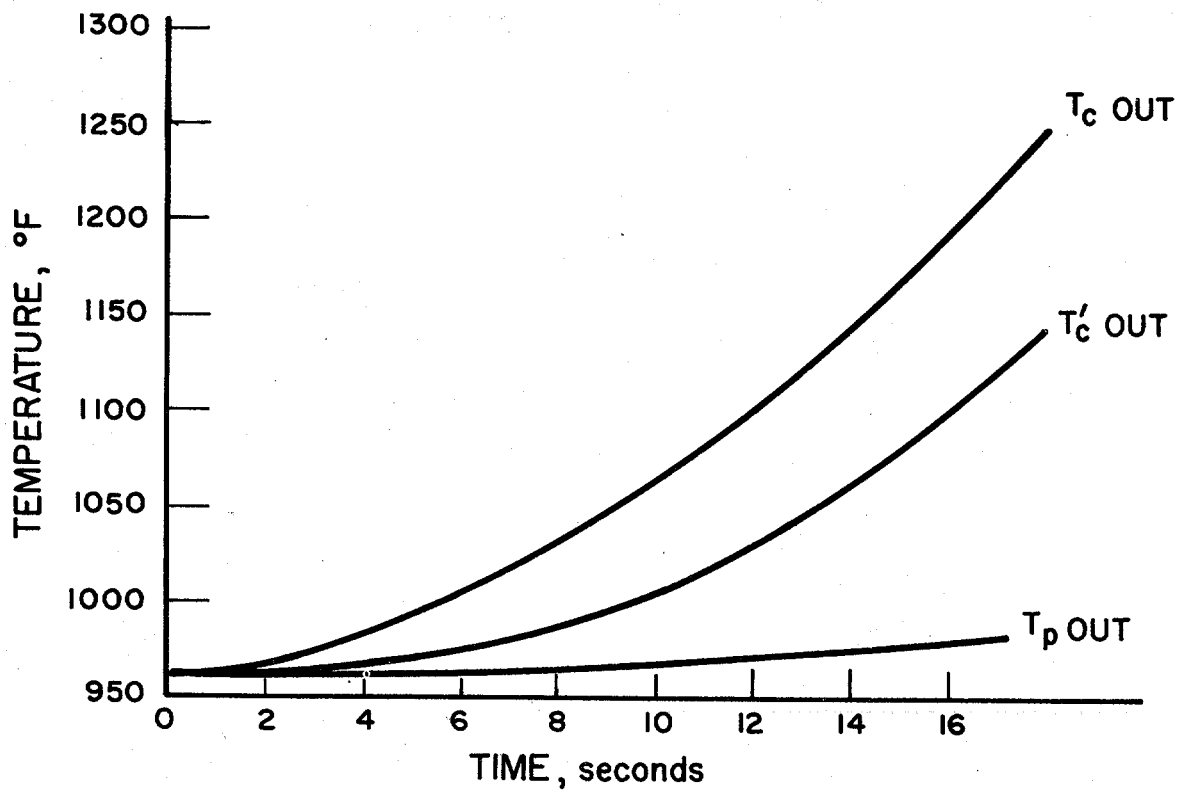

T_c OUT = COOLANT CHANNEL OUTLET SODIUM TEMP.

T'_c OUT = T_c OUT AS INDICATED BY THERMOCOUPLE WITH A 5 sec RESPONSE TIME

T_p OUT = REACTOR SODIUM OUTLET TEMPERATURE FROM UPPER PLENUM

Fig. 13. Effect of Thermocouple Response Time

with temperature and flux; rods should effect the faster control of the two. Figures 14 and 15 show the effects on coolant channel outlet sodium temperature and power caused by continuous rod motion and continuous change of pump speed.

4. Simultaneously interruption of reactor power and sodium flow to minimize transients. Figure 16 shows the outlet coolant channel sodium temperature as a function of time for scrams with different delay times between rods and pumps. Ten per cent negative reactivity is representative of the four safety rods and the 15 per cent final flow is a combination of the auxiliary system (5 per cent) and thermal convection (10 per cent). Actual reactor behavior may be somewhat different than Fig. 16. However, these curves are felt to be the best approximation possible at this time.

B. REACTOR PHYSICS (F. L. Fillmore)

Reactivity Studies and Flux Perturbations - The reactivity control by 1.5 per cent boron-nickel rods was valuated for the wet critical reactor condition. The values obtained are listed in Table III along with those previously obtained for the hot-poisoned case.

TABLE III

HOT-POISONED AND WET CRITICAL VALUATION OF 1.5 PER CENT BORON-NICKEL RODS

	Hot Poisoned	Wet
1 rod on axis	3.2 dollars	3.8 dollars
4 rods	10.6 dollars	12.9 dollars

The reactivity loss due to flooding the central moderator cell with sodium was found to be 1.3 dollars. The reactivity loss due to increasing the sodium layer between moderator cans by 0.1 in. was found to be 3.9 dollars.

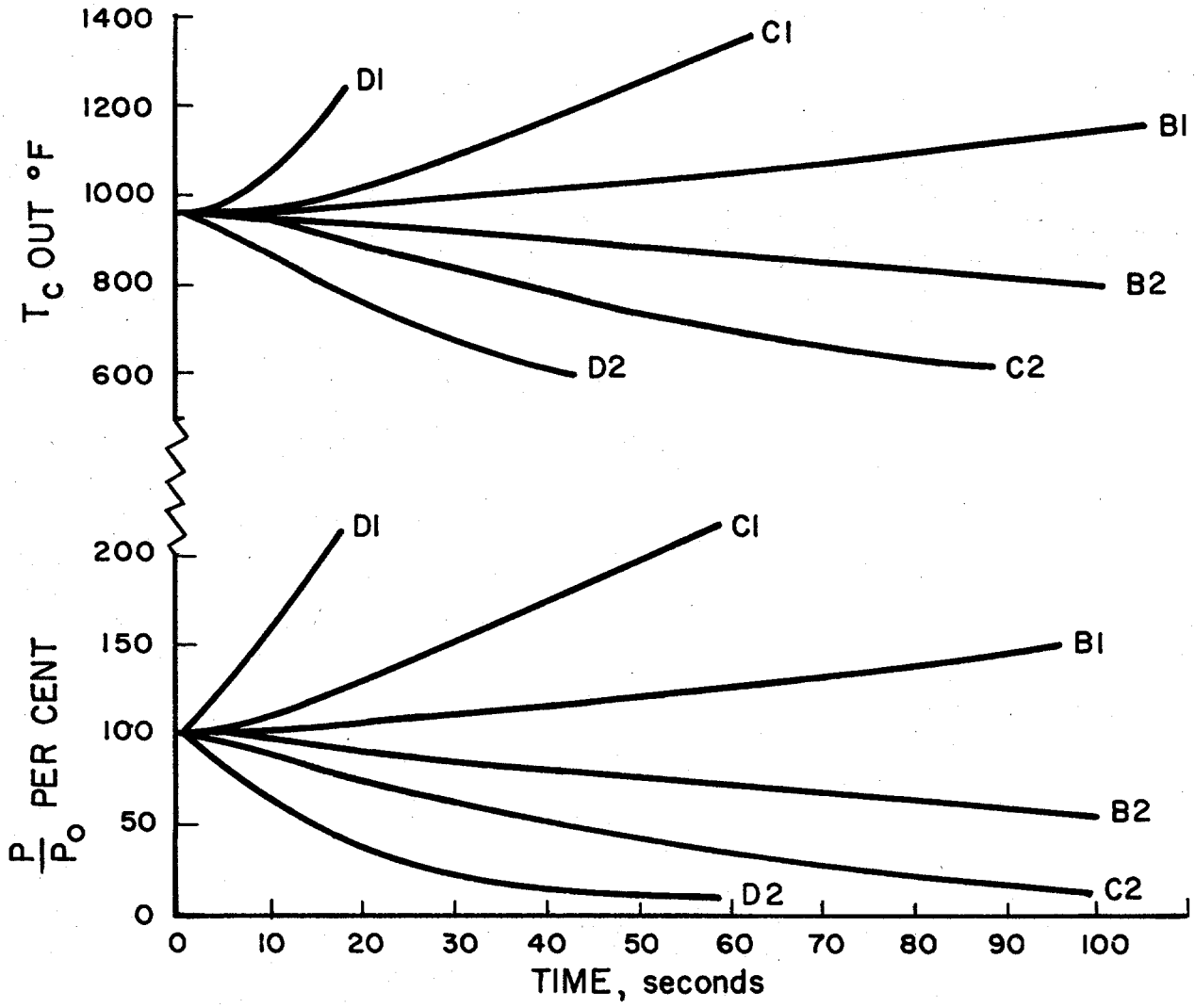

INITIAL CONDITIONS

100% FLOW
100% POWER
RATED TEMPERATURES

B - ONE ROD RATE (SHIM MOTION)
C - FOUR RODS GANGED (SHIM MOTION)
D - REGULATING ROD RATE
1 - WITHDRAWING
2 - INSERTING

Fig. 14. Effect of Rod Motion

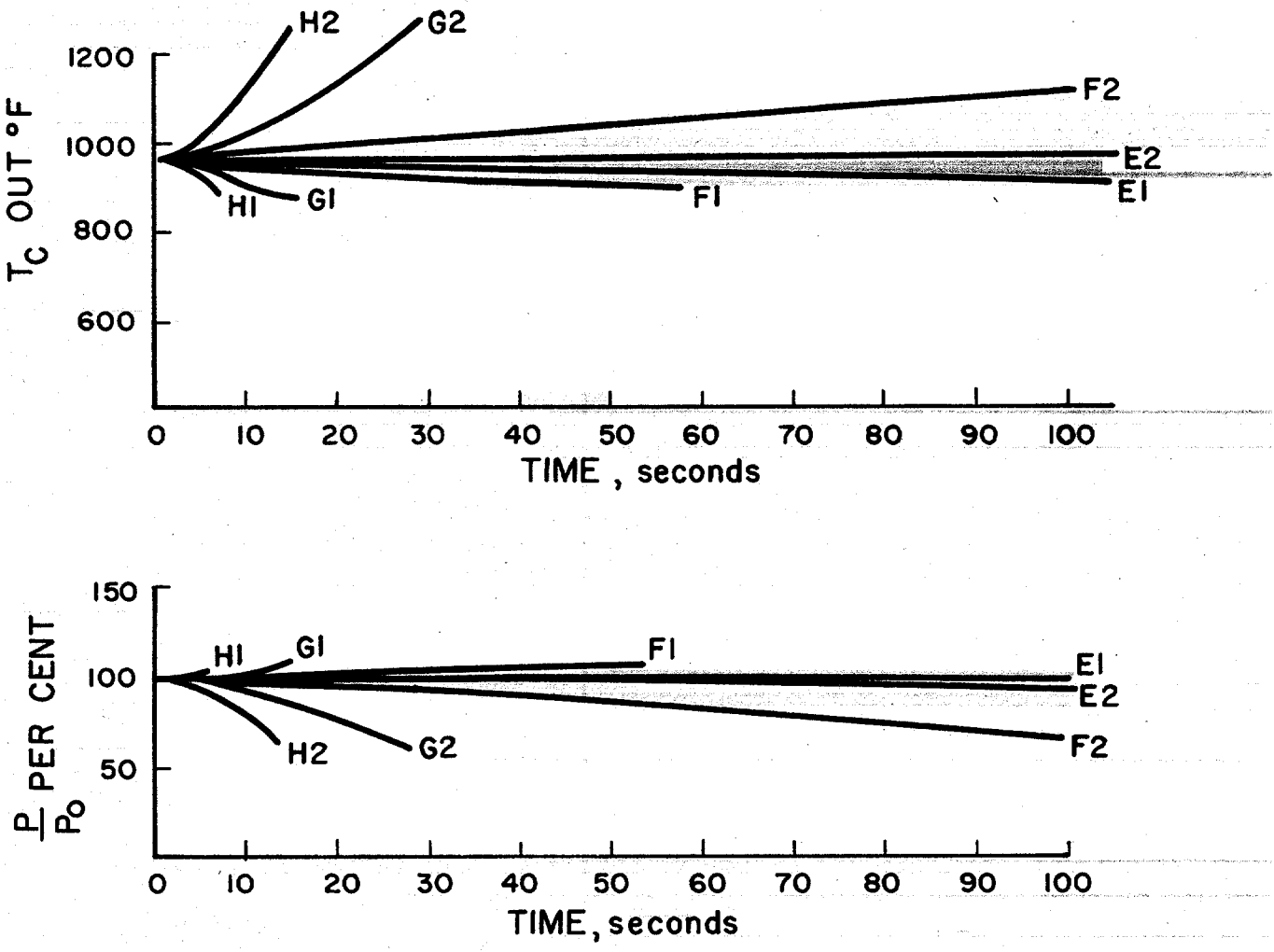

INITIAL CONDITIONS

100% FLOW
100% POWER
RATED TEMPERATURES

E -6% /min
F -30 "
G -167 " (DESIGN LOW RATE)
H -400 " (DESIGN HIGH RATE)

1 - INCREASING SPEED
2 - DECREASING SPEED

Fig. 15. Effect of Pump Boost Rate

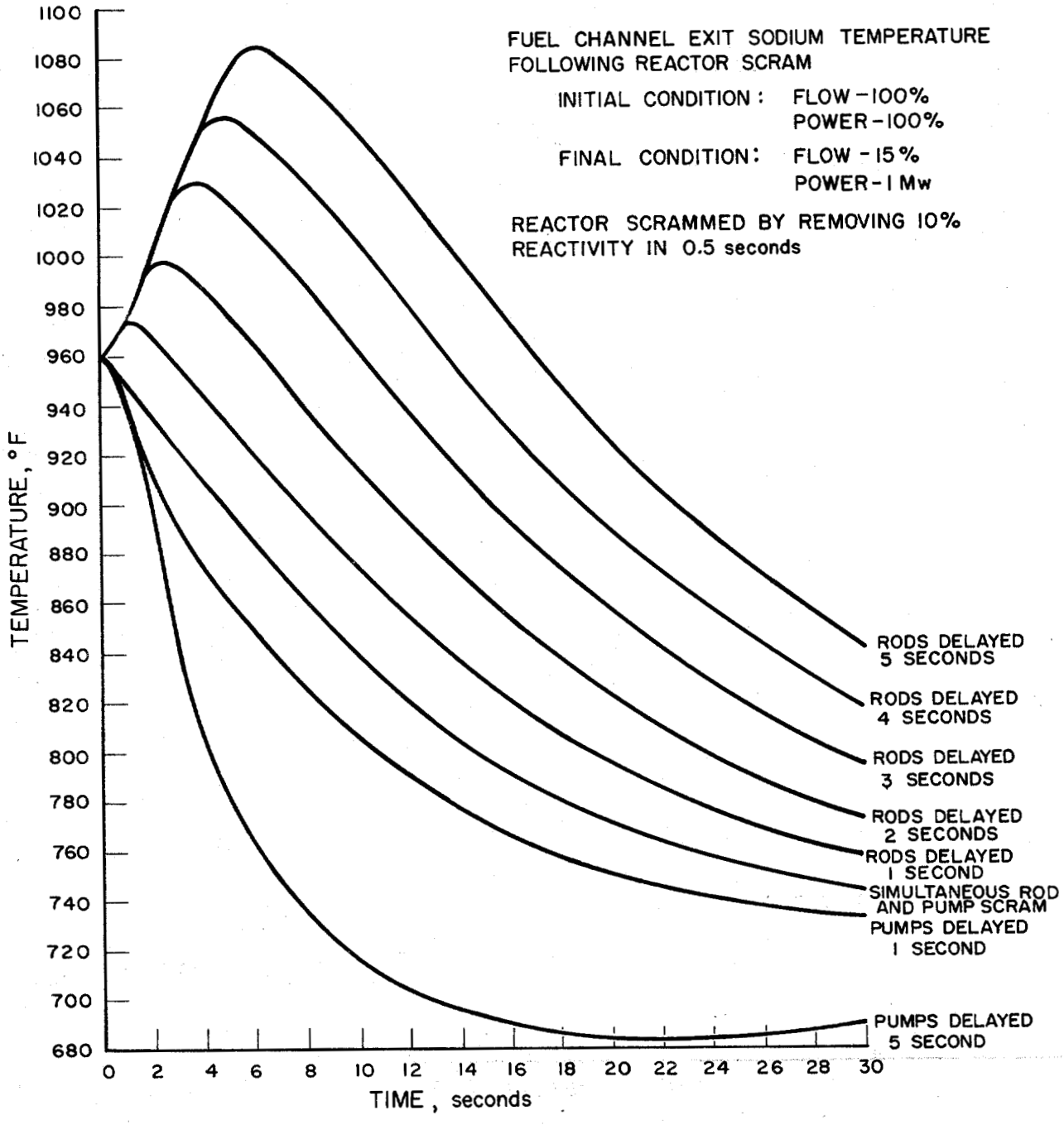

Fig. 16. Effect of Scram Delay Times

IX. LAND, UTILITIES, AND BUILDINGS

(F. C. Burnett)

The rough plumbing in the hot cell basement area was completed and tested. The sump pump opening was dug again and the new sump has now been poured. The hot cell basement area has been backfilled to the final earth grade line.

Construction of the primary sodium service vault and cold trap have been completed except for their plugs. The walls of the sodium service vault have been sodium silicated and the sodium drip pan liner on the floor has been completed.

The main primary heat exchanger has been lowered in place and the sodium drip pan linings are about 1/2 completed for the main gallery only. Both vault walls have been sodium silicated.

The hot dry fuel storage tubes have been set to final positions. The cleaning cells are not to elevation but will be water jetted into place. Moderator can seals are set to elevation.

The SRE hot cell liner has been tack welded in place and now requires wood forms and concrete placement in order to complete it.

The reactor building steel work in the high-bay area is completed, with the panels, low-bay area, and roofing remaining to be done (Fig. 17). This should be completed February 15, 1956. The 75 ton bridge crane has arrived at the site and will be placed in January.

The reactor core tank was placed but did not fit properly. In attempting to fit the outer tank into the clearance holes, the lugs were damaged. The stainless steel core tank, outer tank, and thermal rings were removed from the reactor core and had to be reworked. This has caused a delay of approximately four weeks in the reactor schedule.

X. FUEL ELEMENTS

A. FUEL ROD ASSEMBLY APPARATUS (J. J. Droher and H. Strahl)

Shakedown runs on fuel loading equipment were carried out during the quarter using normal uranium slugs. The regular sequence of operations has been performed on the electropolishing, outgassing, and multi-rod loading rings. The

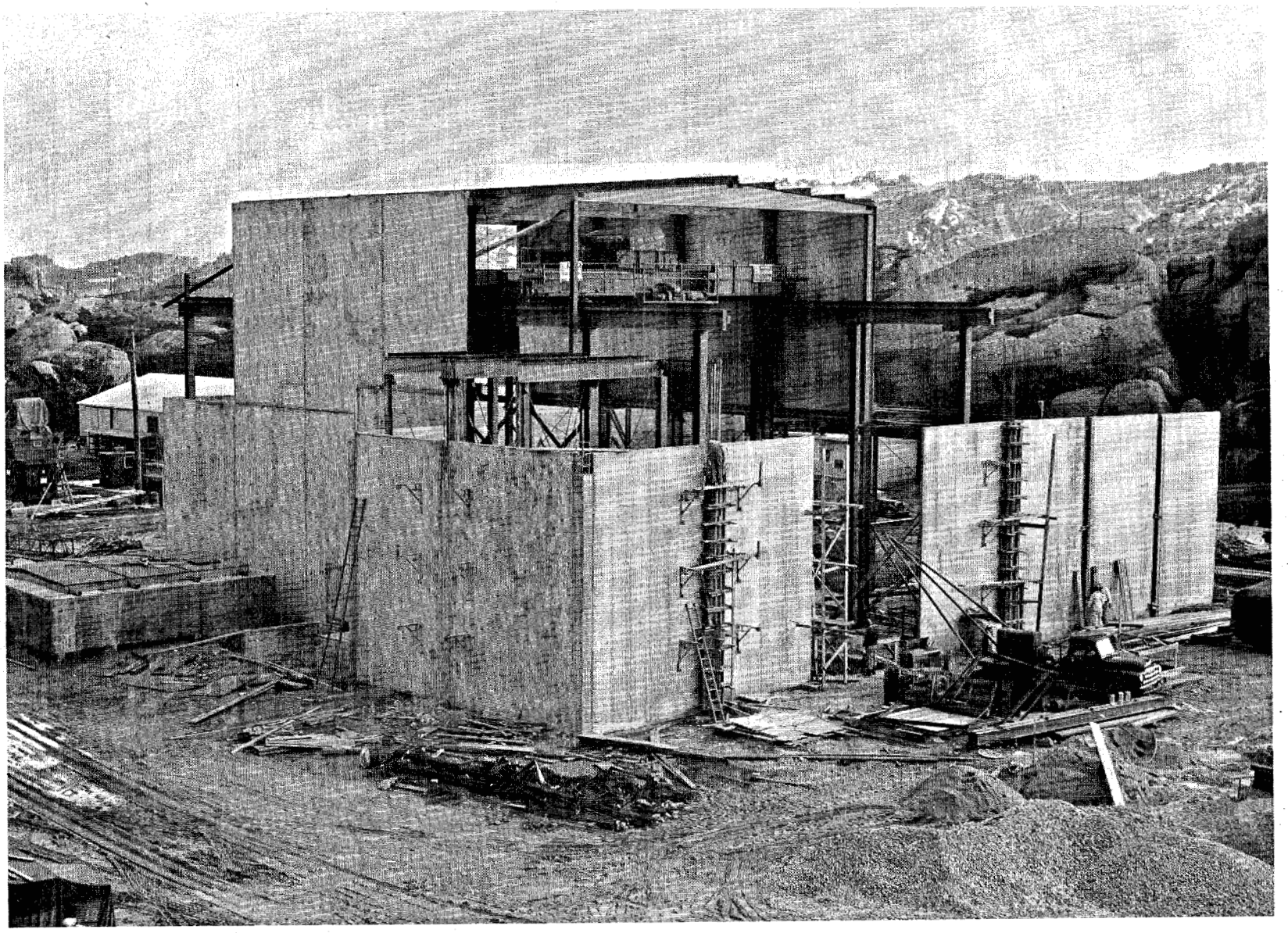

12-28-55

9693-12604

Fig. 17. Reactor Building Showing Structural Progress

expected full load of 21 batches, with 12 slugs in each batch, was used. The NaK bond loader was tested during these runs and no operational difficulties were encountered.

Additional modifications of the weld head have been made; these include improved seals, increased brush capacity, and changes in the geometry of the cap centering head.

A black soot-like material was deposited around the weld and chill block when welds were made under helium at one atmosphere. This deposit was not obtained under argon under the same conditions, so there was some concern that this deposit might be attributed to impurities in the helium. In Fig. 18 this black deposit may be noted around all welds and the top of all chill blocks with the exception of rods numbered 4 and 6, which were welded under argon. A thin sheet of stainless steel was placed over the top of the copper chill block in rod no. 5 to see if the source of this deposit might be in the copper chill block. Chill blocks of aluminum were used around rod no. 8 as a further check on the effect of the chill block material. It is apparent from Fig. 18 that the chill block material is not the source of the black deposit. Spectrographic analysis of this deposit revealed that manganese, chromium, and iron were major constituents indicating that the stainless steel was the primary source of this deposit. Only 2.6 per cent carbon was present, eliminating hydrocarbon as a source of impurity in the helium. Less than 0.01 per cent tungsten and no thorium was found, thus eliminating the electrode as a source of contamination. It is believed that the stainless steel sputters during the welding operation giving off very fine particles which would account for their black appearance. The supression of this deposit under argon is believed due to the shorter mean free path, since argon has a density ten times greater than helium under an equivalent pressure. This will be checked by attempting to weld under argon at 0.1 atmosphere to see if the deposit is obtained.

It is extremely important that the cleansing agents, used for reactor core components, do not contain any boron which might be retained as residual traces. Samples of Alconox, used for cleaning fuel rod jackets, were submitted for boron analysis. No boron could be detected. The limit of this detection is 10 ppm.

Routine production of fuel rods has been started. Approximately 150 jacket tubes have been tested on the Cyclograph, 100 have been trimmed, and 75 have

10-5-55

9693-51136

Fig. 18. Black Soot-Like Deposit Around Welds and Chill Blocks

had bottom end caps welded and leak checked. Shipment of 2700 slugs from the Accountability Station at Downey to the Engineering Test Building vault has made late in the quarter. Weighing in of these slugs has been carried out and 21 batches have been electropolished. Figure 19 shows the "as received" slugs on the left and the electropolished slugs on the right. The remaining fuel loading operations are now beginning and will reach a uniform output flow early in the next quarter.

B. FUEL ROD MODEL (R. Kennedy)

A cutaway rod (Fig. 20) showing the uranium slugs, bond, gas space, and tubing was fabricated for the fuel rod model. Oxidized stainless steel was used to simulate the uranium slugs, while aluminum tubing was machined to simulate the 10 mil NaK bond. This model is being used as part of an unclassified educational display.

Doesn't gravity have something to do with it? Design — ha

C. FUEL ROD DEVELOPMENT

Under presently specified fuel loading conditions, a fuel jacket leak during reactor operation will result in displacement of the liquid metal bond down to the level of the jacket failure. Some possible modifications of the fuel loading procedure to avoid this condition are listed.

1. Reduction of helium pressure during sealing of the jacket.
2. Increase in temperature of helium in jacket during sealing.
3. Increase in level of the liquid metal bond material in the jacket.
4. A combination of the above.

The first two modifications are not feasible for application to the present multi-rod loader. The third modification is the most attractive and the liquid metal bond level will be increased by adding more NaK before sealing the tube.

It is planned to add 7.32 cu in. of NaK which will raise the bond level 12 in. above the top of the slugs leaving 7 in. of gas space. Under a maximum operating temperature of 1200° F the NaK, stainless tubing, uranium, and gas all expand leaving 4.5 in. of gas space under a calculated pressure of 71 psi. This results in a radial stress on the tubing of 2760 psi and a longitudinal stress of 3700 psi (the longitudinal stress exceeds the radial stress because it includes the stress caused by the weight of the uranium). This appears reasonably safe when compared with creep and rupture data for type 304 stainless steel.

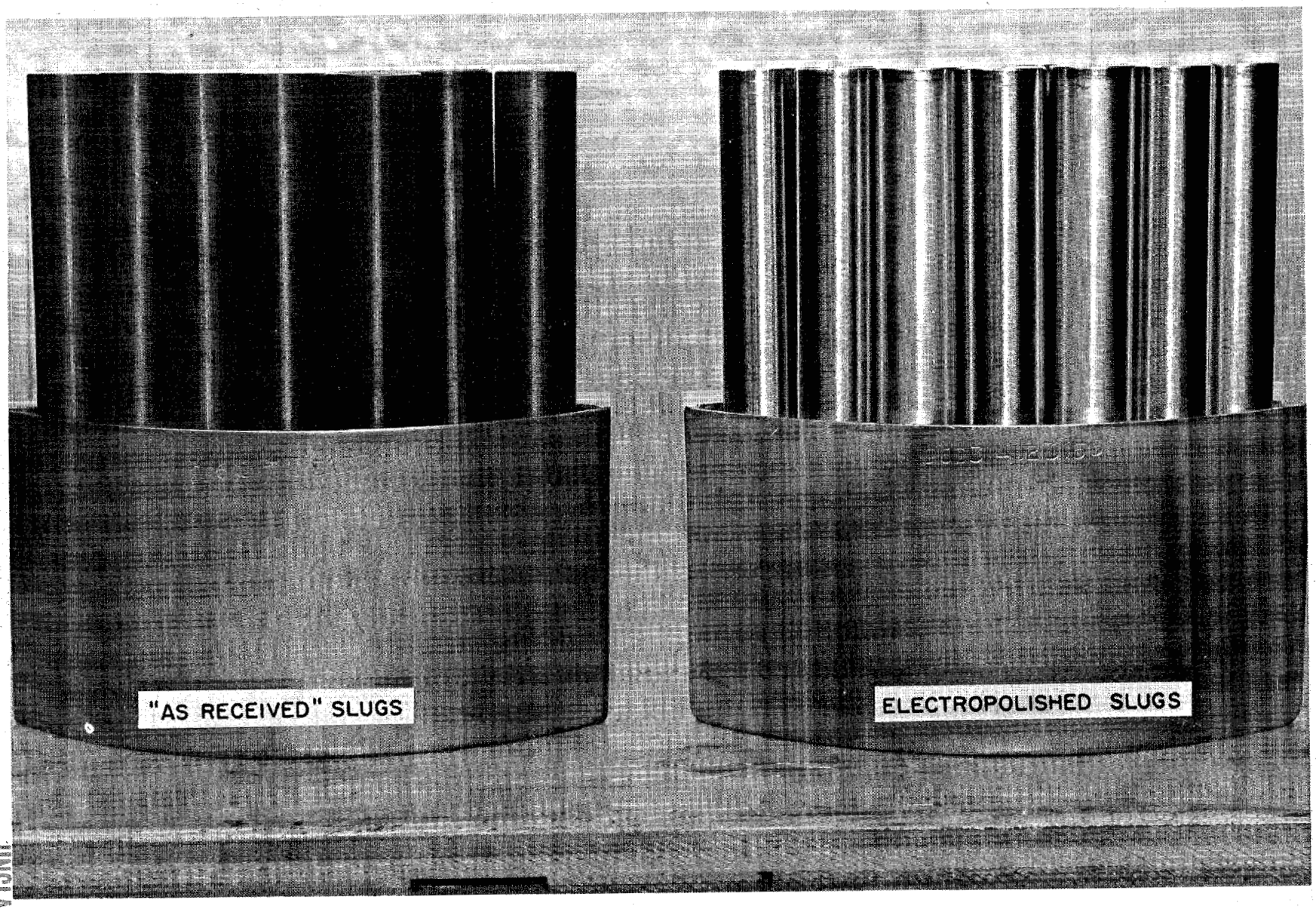

Fig. 19. "As Received" and Electropolished Slugs

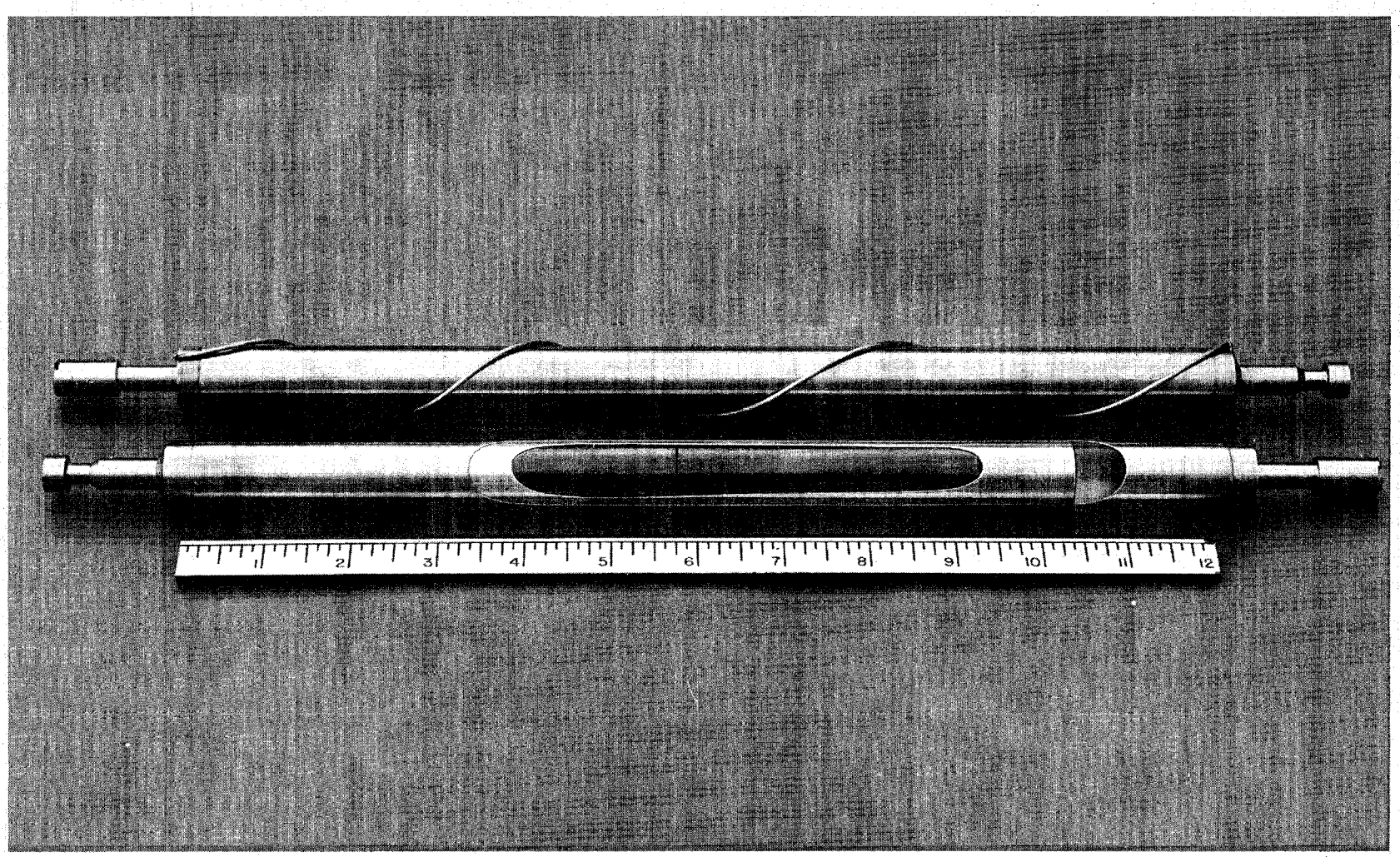

12-3-55

9693 – 51150

Fig. 20. Cutaway Rod for Fuel Rod Model

Prior to this modification, 4.6 cu in. of NaK were added raising the bond 6.1 in. above the top of the slugs and leaving a gas space of 12.9 in. This length of 12.9 in. was for the accumulation of any fission gases. Recent information indicates no substantial increase in pressure will be caused by fission gases since apparently there is very little diffusion through uranium metal slugs of the size being used and under the conditions of the SRE.

D. FUEL ROD TESTING

Cyclograph traces of rods bonded with various sodium potassium alloys were recorded for rods at room temperature and heated to 450° and 600° F. Examination of successive traces (Fig. 21, 22, and 23) shows an approach toward the straight line, which is indicative of uniform bonding, as the potassium content of the bond is increased. The trace labeled no. 1 is for sodium bonding and the numerous deviations from a straight line are indicative of many large voids. Traces numbered 3, 4, and 5 are for bonds of sodium alloyed with 5, 25, and 44 per cent potassium. The trace labeled no. 2 is for NaK eutectic (22% Na - 78% K) and indicates no voids. Thus, successively fewer voids are indicated as the potassium content of the bond is increased, or as the temperature is increased.

As an additional test of bonding voids these experimental fuel rods were pulled at constant velocity through a close fitting induction heater coil. In uniformly heating the fuel element jacket, the unbonded regions cannot lose heat to the uranium slug as rapidly as the bonded regions and hence should overheat. Figure 21 shows a portion of all rods tested. The 100 per cent sodium bonded rod is at the left. The numbers of oxidized regions are readily apparent. The rod containing 5 per cent potassium is the second from the left and the discolored area may be seen near the bottom of the picture. No discolored area was obtained in the other 3 rods. All the rods were tested in this manner. The jackets of the well bonded rods heated to above 500° F (as determined by stroking with tempilstick crayons) but no overheated regions were apparent. On the other hand, the poorly bonded rods did exhibit overheated regions manifesting themselves as badly oxidized spots on the jacket tubing. The greatest quantity and the largest voids appeared on the sodium bonded rods, the next largest number on the rod containing 5 per cent potassium in the bond, and none was detected in these rods containing 25, 44, and 78 per cent potassium.

11 – 18 – 55

9693— 51143

Fig. 21. Cyclograph Traces

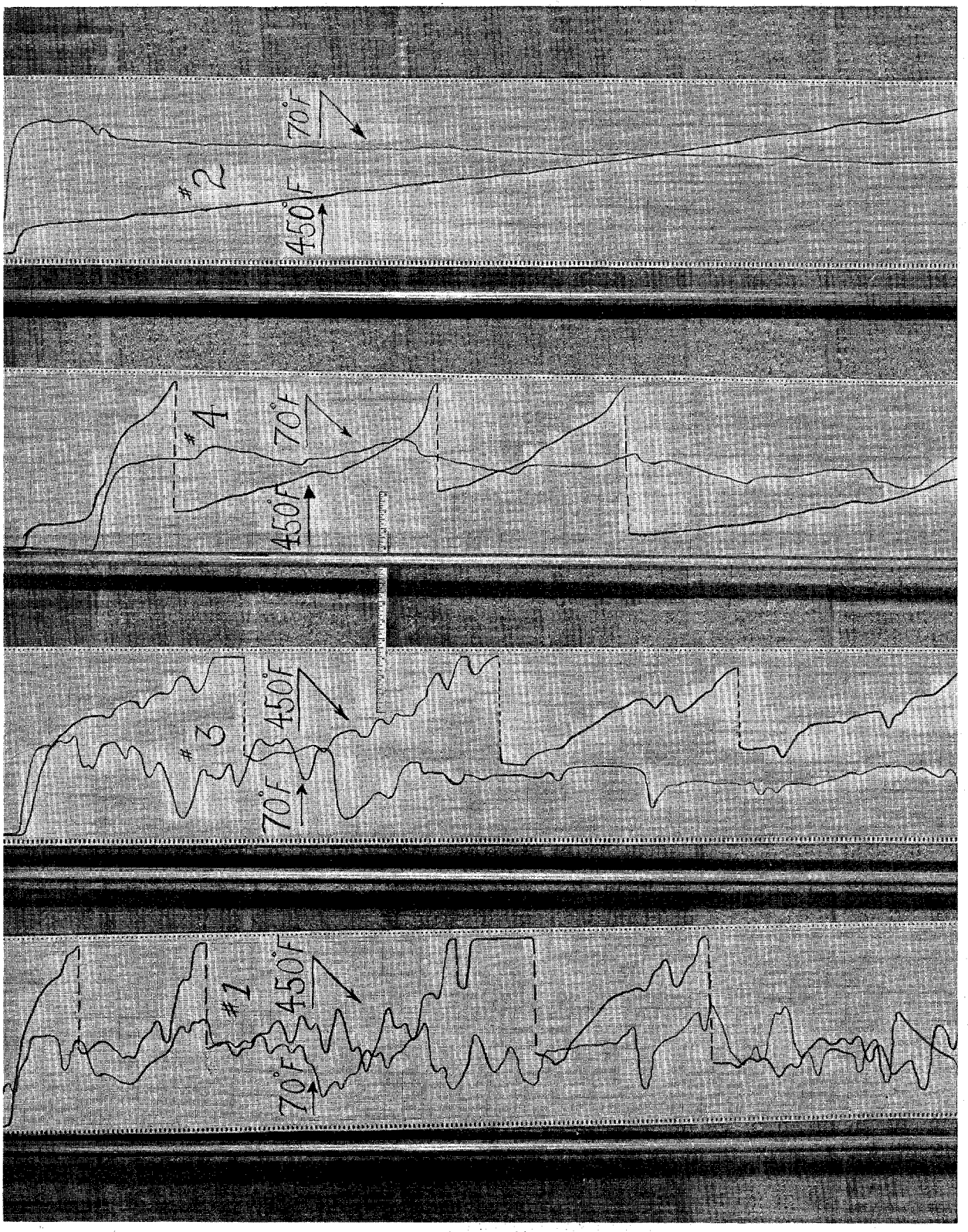

Fig. 22. Cyclograph Traces

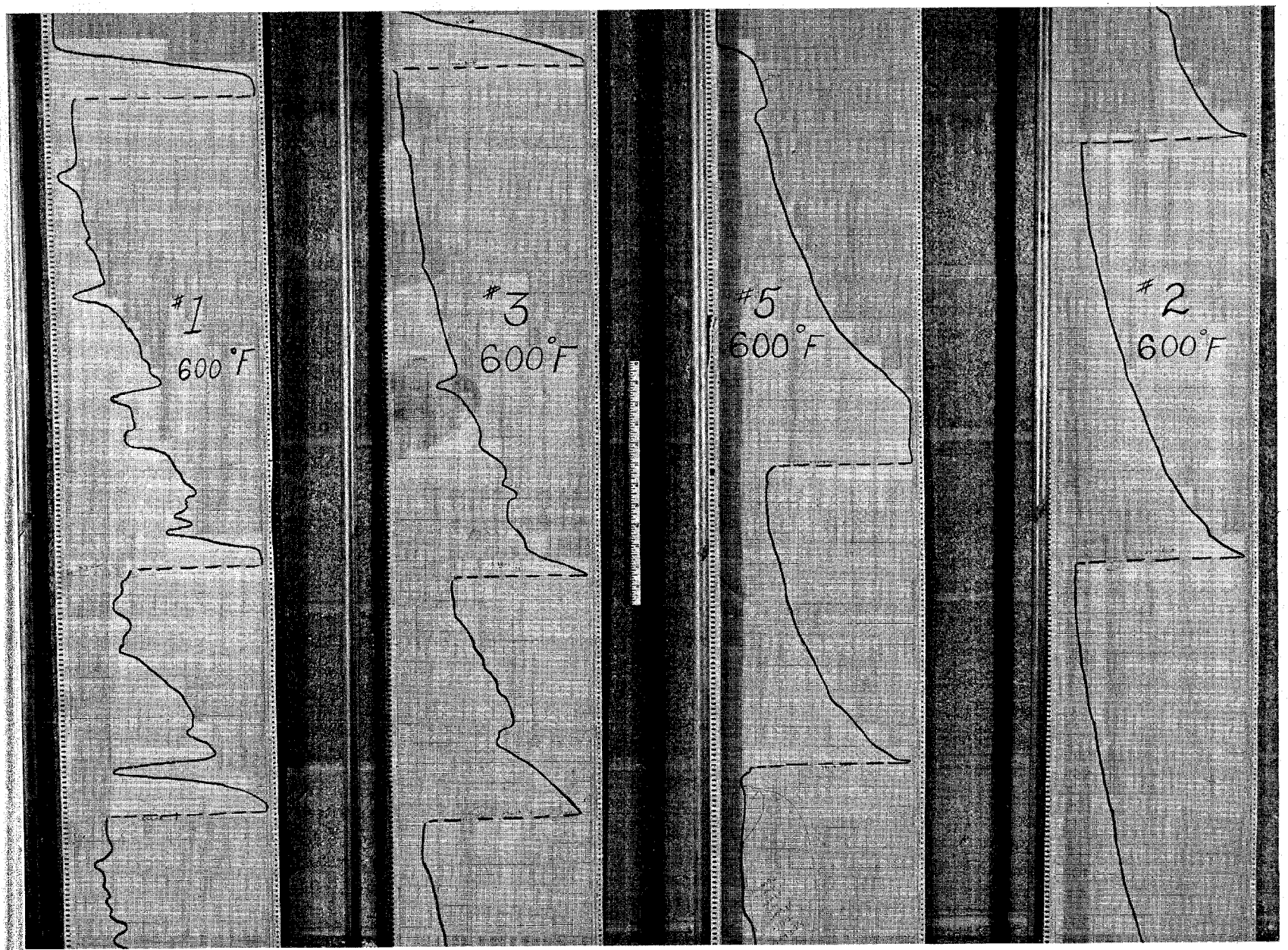

1-13-56

9693 - 51186

Fig. 23. Cyclograph Traces

These tests were repeated for cases having the bond molten before passing through the induction heater coil. The rods were soaked at 450° F and 600° F and pulled through the coil at the same power setting and velocity as the room temperature test. No discolored areas were observed. It was calculated that the increase in electrical resistivity with temperature caused an increase in the effective depth of penetration of heat from 10 mils to 20 mils. Therefore, the rods were pulled through the coil at successively slower velocities. Even at velocities as low as 1/4 of that in room temperature tests it was difficult to obtain oxidized or "burned" spots on the jacket. However, a few spots were obtained on the sodium bonded rods. Finally, autoradiographs, which were made of all the experimental fuel rods, show a correlation between dark regions indicative of voids, and void regions shown by the other tests.

The rods were then stripped of their jackets. As was expected, the 12 slugs in the sodium bonded rods had numerous unbonded regions. These slugs (Fig. 24) showed the regions bonded with sodium (which rapidly turned white as the sodium oxidized in air) and the unbonded regions. Voids coincided with many of the external burned regions (Fig. 25) caused by the induction heating tests. The eutectic NaK bonded slugs were quickly dumped into mineral oil and all were uniformly coated with NaK. Photographs of the rods bonded with the intermediate alloys could not be obtained as the bond ignited immediately upon exposure to air.

All of these tests confirm previous findings with the cyclograph that, (1) both the number and size of voids decrease, but do not necessarily disappear entirely, when the bond is molten, and (2) increasing the amount of potassium decreases the number of void indication.

XI. MODERATOR CAN FABRICATION AND TESTING

A. MODERATOR CAN TESTING PROGRAM (J. A. Leppard and S. Bain)

The second retort test on the 35 mil wall, one-scallop can, previously described,[4] was completed after a continuous period of 36 days at reactor temperatures. The can, which remained leak tight throughout the test, was in good condition at the end of test. It was previously reported that the top head "oil canned" upward during the first test. This condition remained unchanged during the second run After the can was sawed apart the top head was found to be permanently deformed.

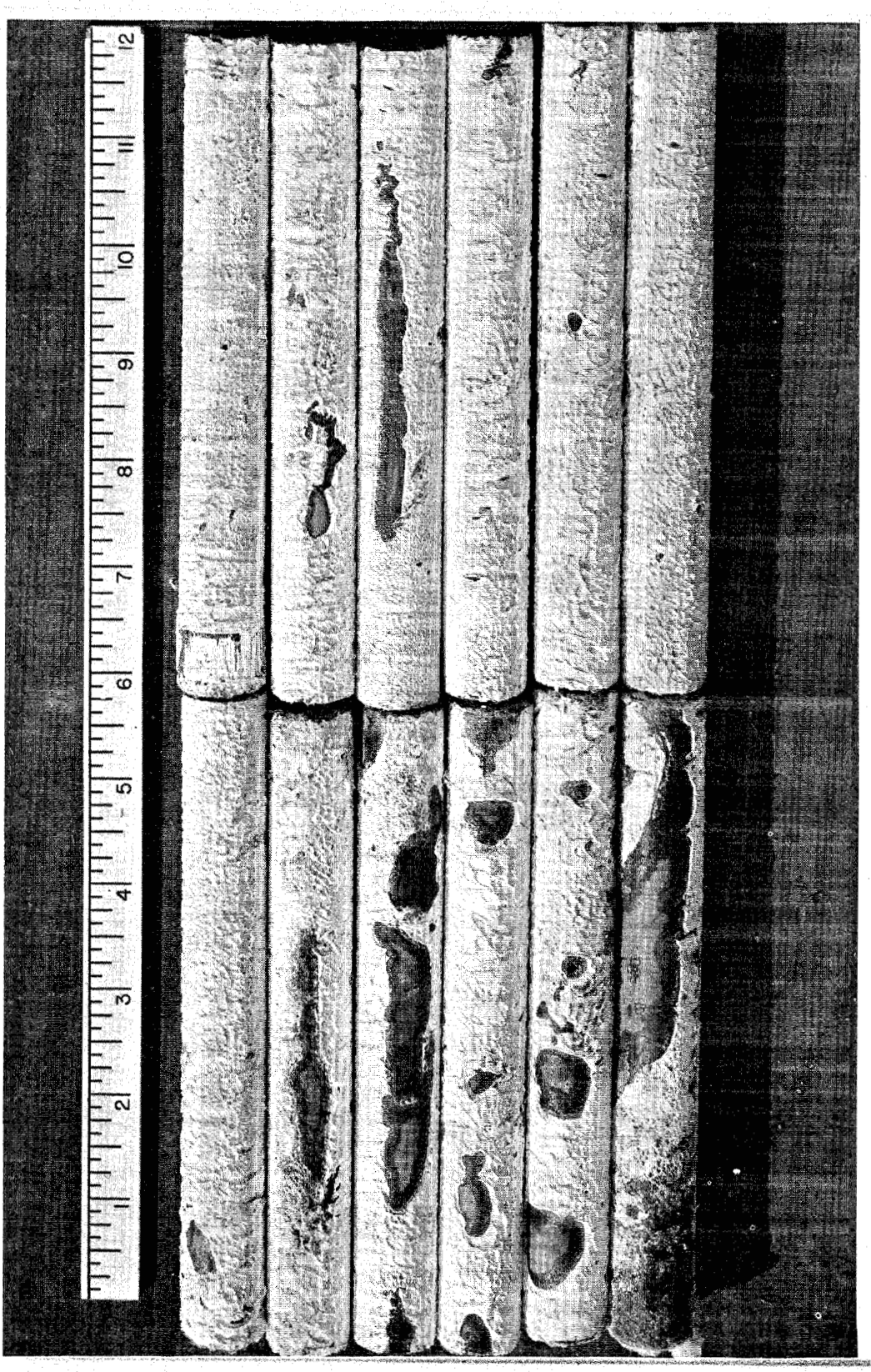

12-3-55

9693—51149

Fig. 24. Slugs Showing Regions Bonded with Sodium

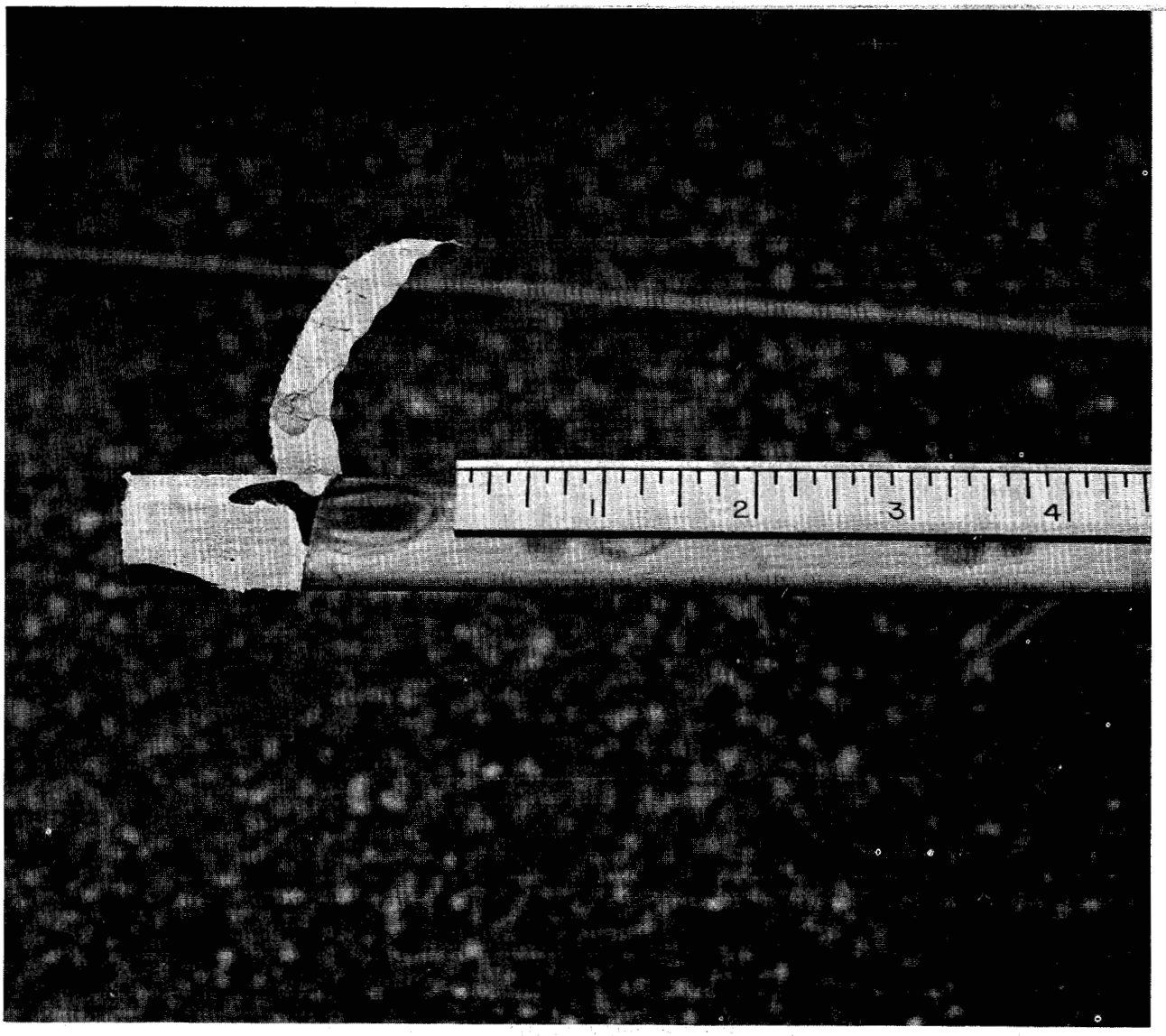

12-3-55 9693 - 51157

Fig. 25. Slugs Showing Voids Coinciding with Many External Burned Regions

Careful measurement of all parts indicated that the central coolant tube (35 mil Zr) had grown 3/16 in. in length, making the deformation of the top head. Also after the can was sawed open no sodium (from the snorkel tube source) had diffused down into either the breather tube, condenser cup or graphite.

An additional 35 mil wall Zr moderator can containing TSP graphite is being tested in the retort at reactor temperature. One purpose of this test is to determine if any out-gassing of the graphite will occur at the test temperature. The can was initially evacuated and then filled to 10 in. Hg psia with helium in the same way that production cans will be done. At the reactor temperature gradient condition the pressure increased to 21 in. of Hg absolute without any indication of out-gassing.

B. MODERATOR CAN HEAD FLEXURE TESTS (M. Tarpinian)

Using the apparatus described in a previous quarterly progress report,[4] we tested 2 more can head specimens. An 8-inch section of a two-scallop moderator can was flexed under sodium at 1025° F at a rate of 1 cycle per 9 minutes through a downward displacement of 0.09 in. per head. A graphite core with a 1/4 in. relief at the ends was encased in the can. Failure occurred after 666 cycles. Although no cracks were visible, a dye penetrant check showed defects in both head assemblies. As in the case of the first can head, the cracks were in the tube metal at the edge of the weld.

During the removal of the graphite core, several of the longitudinal side wall welds split down the middle of the welds. Consequently, hardness and bending tests were performed to compare welds with specifications. Rockwell hardness measurements indicated a hard weld; the hardness value of the parent metal was RA 49 while the weld was RA 55. This was confirmed by the bending tests which showed failure in the weld up to a bending radius of 0.16 in. (about 4T) although the parent metal did not fail even down to 0.035 in. radius (about 1T). Similar tests made on specimens cut from the original full size can verified the findings above. Therefore, brittleness of the welds was not due to cycling under sodium, but was inherent in the fabrication process.

Previous to flexing, a second two-scallop can head specimen was heated to 1300° F for about 25 minutes to anneal the welds. Cycling was begun after cooling to 1040° F and after 23 cycles failure occurred. Upon removal it was

found that the can had collapsed. On one side the wall had been deformed inward about 3 in., while the remaining sides showed a smooth concave deformation. Both heads were badly bent downward at the sides. Again, the leak occurred in the weld joint between the through tube and the can head. Because of repeated failure of the same joint between the can head and coolant tube, considerable effort is being expended to obtain a more reliable joint.

Before cycling, all can head specimens were static-load tested to a displacement of 0.09 in. per head, both at room temperature and at operating temperature. The force ranged from 360 to 400 lb. Also, for a given specimen the force required at room temperature and at operating temperature was the same within the limits of measurement error.

XII. HEAT TRANSFER

A. SIX INCH WEDGEPLUG VALVE TESTS (J. C. Flint)

Tests have been completed on Freeze Seal No. 2 for the 6 in. oval port Wedgeplug test valve at 3 temperatures, 450° F, 850° F and 1250° F. This freeze seal is located about 3 in. away from the flange face in an effort to reduce the heat load on the seal. In addition, the thermal insulation on the valve is stopped at the flange face leaving the thin outside sleeve of steel, connecting the seal to the flange, open to the atmosphere.

With the seal thus isolated to this extent from the flange it was possible to stop cooling flow entirely, with the valve at 450° F, and not lose the freeze seal. A drawing of the freeze seal and valve flange with thermocouple positions are shown in Fig. 26. The temperature gradients from the hot flange face to the cool end of the seal mechanism for various valve temperature conditions are shown in Fig. 27.

Tests were made by bringing the valve up to required temperature by using "full" water flow (10 lb/min). Temperature gradient readings were taken and heat loads were calculated from the water flow and water temperatures. With the valve at a given temperature, the water flow was reduced in 2 lb/min. steps.

A seal is formed nearest to the flange under conditions of low valve temperature and high water flow (see Curve 1, Fig. 27). The seal is formed farthest

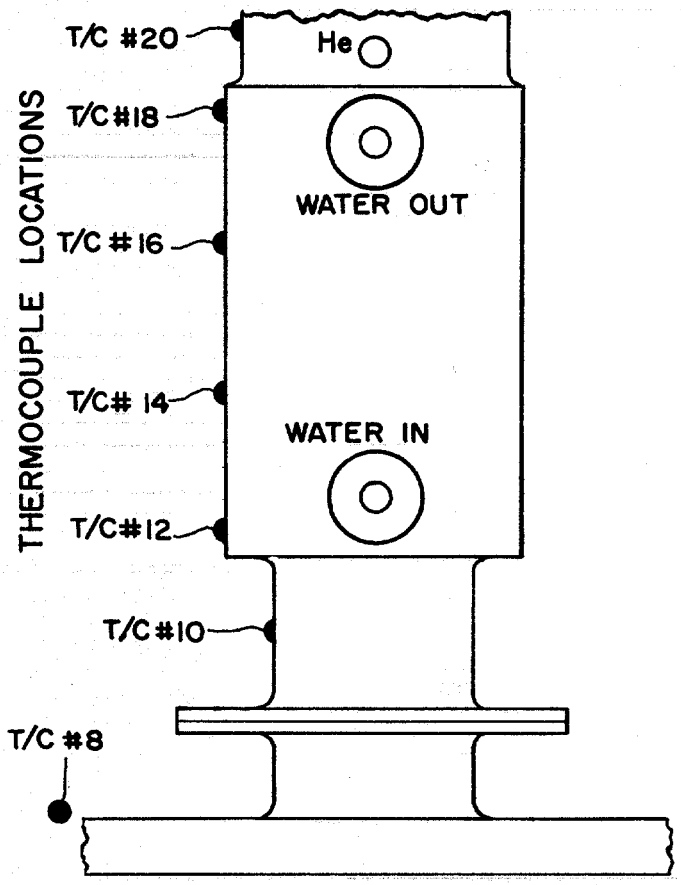

Fig. 26. Thermocouple Locations for the Preliminary Test of Freeze Seal Number 2

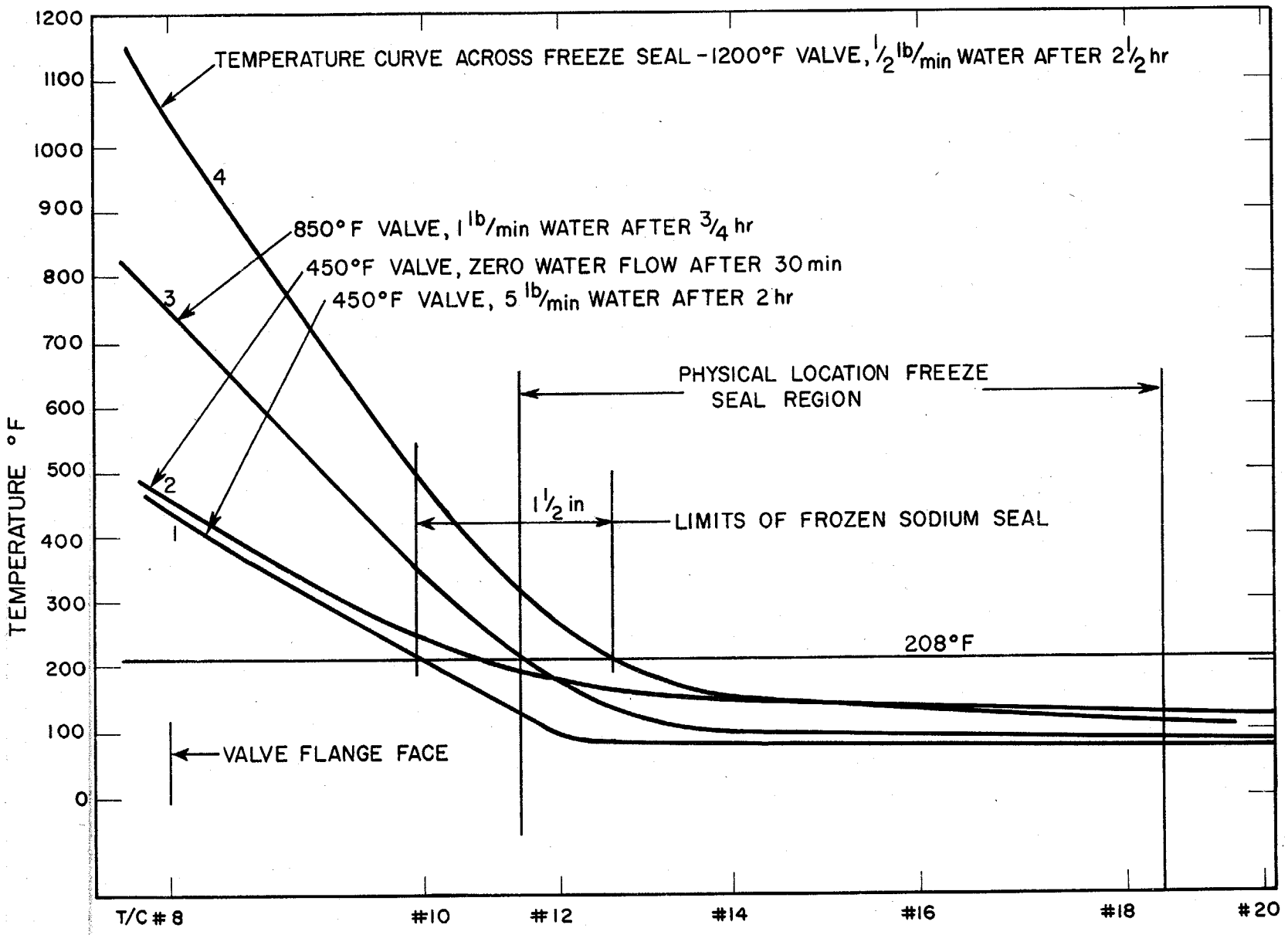

Fig. 27. Six Inch Valve Concurrent Flow Tests Showing the Temperature Gradients Across the Number 2 Freeze Seal

from the flange when the valve is hottest and water flow is at a minimum (see Curve 4, Fig. 27).

The graphitized asbestos stem packing used to keep a helium atmosphere on the frozen sodium in the seal, worked well and did not bind or restrict shaft. However, some helium will bubble into the valve when the shaft is rotated. This is caused by the fact that the shaft is not concentric with the housing or freeze seal. A new seal is formed quickly and even though the shaft is kept turning, no additional helium seems to flow. The amount of helium passed is so small that there is little drop noticed on the helium backup pressure gage. The valve operated easily at all temperatures. The heat loads on the freeze seal for both high and low water flows were:

1. 150-210 Btu/hr for the 450° F valve temperature run
2. 540-1130 Btu/hr for the 850° F valve temperature run
3. 750-1200 Btu/hr on the 1250° F valve temperature run.

On the basis of these data the freeze seal design has been released and the production units are being manufactured.

Tests have been completed for measuring sodium leakage through the valve when it is in the "closed" position. The valve was considered "closed" when the plug was driven forward as far as possible, with 150 ft-lb of torque on the hand-wheel. Table IV indicates leak rates.

TABLE IV

SODIUM LEAK RATES

Pressure (psi)	Valve Temp. (° F)	Leak Rate (gal/hr)
10	500	0.5
30	500	2.0
10	1000	4.85

The next disassembly of the valve may show the causes of this leakage.

Two main factors that might lead to this leakage are warpage due to thermal cycling on a non-homogeneous casting and slag inclusions in the valve seat.

It may be necessary to sodium soak the two production valves to check their performance prior to installation in reactor piping. The reason for sodium soaking the valves is to check for exploded inclusions and pitting with associated porosity, particularly in the valve seat.

B. LIQUID SODIUM LEVEL GAGE PROGRAM (J. C. Flint and J. R. Charles)

Of the 4 types of gages that were being tested, two have been eliminated for use in the reactor. The two remaining gages, which are electrical coils, are being tested. One has completed tests up to 1000° F.

The latter consists of a differential coil enclosed in a probe that can be lowered into a 1 in. thimble in the tank to be measured. The gage has operated continuously in a 500° F air atmosphere and it measures sodium level with an accuracy of ± 1/32 of an inch. No tests have been made to determine its life-time at 1000° F. The coil has been used operationally to measure sodium level at 1000° F but only for a maximum time of about 3 min. at that temperature.

Because the coil resistance increases with temperature, the accuracy drops to about ± 1/16 in. at 1000° F. Another unit of this type is being built for life tests since the first unit is still in use operationally on two other tests. Figure 28 shows the level probe and indicator except for 2000 cps oscillator which is used to drive the unit. The probe has since been fitted with a flexible steel rule for measuring its penetration into the tank. The operation involves lowering the probe into the thimble and tuning for a maximum reading on the water and then reading the depth of penetration from the tape.

The last gage is a redesign for high temperature of the ANL solenoid-type gage used on the EBR II. This gage is being built at present for a one in. thimble and an expected 1000° F maximum operating temperature.

C. TUBULAR HEATER EXPERIMENT (M. Nathan)

The tubular heater experiment was completed during the quarter. The purpose of the experiment was to obtain information for the design and operation of heaters used for regulating SRE sodium-coolant piping temperature.

The test apparatus consisted of a 6 in. nominal, schedule 40 stainless steel 304 pipe to which tubular heaters were affixed, spaced 180° apart. The heaters were held to the pipe by means of 1 in. wide stainless steel T-bolt clamps spaced 12 in.

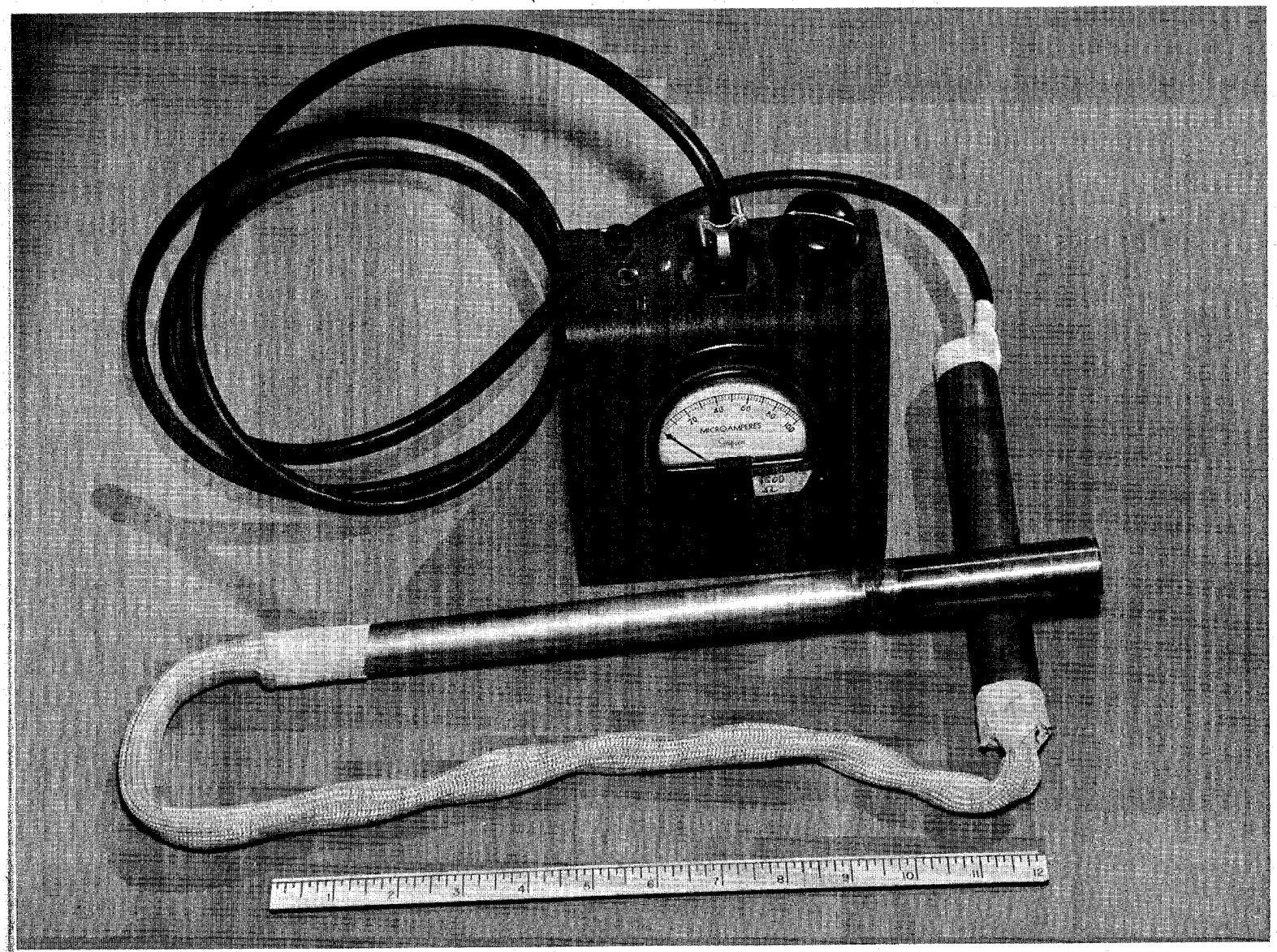

Fig. 28. Level Probe and Indicator

Stainless steel shim stock (0.003 in. by 6 in.) was placed over the entire effective heating length of the heaters and held in place with bands such as used for holding pipe insulation. Two layers of Kaylo insulation, each of 2 in. thickness, were than applied over the entire length of pipe. Figure 29 shows the test setup before the installation of Kaylo insulation.

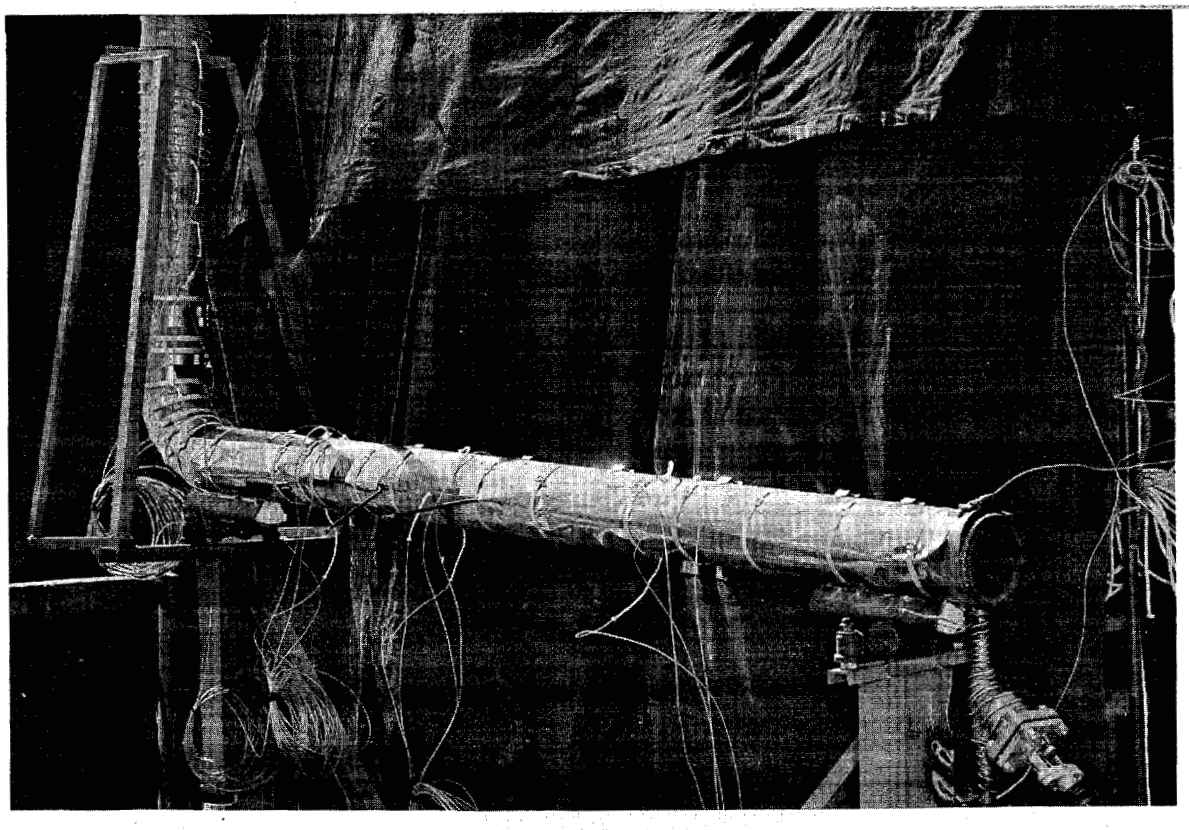

Fig. 29. Tubular Heater Test Setup Minus Kaylo Insulation

Tests were performed to determine the time required to bring the average pipe temperature from ambient to 350° F. Similarly, after admitting sodium to the system, tests were performed to determine time required to heat sodium from 350° F to 750° F. The results of these tests together with test conditions are tabulated in Table V.

D. PLUGGING INDICATOR TEST LOOP (M. Nathan)

Construction of a sodium loop to test the tetralin-cooled plugging meter proposed for the SRE was completed. The plugging meter consists of an economizer, a tetralin-sodium heat exchanger, electrical heaters for controlling the

TABLE V

TIME TO RAISE AVERAGE PIPE TEMPERATURE FROM AMBIENT TO 350° F

Test No.	Pipe	Power Density w/linear in. Pipe*	Temperature Range (°F)	Time (hr)
1	Empty	4.5	62 - 350	10.8
2	Empty	1..12	73 - 164†	11.5
3	Contains Sodium	4.5	349 - 412	18.5
4	Contains Sodium	18.0	350 - 750	6.6

*The value of power density given is for that portion of the pipe having heaters spaced 180° apart and includes no allowance for the pipe section between heater terminals.

†Equilibrium was attained at these temperatures, i.e., the heat input equalled the heat losses through the insulation.

rate of cooling, and a plugging valve. In place of the regularly used plugging disk, a one-inch, Y-type bellows sealed valve has been used. The face of the valve plug has been perforated with holes and the plugging temperature is obtained from a thermocouple on the valve seat.[11]

In the operation of the plugging valve, the entire sodium flow passes through the holes in the valve seat. Provision is made in the valve plug to permit the sodium flow through the holes to continue downstream through the meter. After a plugging determination, the buildup of Na_2O in the holes of the plug is removed by opening the valve halfway and permitting hot sodium to redissolve the oxide.

Operation of the experimental loop was initiated and sufficient thermal equilibrium data were obtained for us to establish the design of the SRE plugging meters. Tests are in progress to determine the recommended number of holes and hole size to use in the plugging valve seats of the SRE plugging meters. In addition, tests are being performed to determine a recommended operating procedure and the proper flow conditions.

E. SODIUM DETECTION (D. L. Whitlock)

The method described previously[4] were continued in this quarter. These tests revealed that sodium detection can be made under ideal conditions in an SRE control or safety rod thimble. By using distilled water as the detector, in conjunction with a pH meter (more sensitive than the previously used detector, thymal blue) sodium can be detected at 500° F if the sniffer tube extends to the bottom of the thimble and at 700° F if this tube terminates in the top of the thimble. Neither method is satisfactory if the sodium is covered with an oxide film.

F. COLD TRAP OPERATIONAL TESTS

The cold trap which was installed on the sodium pump loop has been removed. The proposed modified economizer will be substituted for the earlier design. The cold trap is being cut open and will be examined and cleaned before the next test.

G. SIX INCH SODIUM PUMP LOOP (R. Cygan and R. W. Atz)

A relatively large (several quarts) leakage of lubricating oil into sodium through shaft seal resulted in a mixture having a higher melting point than sodium. This mixture could not be purified by low temperature filtration through a sintered stainless filter and had to be removed from the system by draining and steam cleaning. The portions that were removed by draining formed a coke-like mass upon solidification. As a result of this all the pump oil bearings have been replaced with sealed grease packed bearings. The latter modification has resulted in very satisfactory bearing performance with no lubricant loss. The lubrication test program has been discontinued.

Two new freeze seals have been fabricated and tested. The first unit was fabricated with a coil of 3/8 in. OD stainless tubing as a single helix having a welded manifold return. A second cooling region was built into the seal flange. The seal performed satisfactorily with a tetralin flow of 3.6 gpm at all speeds and temperatures tested (1200 rpm, 1200° F). No leakage was observed during test.

The second unit was machined from a solid stainless forging so that no welds are in contact with the sodium. The cooling passages consisted of two concentric annuli 1/8 in. wide with a 1/8 in. thick flow divided between them. Coolant flow was downward in the annulus (shaft side) and upward in the outer annulus. Performance was satisfactory at all shaft speeds and temperatures tested (1500 rpm, 1200° F).

A small quantity of sodium was extruded in the form of shavings or chips from the seal. It amounted to less than 1 g for over 100 hr of operation. This would amount to about 1/4 lb for a year's operation which can certainly be tolerated from a heat conduction standpoint. The coolant pressure drop of this unit was the lowest of any design tested thus far.

Fabrication of the auxiliary pump loop has started and is now about 25 per cent complete.

H. FUEL ELEMENT DEFLECTION STUDY (C. R. Davidson)

A one to 3.5 scale model of a SRE fuel element (Fig. 30) was constructed to study the effect of side drag on the element during insertion operations at those fuel channels located near the outlet of the upper plenum chamber.

The normal coolant flow rate will probably be reduced ~5 per cent during the fuel element replacement operation. The deflection which the fuel element might experience would be due to forces exerted by any horizontal components of the upward flow through the empty fuel channel which amounts to about 40 per cent of the total flow, and the horizontal cross flow in the upper plenum toward the outlet (Fig. 31). It was conceivable that sufficient force could be exerted on the fuel element to buckle or deflect it enough to make insertion difficult.

In the experiment, the fuel element was suspended in two ways incorporating the extremes of the situation expected in the SRE. One method was the free suspension of the hanger rod from a wire, the other that of rigidly clamping the hanger rod at the top. The experiment was run under these conditions with varying water flow rates, with and without the empty fuel channel plugged, and with various water levels in the upper plenum.

The method of observing the deflection in the preliminary experiments utilized a pen on an arm which was attached to the hanger rod 40.5 in. down from the point of suspension. The length of the arc traced by the pen on a vertical pad of paper was taken to be the deflection experienced by the fuel element at that point.

The observed deflections were negligible at flow rates of around 5 per cent of the equivalent SRE flow rate for both types of suspension and were due almost entirely to the cross flow current. At flow rates approaching operating flow conditions, the deflections increased by a factor of ten but were still of a magnitude less than that which would give difficulty. Forces causing the deflection, however,

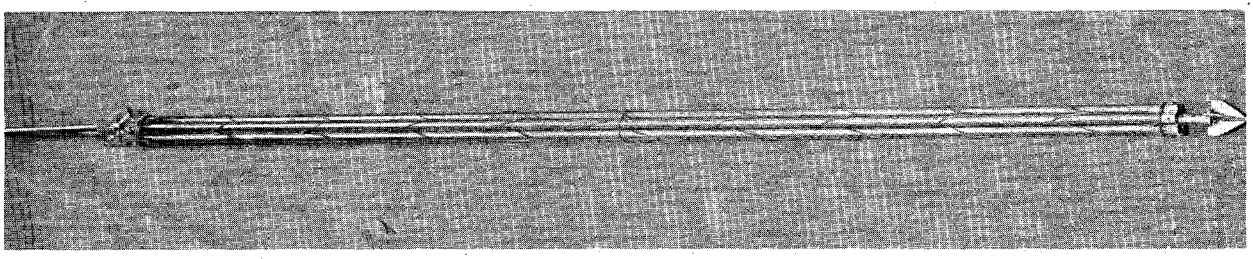

Fig. 30. SRE Fuel Element Model

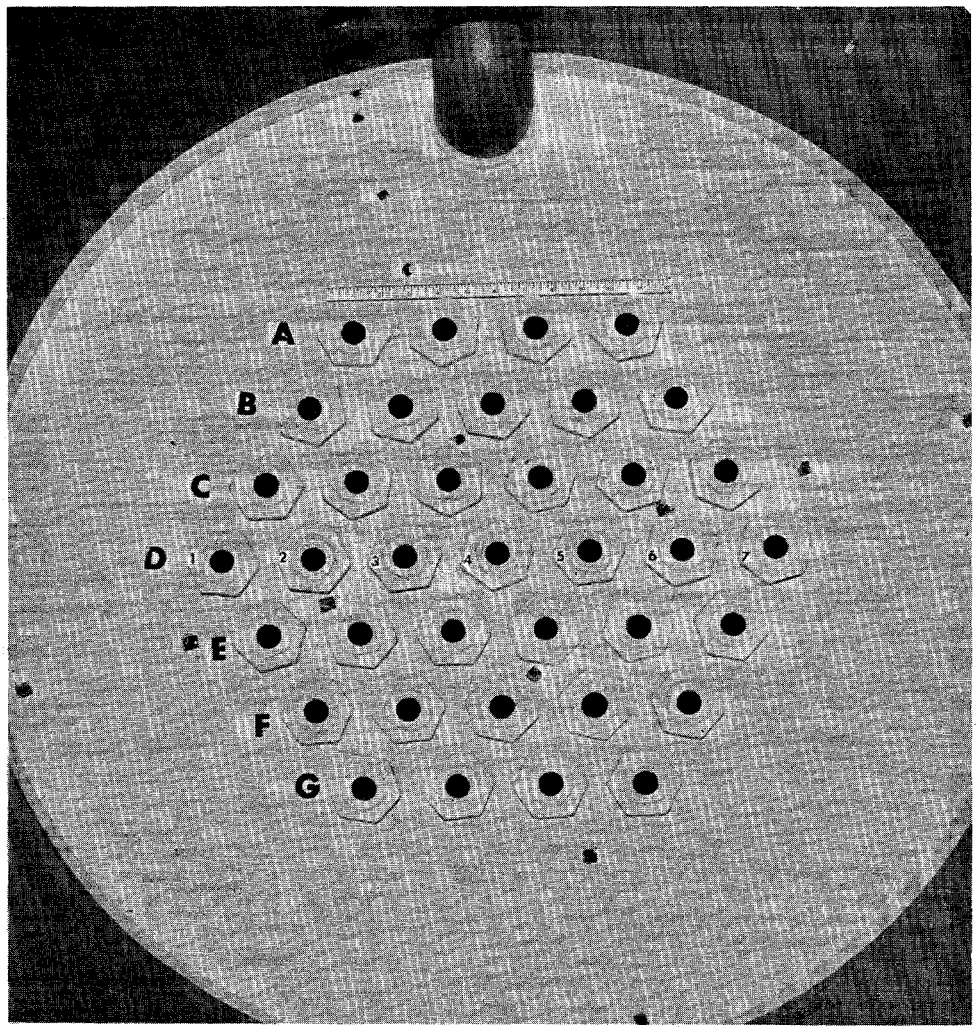

Fig. 31. Upper Plenum Showing Fuel Channels

were about evenly divided between those of cross flow current and the flow through the empty fuel channel. Lowering the coolant level in the upper plenum 20 per cent resulted in no visible effect at 5 per cent flow and about 25 per cent increase in deflection at normal flow.

In view of the small deflections observed and the difficulty of correlating the experimental results with conditions in the SRE, a more rigorous experiment is not planned.

I. SRE FUEL ELEMENT ORIFICE CALIBRATION (C. R. Davidson)

The relative coolant flow in a given fuel channel in the SRE is determined by the total pressure drop across the channel. As some fuel elements are expected to have a greater power output than others due to their particular location in the reactor, a proportionately greater coolant flow should be distributed to these channels if a uniform horizontal temperature profile is to be obtained in the reactor. This is accomplished in SRE by the proper scheduling of orifices. Calibration of these orifices at varying flow rates is the purpose of this work.

The hydraulic model tank system was modified to incorporate a 6-ft length of 2.804 in. ID pipe, equipped with straightening vanes at one end and a test section at the other. The pressure taps were located 2-1/2 pipe diameters upstream and 8 pipe diameters downstream from the orifice plate (Fig. 32). The orifice plate assembly (Fig. 33), which consisted of spear point, orifice plate and spacer, was mounted co-axially in the pipe (Fig. 34).

The pressure drops were observed on a U-tube manometer by using water over 2.95 specific gravity oil while flow rates were obtained from a standard orifice meter. A bypass line simplified control of the flow rate through the test section and tended to dampen out flow fluctuations. Water temperatures were observed with thermocouples mounted downstream from the test section and with the orifice meter.

Calibration runs were made for orifice hole diameters of 0.250, 0.375, 0.500, and 0.625 in. with the orifice assembly mounted co-axially and 0.250 in. diameter mounted eccentrically in the test section. The data are being analyzed.

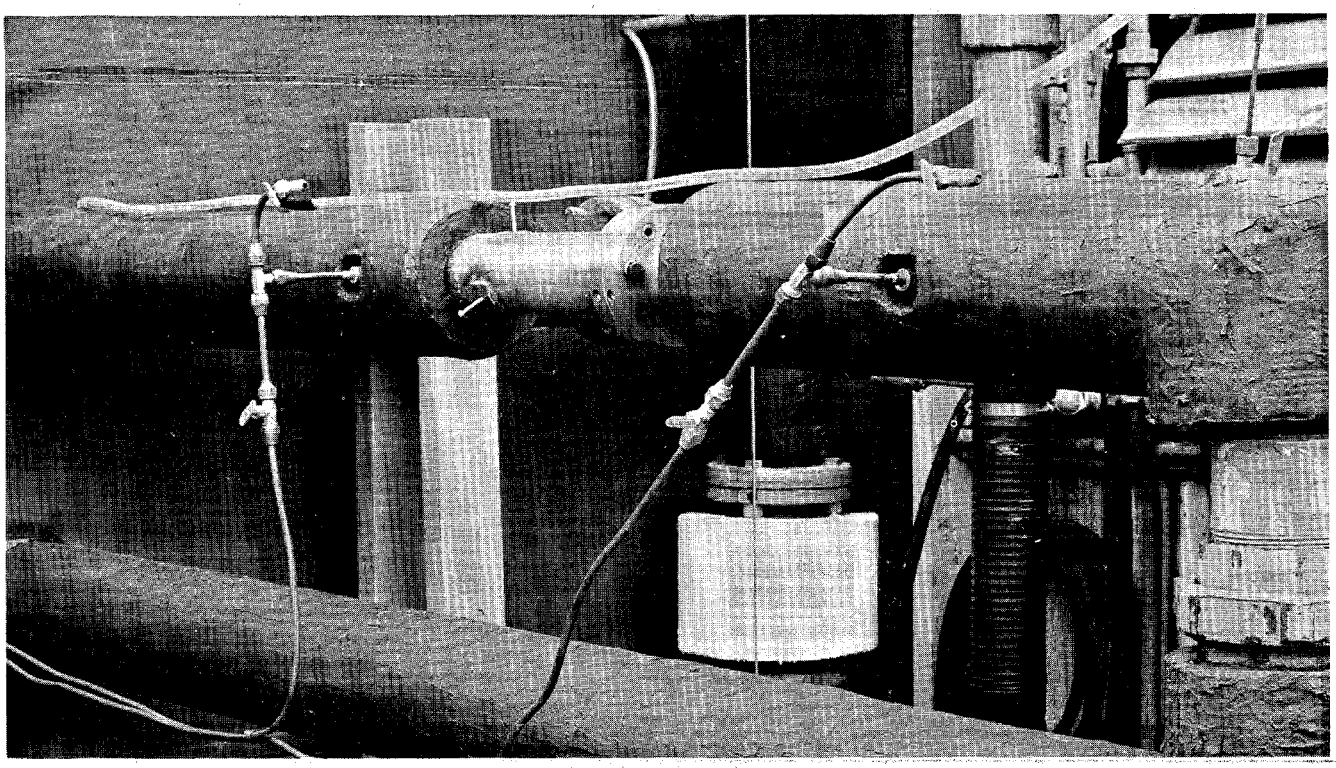

Fig. 32. Orifice Plate Showing Pressure Taps

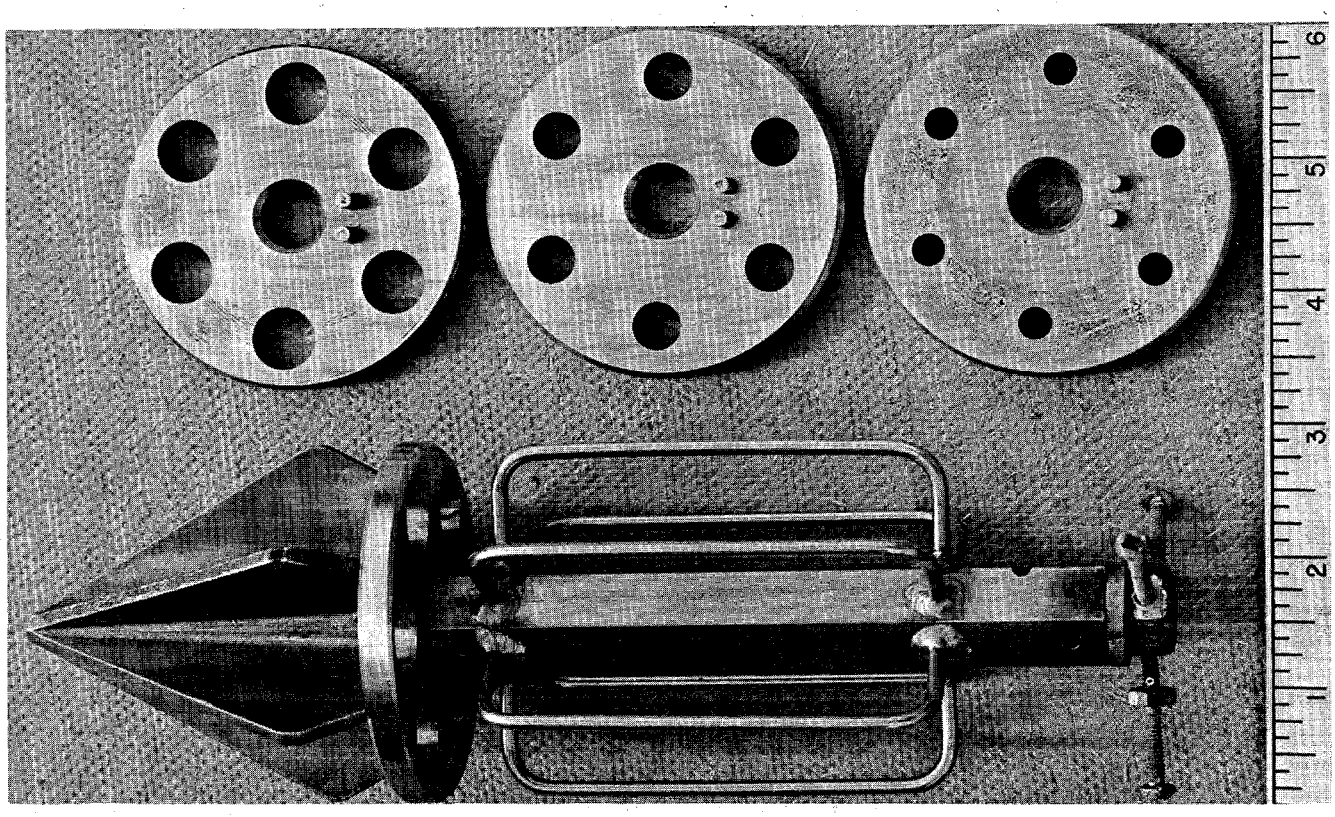

Fig. 33. Orifice Plate Disassembled

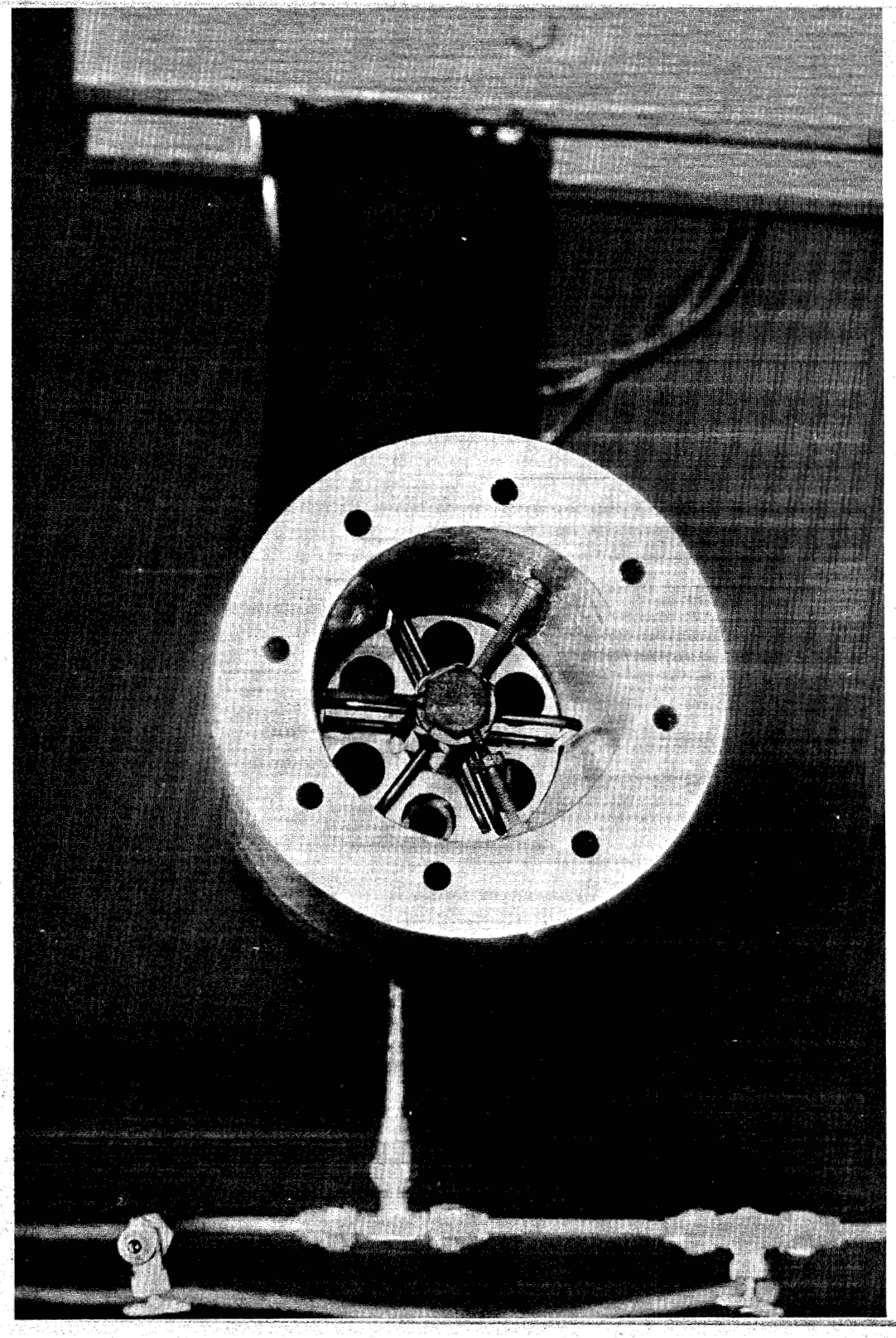

12-5-55

9693-54310

Fig. 34. Orifice Plate Assembly Mounted Co-Axially in Pipe

J. SRE EVAPORATIVE COOLERS (F. Herrmann)

Heat transfer and pressure drop were re-evaluated for use of tetralin in place of toluene and new rated and overload capacities were determined.

K. SRE MAIN AIR BLAST HEAT EXCHANGER (W. Hoschouer)

The air blast heat exchangers are scheduled for delivery May 17, 1956.

XIII. INSTRUMENTATION AND CONTROL

A. INSTRUMENTATION (J. Bauer)

1. Reactor Area - The heaters and thermocouples on the cylinder support rings are completely installed. All stainless steel sheathed thermocouples have been placed on the reactor tanks.

2. Control Room - Installation drawings and wiring diagrams for the control room have been released. Sheet metal work for the majority of the panels has been completed and the wiring of panels BB, CC, DD, and EE is nearly complete. Analog computer studies by the Systems Analysis Group simulating the reactor conditions of flow, temperature and scram transients indicate that some minor changes on the present reactor control system will have to be made.

3. Sodium Piping Area - Sheet metal work on auxiliary sodium instrument panels has been started. Drawings locating heaters, thermocouples, and leak detectors on all sodium tanks and piping were released.

4. Instrument Pickups - Assembly drawings of the sodium flowmeters were released. An investigation of the various methods of calibrating the main flowmeters was made. Because of schedule and installation difficulties, it was decided to calibrate the flowmeters in the experimental pump loop and check them after installation in the SRE.

A sodium instrumentation survey trip was made to several companies who work with sodium. Information obtained during this trip has led to further development on a long coil type sodium level indicator for use in the SRE. Tests will be made on the new design as soon as possible.

An instrumentation list identifying all instruments used in the reactor building, the radioactive waste area, and the toluene and nitrogen pad areas, with the

exception of those in and about the reactor vessel has been released. Instrument installation drawings for all pneumatic instruments were also released.

5. Electrical Power - The Phase "A" electrical contract is estimated to be 78 per cent complete. All initial drawings for Phase "B" of the electrical contract have been completed. Phase "B" includes the balance of the electrical work on the reactor building with the exception of top shield wiring and ion and fission tube installations.

B. CONTROL ROD SYSTEMS

1. Control Rod Lead Screw Development (A. E. Miller and R. Douglas) - Lead screw tests are continuing at Saginaw Steering Gear, a division of General Motors Company.

During this period the Haynes 25 screw previously tested[4] was remachined and tested. This test was made to demonstrate the adequacy of the apparatus which had been modified after the earlier tests. The test was made under the following conditions:

load - 100 lb tension
balls - Haynes 25
speed - 300 rpm
stroke - 14.5 in.
atmosphere - argon, 1/4 in. H_2O pressure
temperature - 875° F
lubrication - none

The test was ended after an increase in the torque required to drive the screw was noted. This occurred after 6 hours and 21 minutes or 900 cycles.

Examination of the specimen revealed that the screw and nut was badly oxidized and the races slightly damaged. The balls were badly deformed showing readily visible flat spots as well as signs of serious abrasion.

The oxidation of the specimen in the above described test indicated a need to improve the furnace seals. After the seals were improved the screw and nut were again tested after being vapor blasted. Conditions of this test were identical to those of the previous test with the exception that the specimen was lubricated with molybdenum disulfide and the damaged Haynes 25 balls were replaced with

steel bearing balls. This test was terminated after 615 cycles. Subsequent examination of the specimen revealed very slight oxidation and no further damage.

The furnace seal was still further improved and a new Haynes 25 screw with nickel bonded chrome carbide balls was tested under the following conditions:

load - 100 lb
speed - 220 rpm
stroke - 10 in.
atmosphere - argon, 1/4 in. H_2O
temperature - 875° F
lubrication - molybdenum disulfide

This test was interrupted when the pressure regulator controlling the furnace atmosphere failed. The specimen was undamaged although oxidized. After cleaning and lubricating, the test was continued and has logged 100 hours to date.

2. Prototype

a. Control Rod (R. Douglas, S. Elchyshyn, and A. E. Miller) - The prototype control rod with the 316 stainless steel screw was reassembled and placed in the process cylinder. The rod was cycled over a 5-ft traverse up and down for a total of 688 cycles. The temperature schedule is shown in Table VI.

TABLE VI

TEMPERATURE SCHEDULE OF CYCLED PROTOTYPE CONTROL RODS WITH 316 SS SCREW

Cycles	Temperature° F
50	70
33	525
25	650-700
10	730
50	960
55	960-1025
465	1065

The rod was maintained at 1065° F for two weeks while cycling at this temperature. At the end of a total of 688 cycles the rod jammed.

After we had cut through the thimble, we examined the internal parts and found galling between keys and keyways (Fig. 35 and 36). All other parts of the rod were in good condition.

The control rod thimble has been rewelded and the keyways remachined. New molybdenum keys with sulfided surfaces have been made to replace the damaged keys and the control rod assembled. The prototype rod is now cycling at temperature.

b. Control Rod Drive - Two Speed (S. Kuhnhoffer and A. E. Miller) - In conjunction with the above test, the prototype control rod drive was used. During the test the rate of inert gas leaks from the assembly gradually increased until the pressure changed at the rate of 0.33 psi per hour. This loss was due primarily to a leak through the rotating O-ring seals in the drive. These seals rotate in an aluminum housing in which deep grooves were worn. This housing has been replaced by steel to prevent this reoccurrence.

C. SAFETY ROD SYSTEM

1. Latch (S. Kuhnhoffer and A. E. Miller) - The chrome plated latch was "soaked" for 500 hr at 1100° F under a load equivalent to the weight of the pull tube and rings. The torque required to release the latch after "soaking" was excessive (greater than 100 lb-in.) and indicated self welding. The chrome plating has been removed from the latch parts and silver plating substituted on half the surfaces. The surfaces mating with the plated surfaces are type 316 stainless steel. This latch is now undergoing an identical test to that performed on the chrome plated latch.

2. Snubber (S. Elchychyn and E. C. Phillips) - With Haynes 25 piston rings the snubber has been operated from 70° to 1100° F. Hi-speed motion pictures of tests at 1100° F revealed that only half the snubber volume was utilized because of the pull tube support latch releasing prematurely. Also these pictures showed that the weight representing the rings collided with the end of the pull tube a number of times, instead of once as observed visually. While energy was dissipated by the series of impacts it is expected that the unused snubber volume will easily compensate for this dissipated energy.

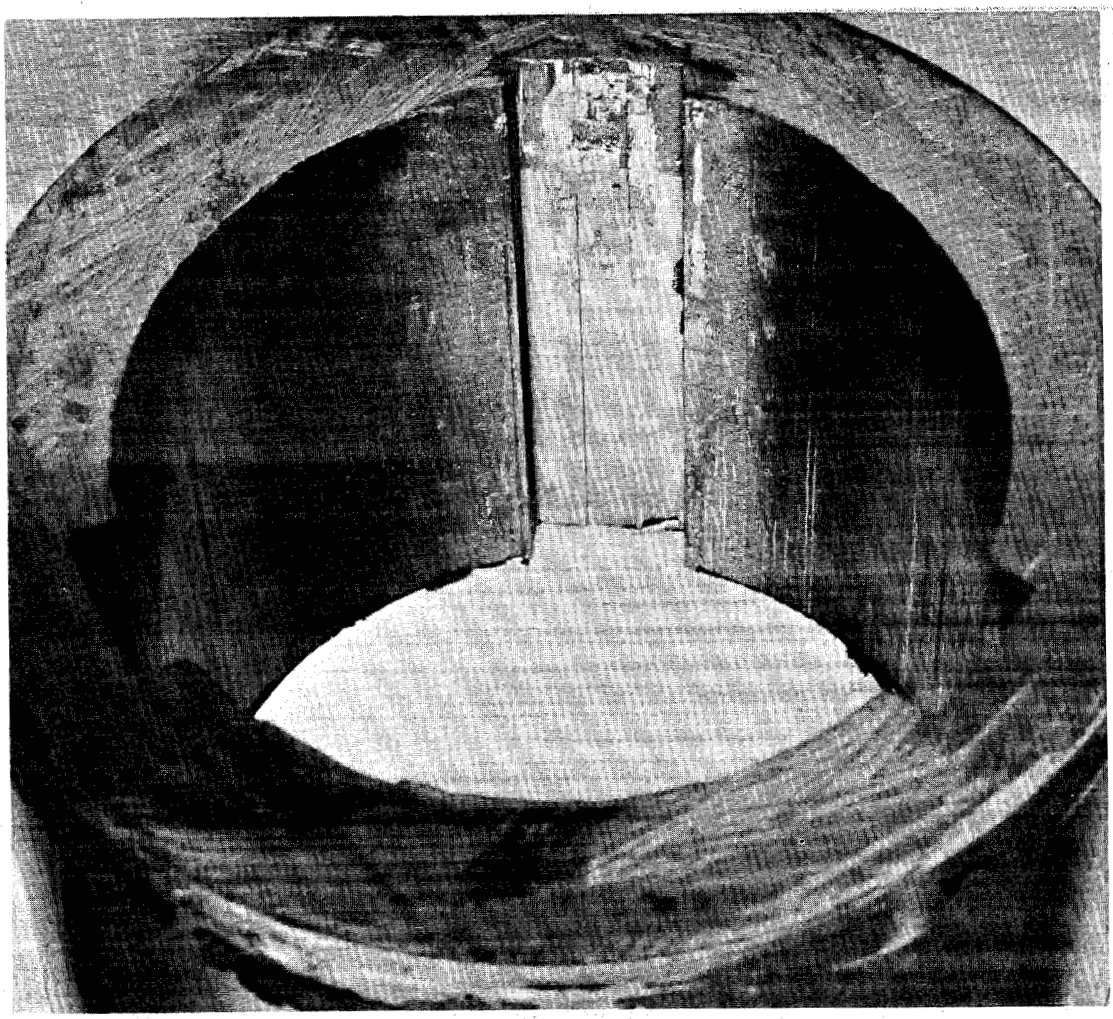

Fig. 35. Section of the Keyway Showing Galling

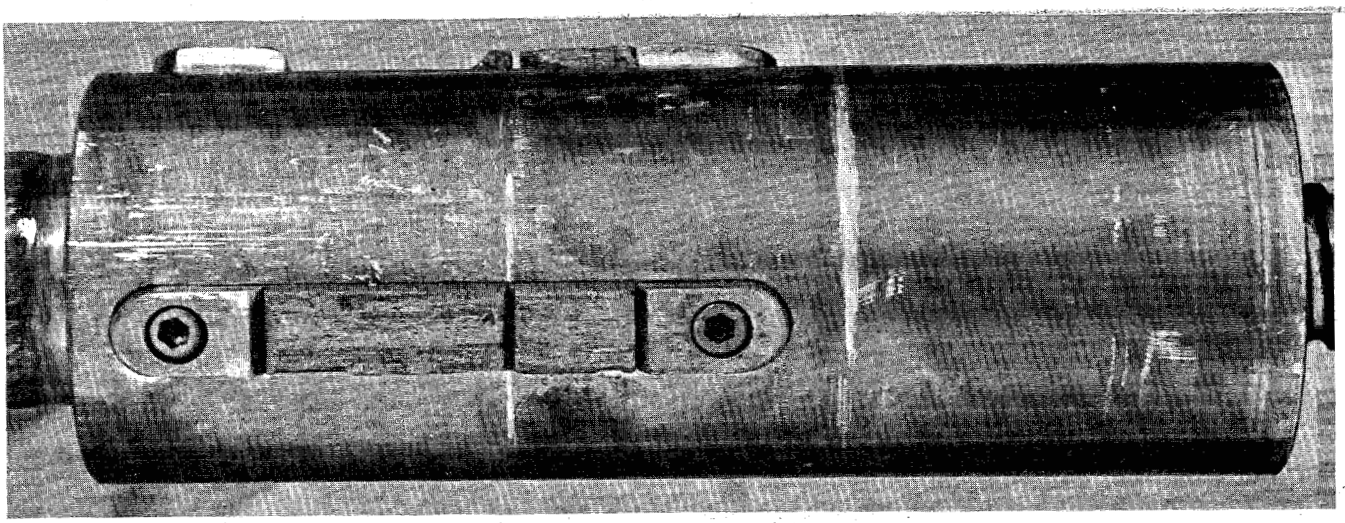

Fig. 36. Key Showing Groove Cut Through Thimble

After a number of tests at 1100° F and 50 hr at this temperature, the snubber ceased to function satisfactorily (pull tube reached end of its travel with an appreciable velocity). This was caused by a decrease of 0.040 in. in the free diameter of the Haynes 25 piston rings. The reason for the unexpected change in dimension of the rings is now being investigated. Information thus far available indicates that the rings were made from material insufficiently cold worked. Rings of larger cross section and greater cold work have been ordered. Rings of the same cross section as those tested, with what is expected to be sufficient cold work, are to be supplied by the manufacturer to replace the ones that failed.

3. Prototype (R. Douglas and A. E. Miller) - At least 90 per cent of the component parts of the prototype control rod have been completed and received. Sub-assemblies of the safety rod are now in progress.

D. CORE TANK GALLING TESTS (E. C. Phillips)

Six core tank galling tests have been made with loading pressures of 200 psig. Two sets lubricated with molybdenum disulfide have been tested. Two sets of 304 CRES against ASTM-A301 have been tested without lubrication. One set of 304 CRES against ASTM-A301 has been tested with metallic sodium added after the specimens were lubricated with MoS_2. A set of 304 CRES against ASTM-A301 specimens has also been tested with metallic sodium between the specimens.

1. 304-A301 - Unlubricated - One set of the unlubricated 304 CRES against ASTM-A301 specimens was tested at 750° F in argon while the other was tested at 500° F in argon. During the first 550 cycles of each test, the specimens were rotated through an angle of approximately 36°. During the last 50 cycles of the test, this angle was increased to approximately 50° (Fig. 37).

During the first 550 cycles of the test at 750° F, the starting torques ranged from 105 to 220 lb-in. while the running torques ranged from 220 to 110 lb-in. The surface damage to the 304 CRES specimen was 0.022 in. while that to the ASTM-A301 was 0.034 in. The surface damage is the distance from the bottom of the deepest pit to the top of largest build up of material on the surface of the specimen (Fig. 38).

During the first 550 cycles of the test at 500° F, the starting torques varied between 325 and 75 lb-in. while the running torques varied between 300 and 110 lb-in

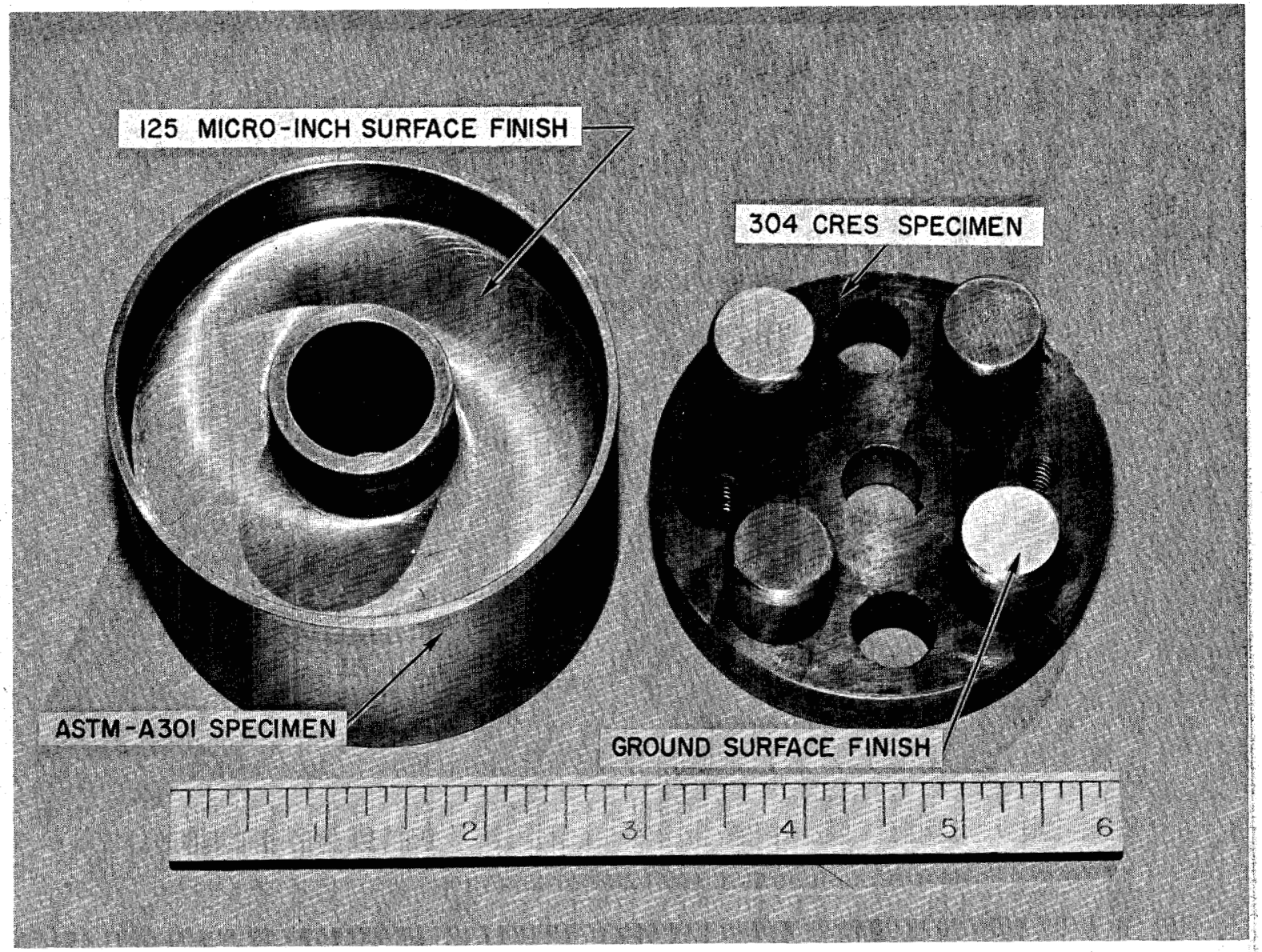

11-3-55

9693 - 52186

Fig. 37. ASTM-A301 and 304 CRES Specimens Before Testing

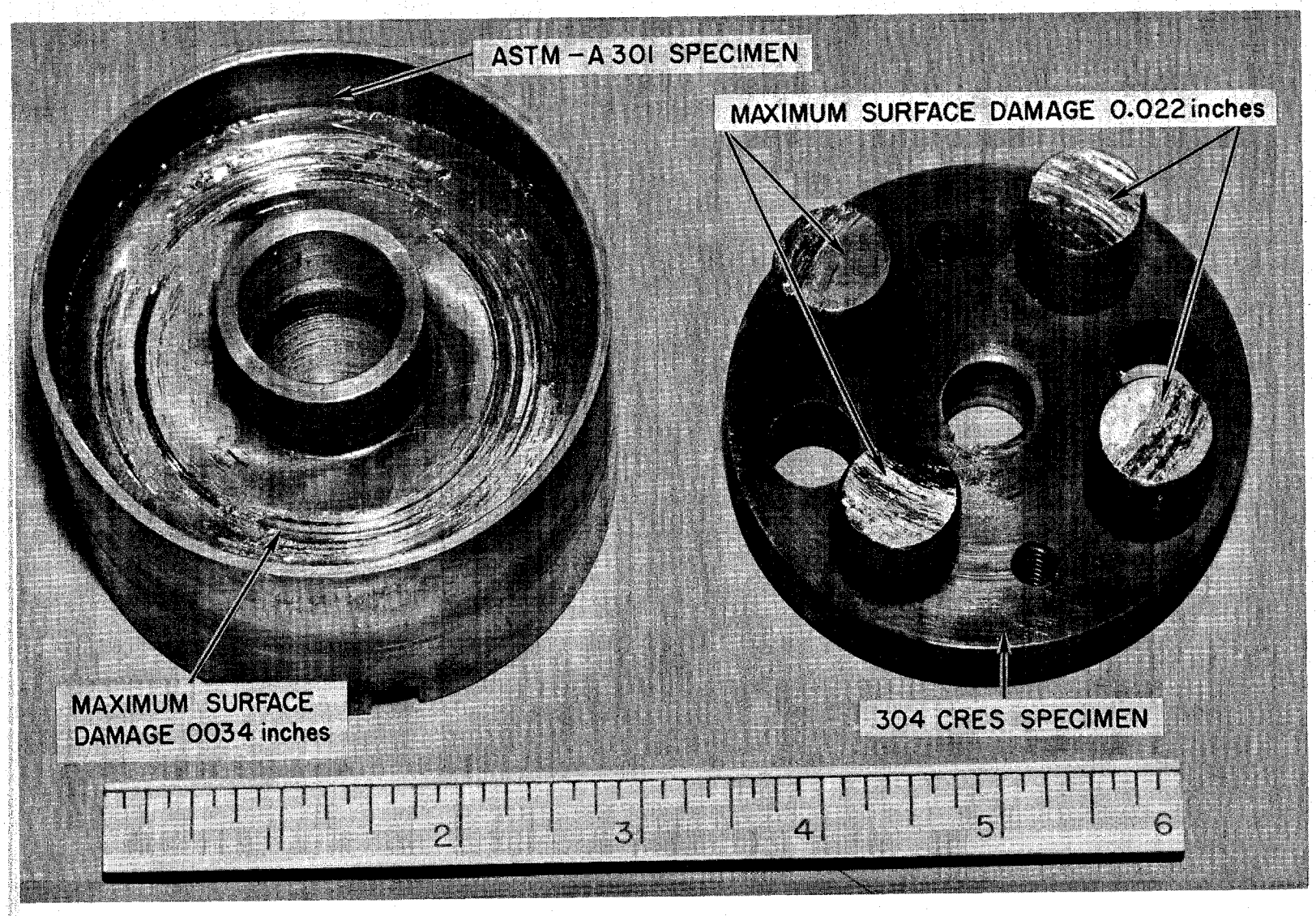

11 – 3 – 55

9693 – 52187

Fig. 38. 304 CRES vs ASTM-A301 After Test Run with No Lubrication

The high torques were experienced only during the first 20 cycles of the test. During the last 50 cycles, the starting torques ranged from 270 to 110 lb-in. and the running torques from 320 to 140 lb-in. The surface damage was 0.030 in. for the 304 CRES specimen and 0.034 in. for the ASTM-A301 specimen (Fig. 39).

2. 304 Haynes 25 Plate - A301, MoS_2 Lubricated - A segmented 304 CRES specimen was cycled against a Haynes 25 plate which rubbed in turn against a specimen of SAE4130. The specimens were generously lubricated with molybdenum disulfide. The specimens were cycled 600 times at 750° F in helium with a loading pressure of 200 psig (Fig. 40 and 41).

The starting torques varied from 14 to 26 lb-in. during the first five cycles as did the running torques. After 168 hr at temperature, 600 additional cycles were run. The starting torques varied from 15 to 70 lb-in. while the running torques varied from 15 to 60 lb-in. The surface damage to the 304 CRES was 0.003 in. while that to the SAE4130 was 0.002 in. There was no visible damage to the Haynes 25 specimen in these tests (Fig. 42).

3. 304-A301 - MoS_2 Lubricated - A 3 peg specimen of 304 CRES lubricated with molybdenum disulfide has been cycled 600 times against ASTM-A301 at 750° F in argon. During the first 550 cycles rotated through an angle of 36°, the starting torques ranged from 15 to 150 lb-in. while the running torques ranged from 12 to 135 lb-in. During the last 50 cycles through an angle of 50°, the starting torques ranged from 110 lb-in. to 50 lb-in. while the running torques varied from 50 to 80 lb-in. The surface damage to the 304 CRES was 0.025 in. while that to the ASTM-A301 was 0.017 in.

4. 304-A301 - Na + MoS_2 Lubricated - A molybdenum disulfide lubricated peg 304 CRES specimen was cycled 600 times against ASTM-A301 at 750° F in argon. Metallic sodium was added to the specimens. The first 550 cycles were rotated through an angle of 36° while the last 50 cycles were rotated through an angle of 50°. The starting torques ranged from 53 to 125 lb-in. during the first 550 cycles while the running torques ranged from 45 to 117 lb-in. During the last 50 cycles, the starting torques varied from 64 to 98 lb-in. while the running torques varied from 117 to 63 lb-in. (Fig. 43).

5. 304-A301 - Na+ Unlubricated - The surface damage to the 304 CRES was 0.003 in. while that to the ASTM-A301 was 0.011 in.

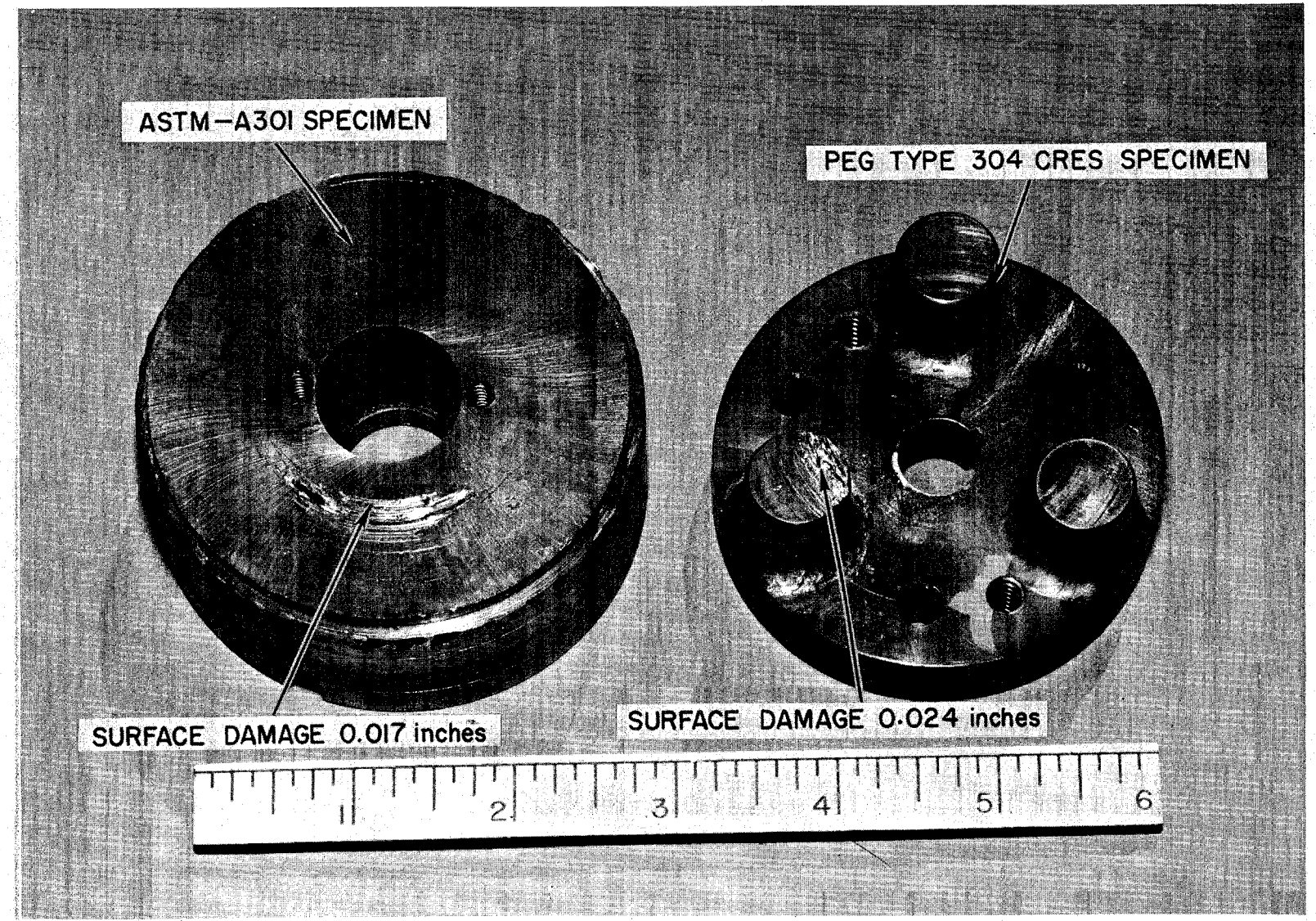

Fig. 39. 304 CRES vs ASTM-A301 After 600 Cycles at 500° F in Argon, 200 psi Loading Pressure

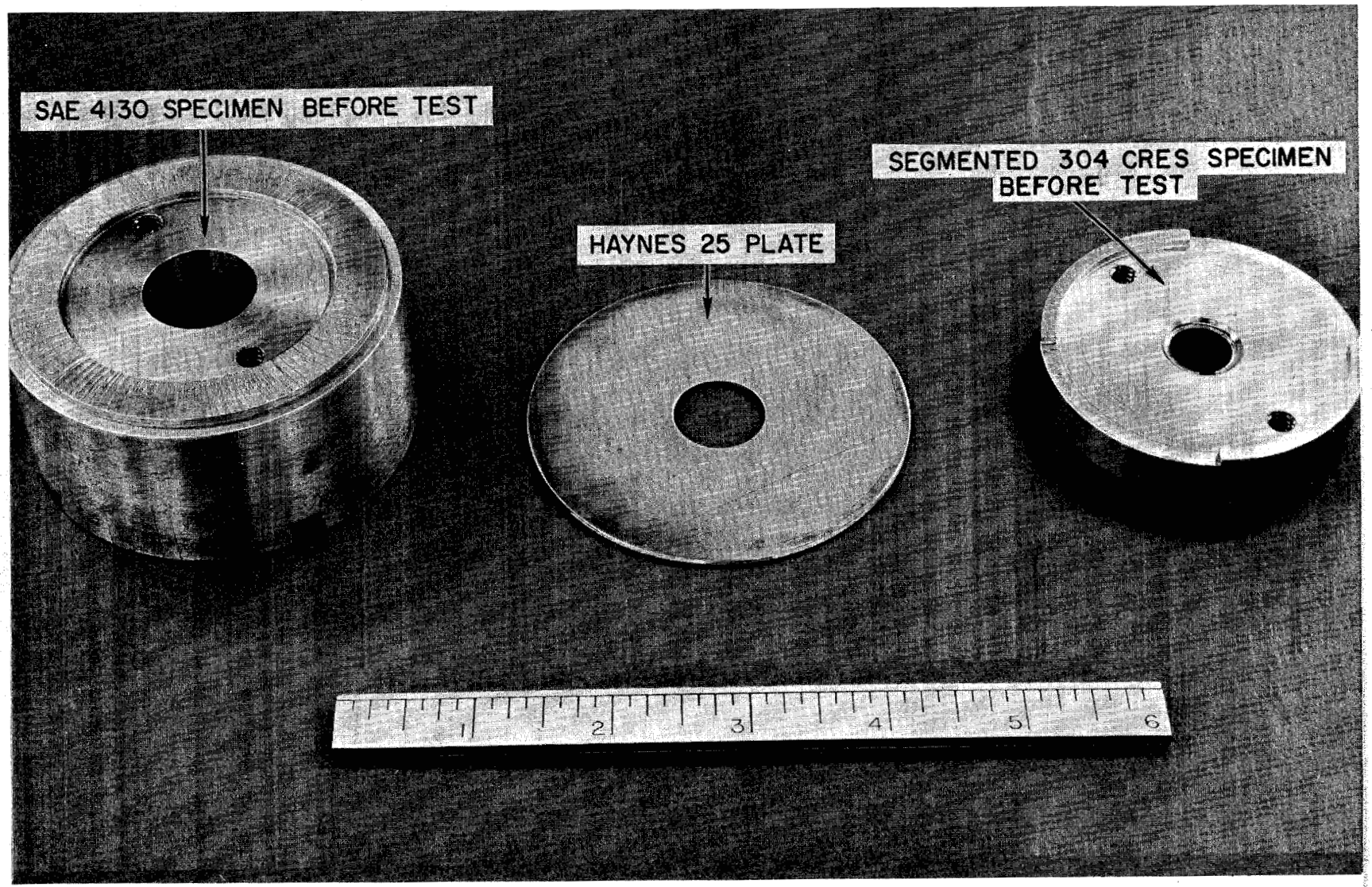

10-10-55

9693 – 5664

Fig. 40. SAE 4130, 304 CRES, and Haynes 25 Specimens Before Test

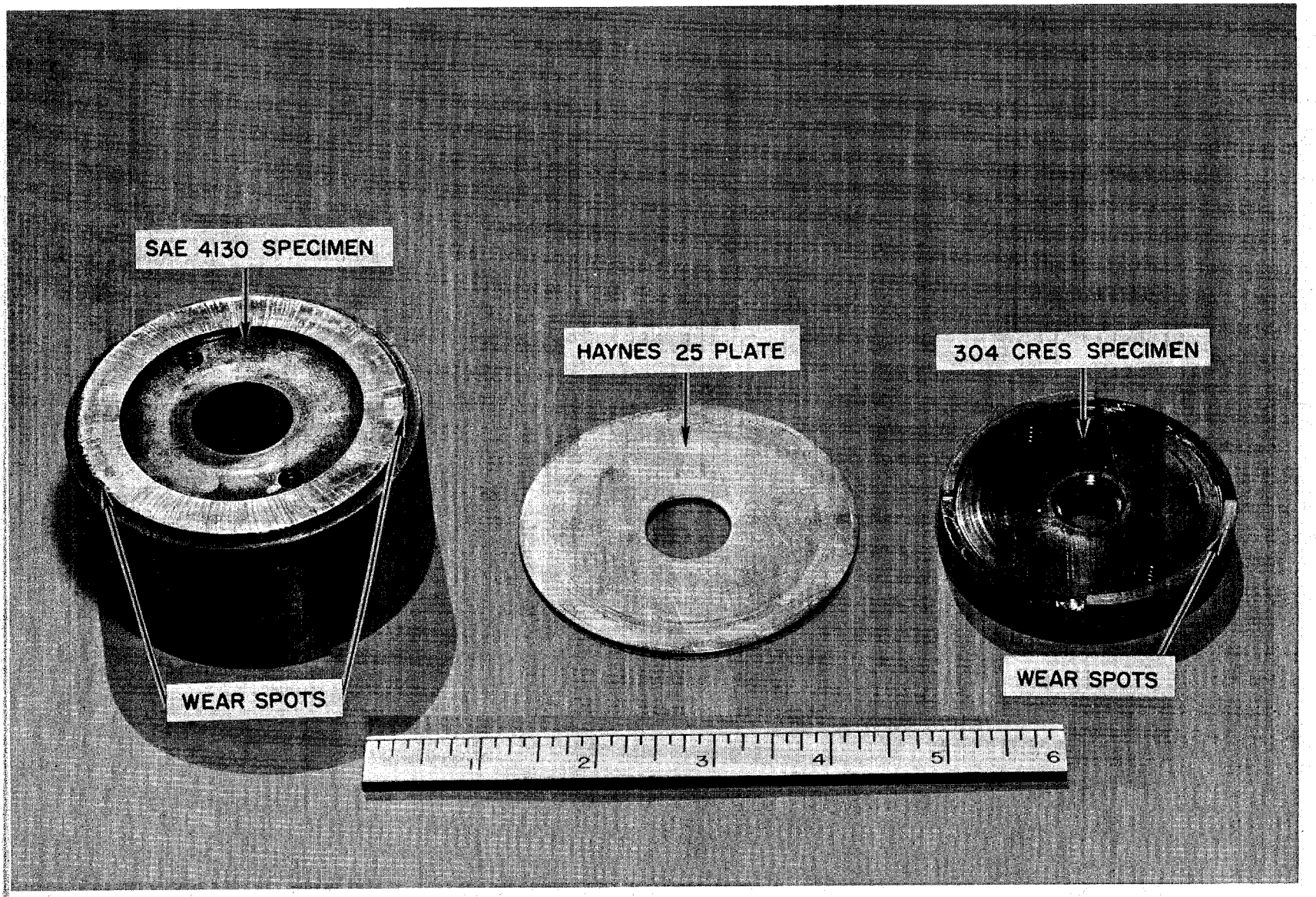

10-25-55

9693 - 52177

Fig. 41. SAE 4130, 304 CRES, and Haynes 25 Specimens After Tests with MoS_2 Lubrication

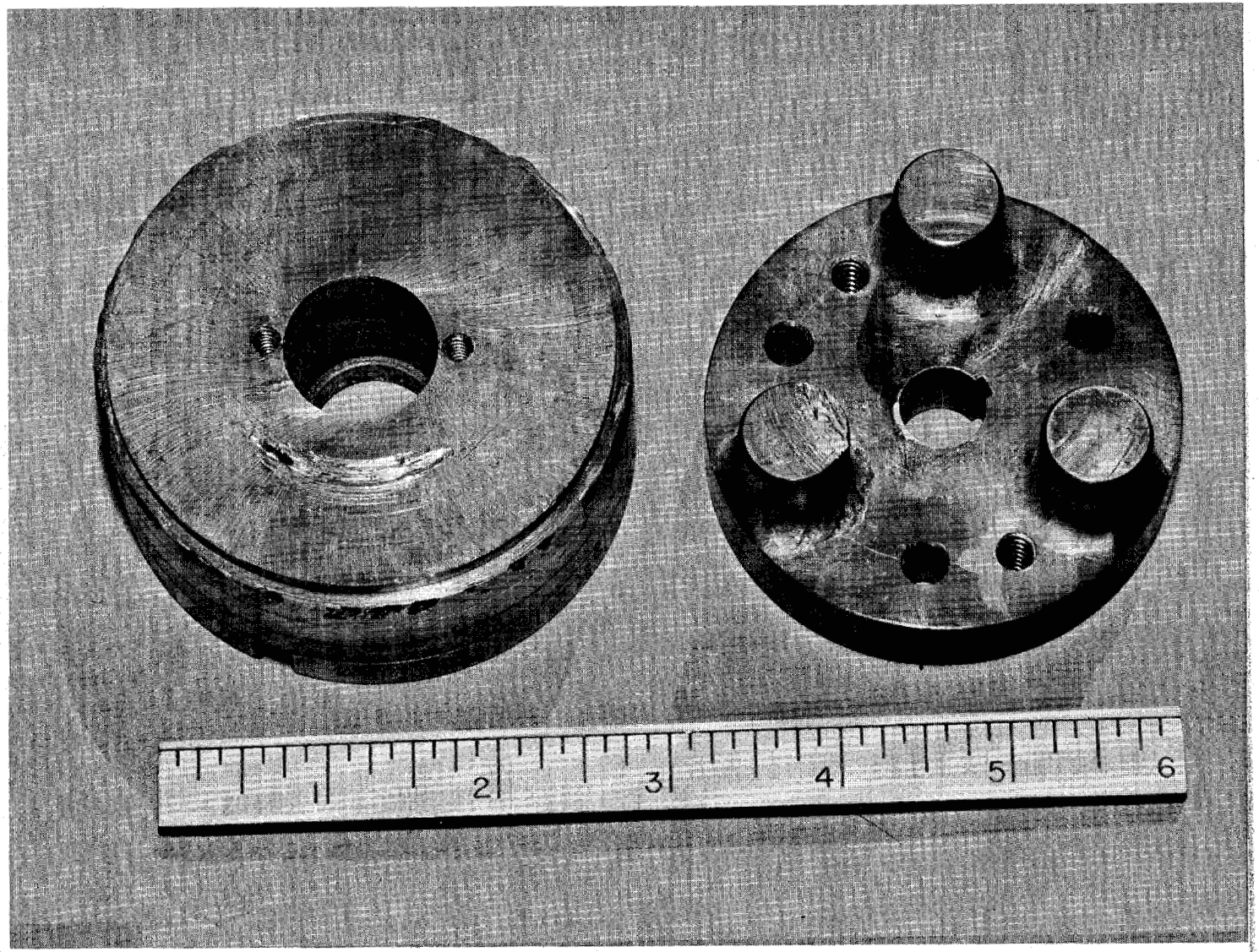

11-3-55

9693—52188

Fig. 42. 304 CRES vs ASTM-A301 After Tests with MoS_2 Lubricaion

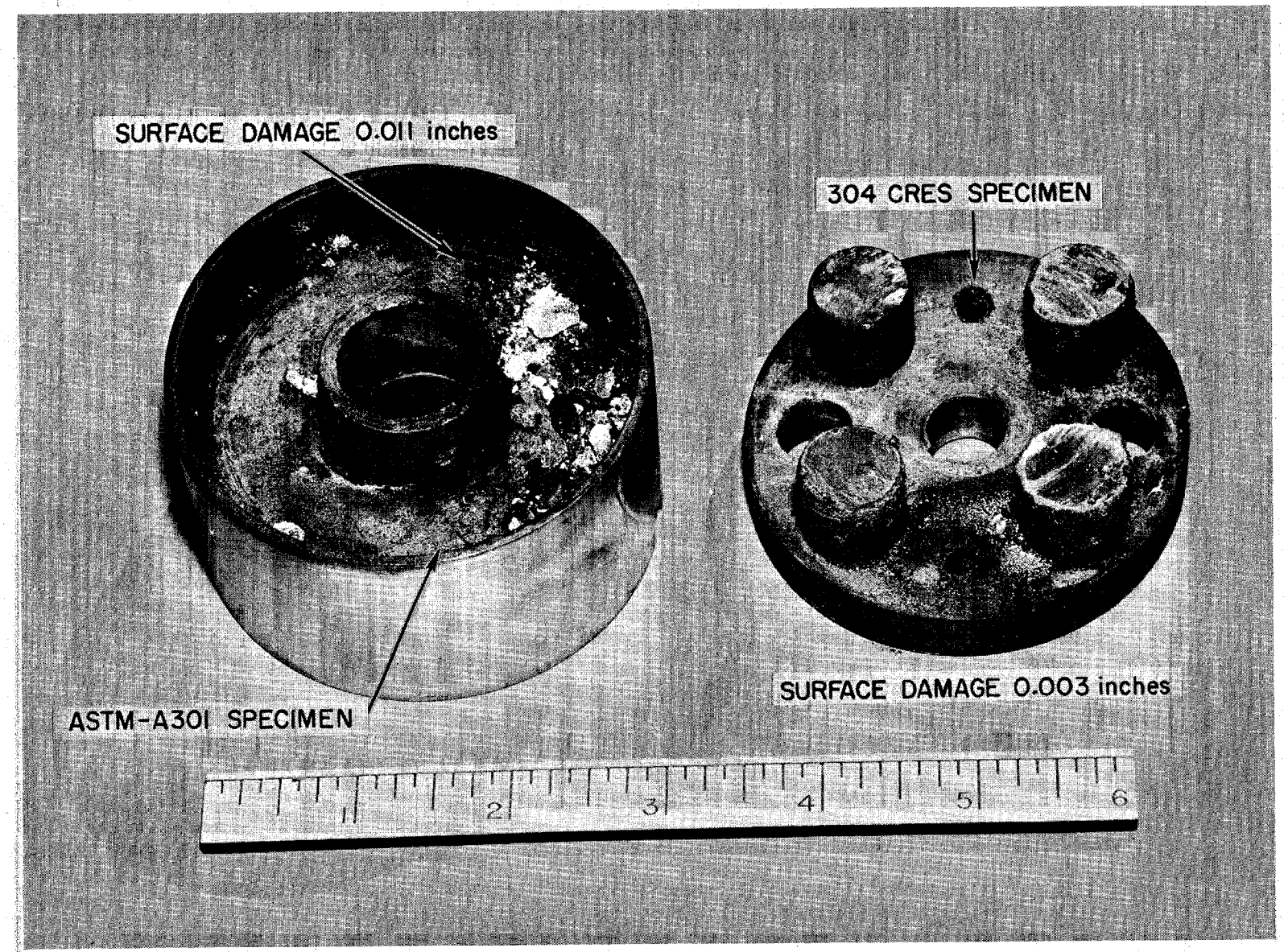

11-7-55

9693-52189

Fig. 43. 304 CRES vs ASTM-A301 Lubricated with MoS_2 with Sodium Added

A similar test was performed cycling 304 CRES against ASTM-A301 in argon at 750° F with metallic sodium placed between the specimens. The starting torque ranged from 55 to 103 lb-in. for the first 550 cycles while the running torques ranged from 50 to 101 lb-in. During the last 50 cycles the starting torques varied from 70 to 95 lb-in. while the running torques ranged from 67 to 87 lb-in. After the test the specimens showed little evidence of wear. The sodium was free of oxidation and had wetted the rubbing surfaces (Fig. 44).

E. MoS_2 IRRADIATION EXPERIMENT (K. Horton)

The control rod mechanism in the SRE incorporates a ball screw drive operating at elevated temperatures. It is proposed to use MoS_2 as a lubricant for the ball screw; however, very little is known of the effects of irradiation on MoS_2. A preliminary experiment in the statitron indicated a change in orientation of the MoS_2 on a specimen. This test was conducted at room temperature and the results cannot be extrapolated to elevated temperatures. For this reason it has been decided to irradiate MoS_2 at various temperatures in the gamma facility at MTR. It is proposed to measure the coefficient of friction of MoS_2 before and after irradiation.

Small cylindrical specimens of A-301 and 304 stainless steel, Haynes 25 alloy, and molybdenum were coated with MoS_2 (the MoS_2 was produced in situ), and a rig has been built to measure the coefficient of friction of the MoS_2 coated specimens. These specimens are to be canned in stainless steel containers filled with helium. Clam shell heaters will surround the specimen containers and Super-X insulation will be used to allow for three separate hot zones. These hot zones, and the specimens therein are: A-301 and 304 stainless steel at 500° F, Haynes 25 alloy, 304 and A-301 at 800° F, and molybdenum and Haynes 25 alloy at 1100° F. The entire apparatus is canned in 61S-T, 3.0 in. OD. The aluminum tube fits between the spent fuel elements in the gamma canal at MTR. Thermocouples sealed to each specimen container will be wired to Brown Electronic controller-recorders for temperature control. The thermocouple leads will be brought from the 3.0 in. aluminum to the surface of the gamma canal through a 0.625 in. OD aluminum tube shaped as a spiral (to prevent scattered gamma rays from reaching the air above the canal).

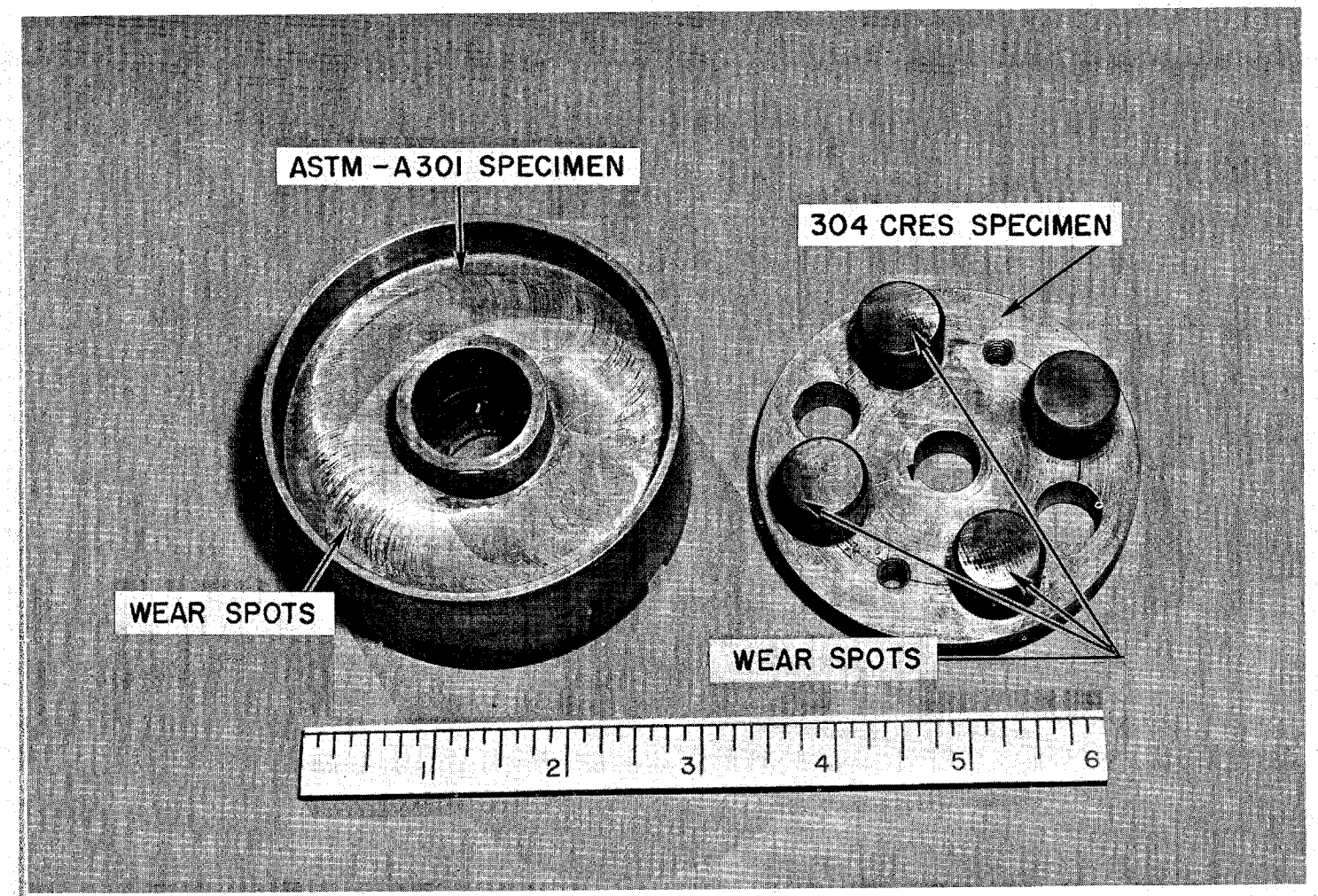

11 – 9 – 55

9693 – 52190

Fig. 44. 304 CRES vs ASTM-A301 Lubricated with Sodium

All materials necessary for completion of assembly of the apparatus to irradiate specimens in the gamma facility of the MTR are on order. The various specimens (A-301 and 304 stainless steels, molybdenum, and Haynes 25 alloy) have been machined and coated with MoS_2. The coefficient of friction of the MoS_2 is being determined by using strain gages for friction force measurements prior to gamma-irradiation. The stainless steel specimen cans have been partially assembled, awaiting the completion of friction measurements of the specimens. One specimen can has been completely assembled and heated to 1100° F to test for leak tightness of the enclosed MoS_2 coated specimen.

XIV. SHIELDING

A. TOP SHIELD (L. A. Wilson)

Calculations performed over 18 months ago relative to the shielding requirements for the top shield are being reviewed and brought up to date. The principal design change which has taken place is that the thickness of the thermal shield was reduced 3 in. and an appropriate thickness of heavy concrete substituted in its place. The dose buildup factor for the heavy concrete to be used in the top shield was calculated for both point isotropic and plane monodirectional sources by following the method of Goldstein and Wilkins.[12] By this method the effective atomic number of the heavy concrete was found to be 19, while for ordinary concrete a value of 12 was obtained. The dose buildup factors for these concretes are listed in Table VII. These were fitted to a quadratic form which is used in the analysis of the dose rate from capture gamma rays generated in the shield itself. The constants so derived are listed in Table VIII. The capture gamma ray spectrum of the heavy concrete was also evaluated and is listed in Table IX. (See also Fig. 45. The composition of the heavy concrete is included in Table IX, while that for ordinary concrete is taken from data published by the National Bureau of Standards.[13] The formulas used in the capture gamma ray portion of the analysis are being fitted to a nomograph because of the multiplicity of variables involved in this formulation.

B. FUEL HANDLING COFFIN (R. L. Ashley)

Samples of the rolled lead, now being machined for the fuel handling coffin, were examined during a visit to a supplier. A fair amount of porosity existed in

TABLE VII

DOSE BUILDUP FACTOR (B_r)-POINT ISOTROPIC SOURCE

Point Isotropic Source Heavy Concrete (Z=19)							
E_o, Mev \ $\mu_o r$	1	2	4	7	10	15	20
0.5	2.15	3.7	7.6	16	27	52	85
1	1.96	3.1	5.9	11.7	18.6	33	51
2	1.77	2.53	4.4	7.7	11.6	18.2	26
3	1.6	2.25	3.65	6.0	8.6	13.3	18.5
4	1.5	2.0	3.1	5.0	7.0	10.5	14.5
6	1.39	1.8	2.65	4.1	5.8	8.8	12.4
8	1.30	1.62	2.3	3.5	4.8	7.3	10.2
10	1.24	1.5	2.05	3.0	4.15	6.4	9.2

Plane Monodirectional Source Heavy Concrete (Z=19)							
E_o, Mev \ $\mu_o r$	1	2	4	7	10	15	20
0.5	2.3	3.35	6.1	10.8	17.5	30	46
1	2.04	2.95	5.1	9.0	13.3	21.5	31
2	1.77	2.45	3.95	6.4	9.1	14	20
3	1.6	2.2	3.4	5.4	7.4	11.3	15.5
4	1.5	1.98	3.0	4.6	6.3	9.3	13
6	1.39	1.75	2.55	3.8	5.2	7.7	10.5
8	1.3	1.6	2.23	3.24	4.4	6.5	9
10	1.24	1.5	2.0	2.9	3.9	5.9	8

Ordinary Concrete (Z=12)							
E_o, Mev \ $\mu_o r$	1	2	4	7	10	15	20
0.5	2.4	4.4	10	23	42	87	155
1	2.05	3.35	6.7	13.5	22	39	61
2	1.8	2.65	4.7	8.2	12	19	26.5
3	1.65	2.35	3.8	6.2	8.7	13	17.5
4	1.53	2.1	3.25	5.05	6.9	10.1	13
6	1.43	1.86	2.7	4.05	5.45	7.8	10.2
8	1.35	1.7	2.36	3.45	4.5	6.4	8.2
10	1.3	1.55	2.14	3.0	3.9	5.5	7.1

Ordinary Concrete (Z=12)							
E_o, Mev \ $\mu_o r$	1	2	4	7	10	15	20
0.5	2.5	3.9	7.7	15	25.5	48	80
1	2.15	3.2	5.9	10.2	15.5	25	37
2	1.8	2.6	4.1	6.7	9.6	14.3	19.5
3	1.65	2.3	3.5	5.5	7.5	10.5	14
4	1.53	2.04	3.06	4.65	6.2	8.9	11.5
6	1.43	1.8	2.6	3.8	5.0	7.1	9.4
8	1.35	1.66	2.28	3.2	4.15	5.9	7.8
10	1.3	1.55	2.05	2.9	3.7	5.1	6.5

TABLE VIII

CONSTANTS FOR THE QUADRATIC* REPRESENTATION OF THE DOSE BUILDUP FACTOR

	Heavy Concrete			
	Point Isotropic		Plane Monodirectional	
E_o, Mev	C_1	C_2	C_1	C_2
0.5	1.0	0.16	1.05	0.059
1	0.89	0.083	0.94	0.0285
2	0.74	0.025	0.72	0.0105
3	0.6	0.015	0.584	0.0068
4	0.49	0.0098	0.486	0.0043
6	0.380	0.0094	0.37	0.0051
8	0.294	0.0085	0.288	0.0054
10	0.23	0.0088	0.233	0.006

	Ordinary Concrete			
	Point Isotropic		Plane Monodirectional	
E_o, Mev	C_1	C_2	C_1	C_2
0.5	1.1	0.32	1.2	0.127
1	1.0	0.103	1.07	0.0315
2	0.80	0.029	0.78	0.0075
3	0.663	0.0091	0.642	0
4	0.542	0.0029	0.522	0
6	0.424	0.0009	0.406	0
8	0.344	0.0009	0.328	0
10	0.28	0.0013	0.274	0

* $B(\mu_o r) = 1 + C_1 \mu_o r + C_2 (\mu_o r)^2$

TABLE IX
CAPTURE GAMMA RAYS FROM HEAVY CONCRETE

Composition gm/gm concrete		Cross Section (cm^2/nuc.) x 10^{24}	nuclei/gm x 10^{-24}	cm^2/gm concrete	% of captures	References to Capture Gamma Rays
Fe	0.565	2.43	0.01078	0.0149	89.6	Phys. Rev., 89, 375 (1953)
H	0.0062	0.33	0.5975	0.00122	7.35	Phys. Rev., 92, 211 L (1953)
O	0.332	0.000	0.01879	0.000	0.00	
Mg	0.0079	0.059	0.02476	0.0000115	0.069	Phys. Rev., 83, 519 (1951)
Ca	0.0557	0.406	0.01503	0.00034	2.04	Phys. Rev., 85, 1012 (1952)
Si	0.0245	0.160	0.02146	0.000083	0.50	Phys. Rev., 83, 519 (1951)
Al	0.0055	0.215	0.02233	0.0000264	0.159	Phys. Rev., 83, 519 (1951)
S	0.0008	0.49	0.01879	0.00000735	0.044	Phys. Rev., 85, 1012 (1952)
P	0.0013	0.193	0.01944	0.00000488	0.029	Phys. Rev., 85, 1012 (1952)
Na	0.0005	0.47	0.02619	0.00000615	0.037	Phys. Rev., 83, 519 (1951)
K	0.0006	1.89	0.01540	0.0000175	0.105	Phys. Rev., 85, 1012 (1952)
				$\sigma_{n,\gamma}$ = 0.01661678		

Energy Interval	Photons/100 Captures	Energy Interval	Photons/100 Captures	Energy Interval	Photons/100 Captures
$2.1 \leq E < 2.3$	7.350	$5.5 \leq E < 5.7$	0.084	$8.9 \leq E < 9.1$	0.0
$2.3 \leq E < 2.5$	0.0	$5.7 \leq E < 5.9$	0.259	$9.1 \leq E < 9.3$	2.421
$2.5 \leq E < 2.7$	0.325	$5.9 \leq E < 6.1$	9.652	$9.3 \leq E < 9.5$	0.0
$2.7 \leq E < 2.9$	0.048	$6.1 \leq E < 6.3$	0.025	$9.5 \leq E < 9.7$	0.0
$2.9 \leq E < 3.1$	0.035	$6.3 \leq E < 6.5$	2.160	$9.7 \leq E < 9.9$	0.0
$3.1 \leq E < 3.3$	0.024	$6.5 \leq E < 6.7$	0.002	$9.9 \leq E < 10.1$	0.0
$3.3 \leq E < 3.5$	1.810	$6.7 \leq E < 6.9$	0.034	$10.1 \leq E < 10.3$	0.090
$3.5 \leq E < 3.7$	0.834	$6.9 \leq E < 7.1$	0.003	$10.3 \leq E < 10.5$	0.0
$3.7 \leq E < 3.9$	0.467	$7.1 \leq E < 7.3$	3.186	$10.5 \leq E < 10.7$	0.002
$3.9 \leq E < 4.1$	0.090	$7.3 \leq E < 7.5$	0.042		
$4.1 \leq E < 4.3$	1.916	$7.5 \leq E < 7.7$	32.301		
$4.3 \leq E < 4.5$	1.533	$7.7 \leq E < 7.9$	0.095		
$4.5 \leq E < 4.7$	0.041	$7.9 \leq E < 8.1$	0.001		
$4.7 \leq E < 4.9$	1.041	$8.1 \leq E < 8.3$	0.006		
$4.9 \leq E < 5.1$	1.191	$8.3 \leq E < 8.5$	0.716		
$5.1 \leq E < 5.3$	0.053	$8.5 \leq E < 8.7$	0.021		
$5.3 \leq E < 5.5$	0.132	$8.7 \leq E < 8.9$	0.450		

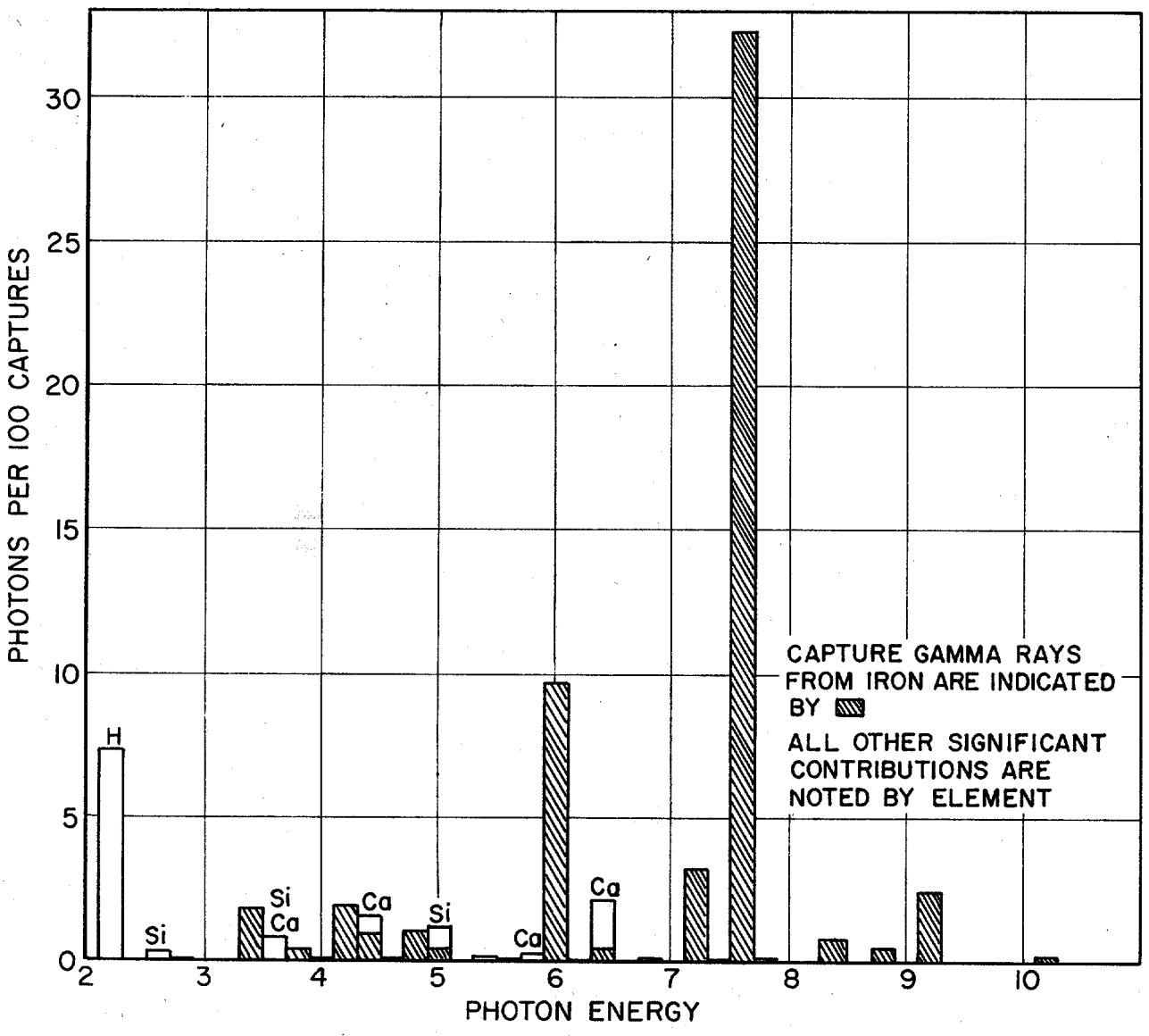

Fig. 45. Capture Gamma Ray Spectrum for Heavy Concrete

the thicker pieces. Tests are being carried out to determine the magnitude of the problem and the effect on the radiation level at the surface of the coffin.

C. GALLERY SHIELDING (A. R. Vernon)

As previously reported,[4] the design of the shoulder supporting the gallery shield blocks permits radiation levels of the order of 30 to 60 r/hr above the gaps between the blocks and the gallery walls. Reduction of these dangerous radiation levels can be accomplished by inserting 2-in. lead slabs along the gallery wall. These slabs would rest on the ledge which now forms a bearing surface for the shield blocks. (It would then be necessary to design a mating recess in the shield blocks.) Calculations were made which indicated that, for a slab 16 in. high and 2 in. thick, the radiation level could be reduced by a factor of about 1×10^3. The cost of the lead required for this modification was estimated to be $12,000, or roughly four times the cost of the 4 in. of lead shielding which, if placed over the gap at floor level, would reduce the radiation level to a tolerance value.

Concerning the problem of painting the gallery and vault walls, calculations were completed indicating that a paint which can withstand a total integrated exposure of 1×10^9 will have a life equivalent to at least 10,000 hr of full power reactor operation. The maximum radiation level occurs along only a small portion of the west wall of the heat exchanger wing of the main primary gallery. In most areas, the paint should last from two to three times as long as that exposed in the maximum radiation field.

D. HOT CELL WASTE DISPOSAL (A. R. Vernon)

The problem of removal of stainless steel cladding, which has been stripped from the fuel rods, from the hot cell was investigated. Assuming a one-year fuel rod life, the activity of the cladding was calculated to be 5.25 c/lb. (The decay period was assumed long enough so that only Fe^{59} and Co^{60} contribute.) This activity corresponds to a radiation level of about 83 r/hr-lb at a distance of 1 ft. A 5-in. iron shield would reduce this by a factor of 28 while 5 in. of lead would give an attenuation by a factor of 1200. Work is continuing on this problem.

E. FUEL CLEANING CELL (R. L. Ashley)

The design of the cleaning cell trench shield plugs was reviewed. The following additions and changes were recommended:

1. Heavy concrete shield blocks 6 in. thick should be added beneath the SE corner of the large shield block over the west trench. This is required to prevent exposure of personnel on the reactor floor and to direct radiation from the pump and cold trap located in the west trench.
2. A shielding step should be added on the south face of the northernmost shield block. As a result, a mating step should also be added along a similar portion of the large north shield block.
3. It will be necessary to add steel shot in the six small trenches feeding between the north trench and the individual cleaning cells. This will necessitate the addition of six retainer rings where these trenches meet the north trench.

F. SODIUM PUMPS (R. L. Ashley and A. R. Vernon)

A major effort of the Shielding Unit during this quarter was devoted to the analysis of the sodium pumps. As a result of the addition of the shot retainer assembly, a maximum vertical gap of 3/32 in. was to exist between the upper half of the assembly and the outer case of the primary sodium pump. Because the outer casing is out-of-round, the maximum gap will be 1/8 in. This situation will result in a 50 per cent increase in the maximum radiation level, which is not expected to exceed AEC tolerance.

Recent developments in the fabrication of the pump shaft housing appear to necessitate the removal of a portion of the brass shielding insert located above the step in the shaft. The effect of removing this shielding was investigated with a recommendation that 7 in. of additional lead be placed in the annulus above the 15-in. lead shield already present. This additional lead will fill the void space which provides a diagonal streaming path when the upper part of the brass shield is removed. The close tolerances required on the 15-in. lead shield need not be maintained on the 7-in. piece.

The use of an oil lubrication system for the main sodium bearing is not desirable. The possibility of oil residue mixing with the primary sodium would aggravate corrosion problems. Oil would also tend to clog the small diameter sodium carrying pipes. Therefore, grease packed bearings will be substituted for the present oil lubricated system.

The use of grease would depend on the magnitude of the radiation field at the bearings. The radiation level at the bearings was calculated; two sources were considered, the sodium within the pump and that exterior to the pump. The maximum dose rate due to sodium within the pump was found to be 2.7×10^4 r/hr, with general levels of about 1.5×10^4 r/hr. The variation is caused by several shielding weak points in the internal structure of the pump. The total dose rate from all external sources (sodium pipe lines, the cold trap, and the heat exchanger) was calculated to be 2.5×10^4 r/hr. The maximum total dose rate, from both internal and external sodium, is thus 5.2×10^4 r/hr. Since a suitable grease may be obtained which can tolerate a total integrated exposure of about 1×10^9, such a grease can be used for a total of 2×10^4 hr of full power operation.

In connection with the above analysis, it is interesting to note that preliminary calculations determining the radiation level around the main primary heat exchanger were completed. The results indicate that the maximum radiation level is 0.9×10^6 r/hr, and this occurs between the two legs of the main heat exchanger, at the surface of either of the headers. The radiation level midway between the two legs of the heat exchanger was calculated to be 0.60×10^6 r/hr, while that midway between the two legs, where the headers meet the rest of the unit, is 0.75×10^6 r/hr. The radiation levels 1 ft above and below these positions were also investigated; in general, they were found to be about 30 per cent lower.

G. SODIUM SERVICE SYSTEM (A. R. Vernon)

Calculations were performed which indicated that no shielding will be required over the E. M. pump pit located in the secondary area. It was recommended, however, that the pit be covered securely and that appropriate warning signs be posted to prevent inadvertent access to the interior of the pit during operation. The radiation levels at the bottom of the pit will be as high as 10 r/hr.

The design of the sodium level indicator was reviewed. It was recommended that the ID of the thimble be decreased 1/8 in. to reduce neutron streaming which could cause excessive radiation levels at the shield surface.

The design of both the shield plug and the mechanical arrangement for sampling sodium in the primary fill tank were reviewed with several modifications suggested in discussions with the Design Group. Calculations of the shielding requirements for removal of a "hot" 30 cc sodium sample were completed.

H. INERT GAS SYSTEM (R. L. Ashley)

Several situations are being investigated in which the present system design permits the uncontrolled release of potentially hazardous quantities of radioactive gases to the SRE environs. A preliminary analysis revealed two such situations, the source in both cases being C^{14} activity produced in the nitrogen atmosphere of the galleries. The first situation arises because analysis has revealed a nitrogen leakage rate between 60 and 260 ft^3/day from the primary galleries as well as the fill tank and disposable cold trap vaults. Calculations completed by members of the Health Physics Group, showed that, were the entire leakage volume to find its way into the reactor room, no inhalation hazard would exist. However, no estimates were made of the relative hazard involved if the gas were to escape from the vaults to the atmosphere. (The atmosphere in the vaults is in direct communication with that in the galleries.) Furthermore, no consideration was given to hazards which would arise if a pipe were to rupture so that fission gases, which were circulating in the coolant stream, would escape. The second source permitting the uncontrolled release of radioactive gases is the constant pressure tank, which again communicates with the atmospheres in the galleries. The original equipment specification for this tank called for its being a gastight container. The supplier has, however, decided to use a membrane seal which will permit leakage to the atmosphere at the rate of about 0.1 per cent per day (1 ft^3/day) and he has requested an exception to this particular point in the specifications. Here again, no estimates have been made as to the possible hazard involved. These situations are currently under investigation.

I. VIEWING DEVICE (R. L. Ashley)

The design of the viewing device was reviewed. The lead shielding contained within the device was rearranged, and about 2 in. was removed. A small amount of neutron shielding was added to attenuate stray neutrons present in the galleries and due to leakage through the thermal shield.

The equipment specification for this device was also reviewed. The viewing device can be used practically anywhere in the reactor building (and possibly in any exterior location, e.g., the fill tank or cold trap vaults) while the reactor is operating, but not in the holes provided in the top shield because of radiation damage and handling problems due to the high neutron and gamma ray fluxes beneath

the reactor shield. Shielding which has been provided in the viewing device would be adequate if the device were used for viewing the core with the fuel remaining in place after shutdown.

XV. REACTOR SERVICES

A. SODIUM SERVICE SYSTEMS (A. M. Stelle, H. A. Ross-Clunis, and G. R. Cogswell)

A disposable cold trap in the sodium service system filters oxides from the sodium before it is stored in the primary fill tank. This disposable cold trap had an economizer similar to that of the cold traps in the heat transfer circuits. Belatedly, it was realized that when the cold trap is used to clean the primary traps, the oxide concentration in the sodium will be high; and therefore, the economizer for the disposable cold trap has been deleted. Controlled electric heating has been added to piping to and from the disposable cold trap.

The disposable cold trap has a boiling fluid circulating system to remove heat from the trap. Whenever sodium from the primary fill tank is being cold trapped, toulene will be used as the circulating fluid. When this is the case, the temperature of the sodium entering the trap will be relatively low, about 350° F. A jacket of toluene around the disposable cold trap would be effective since the boiling temperature of toluene is 232° F. When a disposable cold trap is used to clean the dirty cold trap in the primary heat transfer systems, higher sodium temperatures will be used (about 600° F) so as to effect the oxide transfer as quickly as possible. In this operation, tetralin (boiling temperature, 405° F) will be used as the circulating fluid in order to maintain an efficient working fluid height in the jacket around the disposable cold trap.

Controlled electric heaters were added on the piping to and from each plugging meter. In the plugging meter circuit, there is also a heat exchanger which uses a cooling fluid. By regulating the heaters and heat exchanger, the sodium temperature for a plugging indication can be accurately controlled.

The P and I diagram for the lubricating oil system for the gear boxes in the main air blast heat exchanger has been issued. The oil will be cooled in a heat exchanger using the toluene system for cooling.

A P and I diagram has been issued to cover all the services to the centrifugal pump in the heat transfer circuits.

B. TOLUENE SYSTEM

Tetralin will be used instead of toluene in the cooling system. This change was made in order to reduce physiological and fire hazards. The specific heat of tetralin is about the same as toluene. With the same weight flow, the pressure drop in the piping system is about the same. All of the equipment in the system can work satisfactorily with tetralin.

C. VENT SYSTEM

Hermetically sealed gas compressors were originally contemplated but were found to be unsatisfactory due to the inability to cool the compressors. Belt driven two-stage compressors with jacket and interstage cooling will be used.

A by-pass is being added around all radiation detectors in the vent piping system to facilitate servicing the instruments.

D. PIPING

All process piping in the SRE are getting a final going over in order to pick up all remaining changes.

The fabricated pipe details, or spools, have been completed for all welded pipe under 2-1/2 in. Certain pieces of these will need revision because of equipment changes and additions to the system. This is, however, of a minor nature and is in progress now. Pipe fabrication in our shop at the SRE Site is in progress.

The piping being fabricated by a supplier is virtually completed and delivery is expected early in January, 1956.

The insulation drawings for vessels and piping as well as specifications for these have been released.

The hangers and supports drawings are completed and released.

E. VAPOR TRAP EXPERIMENT (A. N. Gallegos and W. Malay)

Vapor traps will be used at specified locations in the SRE to remove sodium vapor which may be entrained in the exhaust gases. The basic component of an SRE sodium vapor trap is a tank containing packing material to remove the sodium

by combined condensing and filtering action; non-condensables passing through the trap. The experiment was conducted by passing a helium stream through a vessel of sodium and then directing the gas stream (helium plus sodium vapor) through the vapor trap.

Investigations were made using a packing material of stainless steel wool and low helium flow rates ranging from 4.3 cfh to 8.75 cfh. The sodium vessel temperatures throughout the test were of the order of 1000° F. The test results were such that 0.1 to 0.9 microgram of sodium per liter of helium at atmospheric pressure was observed leaving the vapor trap. The sodium concentration in the gas was determined by passing the gas through an indicator solution and observing the color change with a colorimeter.

At the conclusion of the tests, the vapor trap was dismantled. By visual observation, it was noted that considerable sodium had condensed around the inlet to the vapor trap and on the grating at the upstream end of the wool. Inspection of the wool indicated that a major portion of the sodium was trapped by the packing in the initial third of the length of the packing material. The visual observations were confirmed by dissolving the sodium out of the wool with water and analyzing the solution.

A new test series was then initiated using stainless steel wire mesh as a packing and considerably higher helium flow rates. Using flow rates of 60 cfh to 90 cfh and sodium vessel temperatures of approximately 1200° F, exit sodium concentrations from the vapor trap were found to be from 1.810 to 1.891 micrograms of sodium per liter of helium at atmospheric pressure. At the conclusion of the test series, the vapor trap was dismantled and the contents were analyzed by the same method as was used previously, to determine quantitatively the location of the trapped sodium. It was found that considerably less sodium had been deposited at the trap inlet and the grating at the upstream end of the mesh as compared to the previous test series. The trapped sodium was more evenly deposited throughout the entire length of the packing material, although the bulk of the trapping still occurred in the initial third of the packing.

F. FREEZE TRAP EXPERIMENT (A. N. Gallegos)

Test apparatus was constructed to determine the characteristics of the freeze trap designed for the SRE. The freeze trap consists of a coil of 15.5 ft of

stainless steel tubing (1/2 in. OD with 0.035 in. wall thickness) cast in an aluminum cylinder. The principle of operation is that sodium leaking into the coil would freeze in the coil thereby forming a seal. The requested test conditions for the experiment are as follows:

Coil Ambient Temperature	150° F
Sodium Inlet Temperature to Coil	350° - 1200° F
Sodium Pressure	20 - 50 psig

Initial tests, to date, indicate that the coil is capable of solidifying sodium to form a seal, but the data accumulated thus far are insufficient to correlate the results.

G. TETRALIN EVAPORATIVE COOLER TESTS (W. Malay)

To gain some experience and check the rated cooling capacity of the SRE tetralin evaporative cooler, a test was run on a 50 kw evaporative cooler installed in conjunction with the sodium pump loop.

By testing and thus determining the heat transfer coefficients for the 50 kw unit, calculations could then be more accurately made as to the expected performance of the SRE units.

The original plan was to test the 50 kw cooler by using the heat load from the sodium pump loop. However, pump shutdown necessitated that external heater elements and thermal insulation be installed on the return header of the tetralin piping. This was an expedient at best and it was only possible to apply approximately 20 kw of electrical heat input, a little over half of the rated cooler load. Further, it was not possible to pass the rated flow of 33 gpm through the cooler since the total capacity of the two circulating pumps amounted to only 26 gpm.

The test consisted of varying the heat load and tetralin flow rate on the cooler. Flowrators, already installed in the closed tetralin system and calibrated, were used to measure the flow. Cooler inlet and outlet temperatures were obtained by means of surface thermocouples on the piping. These sections of piping were lagged to prevent the effects of the sun from giving erroneous readings.

The calculated coefficients are 216 Btu/hr-sq ft-° F for toluene and 130 for tetralin at a temperature of approximately 100° F. A straight line relationship for the viscosity was assumed in the calculations.

The coefficient for rated flow and heat load was extrapolated to be 50 Btu/hr-sq ft-° F. Since $1/h_i$ was previously calculated, $1/h_o$ + fouling + wall was readily determined. Then assuming that this value is the same for toluene as well as tetralin, a reasonably accurate overall "U" for toluene was calculated to be 69.5 Btu/hr-sq ft-° F. Thus, it is seen the overall "U" for tetralin is about 15 per cent less than that for toluene.

H. HYDROGEN IN HELIUM (W. G. Bradshaw)

Early tests indicated that heated NaK has some effect in reducing the hydrogen content of tank helium (Table X). The most effective results were obtained when Tank A (the first tank) is heated and Tank B (the second tank) is maintained at room temperature. There is no reduction of hydrogen content by NaK when both tanks are at room temperature. Only limited work on the effect of heated NaK was done because of the unavailability of a clean NaK bubbler with heater controls.

The effect of heated NaK on removal of moisture from tank helium was tested (Table XI). The removal of moisture by NaK was not complete. Heating the NaK had no effect.

Because of the possibility of hydrogen formation from a NaK-water reaction the removal of moisture from helium before it is put into NaK was tested. The results with a tube (2 ft long, OD 2 in.) containing freshly activated alumina are shown in Table XI. The best results are obtained when the alumina is kept at room temperature.

TABLE X

EFFECT OF NaK TEMPERATURE ON HYDROGEN CONTENT OF HELIUM

Test No.	NaK T (° F)		Flow Rate		Hydrogen in ppm	
	Tank A	Tank B	(l/min)	(cu. ft./min)	Before NaK	After NaK
1	300	R. T.*	7.9	0.28	3	0.4
2	100	R. T.	15.6	0.55	3	0.1
2a	R. T.	100-170	14.2	0.50	3	0.8
2b	R. T.	170-250	14.2	0.50	3	2.1
2c	R. T.	250-300	14.2	0.50	3	1.5
3	R. T.	R. T.			5.6	5.6

*Room Temperature

TABLE XI

REDUCTION OF WATER CONTENT OF TANK HELIUM

Agent	Temperature (° F)	Water Content in ppm	
		Before Treatment	After Treatment
NaK Bubbler	Room Temperature	900	300
NaK Bubbler	300°	900	400
Alumina Tube	Room Temperature	500	100
Alumina Tube	100° and greater	500	500 and more

I. FUEL HANDLING (J. A. Leppard, S. Elchyshyn and C. M. Keim)

Development work of the fuel handling system has been completed. During this quarter, the process tube sodium system and the fuel handling coffin have remained operable for use in testing other reactor components such as the fuel elements and control rod assembly. Some training of the operating crew in the use of the coffin was accomplished.

A wet vacuum pump was installed in the vacuum system in connection with the cleaning cell. Tests were made in an effort to provide a wet pumping system to eliminate the necessity of using a cold trap during the evacuation after washing. The results proved this plan unacceptable.

In the course of handling the control rod, a sliding O-ring seal on one of the coffin pickup devices failed. The replacement of these O-rings necessitated sufficient disassembly to warrant a complete maintenance overhaul of the coffin. As various parts were removed a careful inspection revealed that only a small amount of sodium had collected on the drip pan and very little had splashed up on the coffin walls. (This sodium comes from the wetted fuel element). The lower end of the guide tubes had a small amount of sodium oxide and/or hydroxide deposit and the O-ring grooves had a rather heavy deposit. The rest of the coffin had no detectable amount of sodium anywhere; it was clean and in excellent condition. These observations were made after the coffin had been used in 24 handling operations involving hot sodium as well as numerous non-sodium operations. A few minor mechanical changes were made at the time of this overhaul.

Fabrication is proceeding satisfactorily. The lead shielding is being machined from rolled sections. Many major components are nearly completed.

XVI. REACTOR OPERATIONS

A. SRE OPERATIONS MANUAL (K. H. Campbell)

Preparation of the SRE Operations Manual has been continued and is approximately 55 per cent complete.

B. REACTOR PERSONNEL TRAINING (K. H. Campbell, F. E. Faris, and K. W. Foster)

The formal training program to prepare reactor operators and maintenance personnel for their jobs on the Sodium Reactor Experiment has been completed. The personnel concerned have been instructed in fundamental reactor technology, have operated the water boiler neutron source, and have received instruction on SRE functional systems and their operation.

Besides participating in that portion of the operators' training program which relates to the SRE systems, the engineers in the Reactor Operations Group have completed a series of studies on various phases of reactor technology. Emphasis here was on the application of basic principles to the SRE.

Five engineers of the Reactor Operations Group visited the SIR site during the month of November to gain experience in the operation of sodium-cooled reactors.

C. PREOPERATIONAL TESTING (D. H. Johnson)

The Preoperational Testing Manual is 70 per cent written. Detailed test procedures for the more complex pieces of equipment and systems are being prepared by engineers of the Operations Group.

Information obtained by operations personnel while visiting the SIR during the first two weeks of November will be an asset in both the completion of the Preoperational Testing Manual and in the performance of the testing program.

REFERENCES

1. A. B. Martin and Guy M. Inman, "Sodium Graphite Reactor Quarterly Progress Report, October - December 1954", NAA-SR-1292, May 15, 1955.
2. A. B. Martin and Guy M. Inman, "Sodium Graphite Reactor Quarterly Progress Report, January - March 1955", NAA-SR-1347, October 1, 1955.
3. A. B. Martin and Guy M. Inman, "Sodium Graphite Reactor Quarterly Progress Report, April - June 1955", NAA-SR-1457, October 1, 1955.
4. A. B. Martin and J. C. Cochran, "Sodium Graphite Reactor Quarterly Progress Report, July - September 1955", NAA-SR-1513, March 15, 1955.
5. F. B. Estabrook and S. W. Kash, "Measurements and Analysis of Uranium - D_2O Lattices" in Nuclear Science and Technology, Vol. I, No. 2, TID-2017, April 1955, pp 157-180.
6. E. R. Cohen, "A Survey of Neutron Thermalization Theory", International Conference on Peaceful Uses of Atomics Energy, UN-611, 1955, p 18.
7. E. R. Cohen - Unpublished Work.
8. J. E. Garvey in "Reactor Physics Quarterly Progress Report, November 1954 - January 1955", NAA-SR-1333, July 1, 1955.
9. F. L. Fillmore - Unpublished Work.
10. F. L. Fillmore - Unpublished Work.
11. I. L. Grey, "Type II Plugging Indicator", APL-Memo-116-7, June 17, 1953.
12. Herbert Goldstein and J. Ernest Wilkins, Jr., "Calculations of the Penetration of Gamma Rays", NYO-3075, June 30, 1954.
13. Gladys R. White, "X-ray Attenuation Coefficients from 10 Kev to 100 Kev", NBS-1007, May 13, 1952.